



Cooperative Research Centre for Coastal Zone Estuary and Waterway Management

Technical Report 32



Acoustic Techniques for Seabed Classification

J D Penrose, P J W Siwabessy,
A Gavrilov, I Parnum,
L J Hamilton, A Bickers,
B Brooke, D A Ryan and
P Kennedy

September 2005



CONTENTS

CONTENTS.....	I
LIST OF FIGURES.....	III
LIST OF TABLES.....	X
1. INTRODUCTION.....	1
2. BASIC CONSIDERATIONS.....	4
2.1. HABITAT AND HABITAT SURROGATES	4
2.2. VERTICAL EXTENT OF BOTTOM HABITAT.....	5
2.3. NON-ACOUSTIC TECHNIQUES FOR HABITAT CLASSIFICATION.....	6
2.4. SAMPLING STATISTICS AND COVERAGE.....	7
3. SONDER BASED SYSTEMS.....	8
3.1. AVAILABLE SYSTEMS	8
3.2. PRINCIPLES OF OPERATION FOR SINGLE BEAM ACOUSTIC BOTTOM CLASSIFICATION SYSTEMS	9
3.2.1. Wavefront curvature and echo shape.....	9
3.2.2. The need for a reference depth	11
3.2.3. Averaging of returns	12
3.2.4. Allowance for slope effects	13
3.2.5. Calibration.....	13
3.3. THE ROXANN SYSTEM	14
3.3.1. Results from North West Shelf and Southeast Fisheries Regions	21
3.4. THE QTC VIEW SYSTEM.....	26
3.4.1. Results from Wallis Lake, NSW	28
3.5. THE ECHOPLUS SYSTEM.....	32
3.5.1. Principles of operation	32
3.5.2. Examples of using ECHOplus	34
3.5.3. Results from Lough Hyne, Ireland	34
3.5.4. Conclusions.....	43
3.6. COMPARISONS OF SYSTEMS.....	43
4. SIDESCAN SONAR	45
4.1. INTRODUCTION	45
4.2. BASIC SIDESCAN SONAR OPERATION.....	47
4.3. CONSIDERATIONS IN SIDESCAN SONAR OPERATION	49
4.3.1. Frequency, range and resolution.....	49
4.3.2. Survey planning	49
4.3.3. Survey speed and ping rates.....	50
4.3.4. Positioning, sidescan deployment and sea conditions.....	51
4.4. EXAMPLES OF CURRENT SIDESCAN SONAR SYSTEMS.....	51
4.5. PROCESSING AND CLASSIFICATION OF SIDESCAN SONAR DATA.....	52
4.5.1. Processing sidescan sonar data	52
4.5.2. Classification of the seabed using sidescan data	53
4.5.3. Automated segmentation of sidescan imagery.....	55
4.6. SEABED SURVEYS AND CLASSIFICATIONS USING SIDESCAN SONAR	56
4.7. USE OF INTERFEROMETRIC SIDESCAN	57
5. MULTIBEAM AND SWATH SONAR.....	59
5.1. PRINCIPLES AND DATA PROCESSING OF MULTIBEAM SONAR SYSTEMS (MBSS).....	60
5.1.1. Processing bathymetry details	61
5.1.2. Processing of backscatter data	63
5.2. SEAFLOOR CLASSIFICATION PROCEDURE.....	68
6. SUBSURFACE SENSING TECHNIQUES	71
6.1. INTRODUCTION	71

6.2.	PRINCIPLES OF SUB-BOTTOM PROFILING.....	71
6.3.	TYPES OF SUB-BOTTOM PROFILERS	74
6.3.1.	High frequency systems.....	74
6.3.2.	Low and medium frequency systems	75
6.4.	INTERPRETATION OF SURFICIAL SEABED PROPERTIES FROM SUB-BOTTOM PROFILERS	77
6.4.1.	Shallow sub-bottom reflectors – links to benthic habitats	77
6.4.2.	The Damuth classification scheme	78
6.4.3.	Quantitative sonar classification.....	80
7.	A COMPARISON AND APPLICATION OF ACOUSTIC SYSTEMS.....	82
7.1.	INTRODUCTION/BACKGROUND.....	82
7.1.1.	State of Victoria Habitat Mapping Project.....	82
7.1.2.	Marmion Marine Park: Area A.....	83
7.1.3.	West End, Rottnest Island: Area B	83
7.2.	OBJECTIVES.....	84
7.3.	EQUIPMENT.....	84
7.4.	SURVEY DESIGN AND PARAMETERS	92
7.5.	DATA PROCESSING METHODS	93
7.5.1.	Reson Seabat 8101 and 8125.....	94
7.5.2.	GeoAcoustics GeoSwath	95
7.5.3.	EG&G 272 analogue sidescan sonar	96
7.5.4.	Klein 5500 multiple beam digital sidescan sonar.....	96
7.5.5.	C-Max CM2 digital sidescan sonar	96
7.6.	RESULTS.....	96
7.6.1.	Validate the Starfix interface to the GeoSwath system.....	97
7.6.2.	Determine the true usable swath width of the GeoSwath systems in varying water depths over varying seabed types	98
7.6.3.	Determine the maximum operating water depth of the GeoSwath.....	99
7.6.4.	Validate the quality of the bathymetry acquired by the GeoSwath interferometric system in comparison with the known quality of the Reson 8101 and Reson 8125 systems	100
7.6.5.	Determine the angular and spatial extent of the data ‘holiday’ under the nadir of the GeoSwath system.....	103
7.6.6.	Determine the required hydro acoustic deliverables for habitat mapping through exchange of technical information with the Coastal CRC, extend the Fugro knowledge base, and derive recommendations for the Victorian Habitat Mapping Project.....	104
7.6.7.	Multibeam bathymetric data deliverables	104
7.6.8.	Multibeam backscatter data – snippets.....	107
7.6.9.	Sidescan sonar	110
7.6.10.	Classification maps	110
7.7.	CONDUCT OF A SYSTEM COMPARISON FOR HABITAT MAPPING PURPOSES OF THE GEOSWATH, 8101 AND 8125	110
8.	ACOUSTIC SYSTEM SELECTION	114
	REFERENCES.....	118

LIST OF FIGURES

Figure 3.1. Interaction of an echosounder ping with the seabed (figure supplied by Andrew Balkin). The left hand side of the figure depicts the energy of the ping as it reflects from a horizontal seabed, and the right hand side shows the cross-section of the ping that is in contact with the seabed at the particular instant. In the centre frames, the back edge of the ping has not reached the seafloor, and a circle is ensonified. In the bottom frames, the back edge of the ping has already reached the seafloor, and an annulus is ensonified.	9
Figure 3.2. The parts of the first and second bottom returns used by the RoxAnn system. Energy of the shaded regions is integrated to form two indices - E1 (for the tail of the first echo – summation begins one pulse length from the echo start) and E2 (for all the second echo). From Hamilton (2001).	10
Figure 3.3. Effect of depth on echo shape for a very short ping. From Clarke and Hamilton (1999).	11
Figure 3.4. Typical echosounder output.	15
Figure 3.5. Scattering geometry and parts of interest of 1 st and 2 nd bottom returns. ...	16
Figure 3.6. RoxAnn system configuration.	17
Figure 3.7. Scatterplot of RoxAnn E1 (roughness) and E2 (hardness) indices with depth collected in the South East Fisheries region (After Kloster et al., 2001b).	19
Figure 3.8. Typical plot of E2 versus E1 together with the RoxAnn Squares, each of which represents one particular seabed type (After Chivers et al., 1990).	20
Figure 3.9. Representative examples of seabed images taken by a 35 mm Photosea 1000 camera system in the SEF area - upper 4 images (after Kloster et al., 2001b) and the NWS study area – lower 4 images (after Siwabessy et al., 1999).	23
Figure 3.10. Map of acoustically derived seabed types along the track, bathymetry and coastline for the SEF study area. ● = soft-smooth (SoSm); ● = soft-rough (SoRg); ● = hard-smooth (HdSm); ● = hard-rough (HdRg).	24
Figure 3.11. Map of acoustically derived seabed types along the track, bathymetry, coastline and benthic habitat types (pie charts) from Althaus et al. (in prep) for the NWS study area. ● = soft-smooth (SoSm) = habitat 4 (H4); ● = soft-rough (SoRg) = habitat 5 (H5); ● = hard-smooth (HdSm) = habitat 3 (H3); ● = hard-rough (HdRg) = habitats 1 & 2 (H12).	25
Figure 3.12. Pictorial plot of four derived fish communities given as pie charts overlaid into four seabed types given as a Cartesian plot of PC1_E1 versus PC1_E2 for the SEF study area. Colour definition for seabed types remains the same with that given previously. ■, ■, ■ and ■ are communities 1, 2, 3 and 4, respectively.	26
Figure 3.13. Pictorial plot of four derived fish communities given as pie charts overlaid into four seabed types given as a Cartesian plot of PC1_E2 versus PC1_E1 for the NWS study area. Colour definition for seabed types remains	

the same with that given previously. ■, ■, ■ and ■ are communities 1, 2, 3 and 4, respectively.	26
Figure 3.14. QTC View system configuration.	27
Figure 3.15. Clusters identified in the Wallis Lake acoustic dataset, based upon a Principal Components Analysis (using QTC Impact software). The ellipsoidal shapes (representing 95% confidence limits) include data points that make up the six acoustic classes (Class 1 = Red, Class 2 = Green, Class 3 = Blue, Class 4 = Cyan, Class 5 = Yellow, Class 6 = Pink).	29
Figure 3.16. Spatial representation of the acoustic data, coded for acoustic class, and plotted on a digital aerial photograph. Aerial photographs courtesy of Land and Property Information, NSW.	29
Figure 3.17. Cluster analysis dendrogram of the sediment data. Ground-truthing sample site numbers are shown on the x-axis. The four main cluster subgroups have been labelled Groups A-D.	30
Figure 3.18. Multi-dimensional scaling plot (MDS) of the sediment data. The four main cluster subgroups, identified in Figure 3.17, have been labelled Groups A-D.	30
Figure 3.19. Cluster analysis dendrogram of the sediment data. Each sample is coded for acoustic class (Figure 3.15) on the x-axis. The four main cluster subgroups have been labelled Groups A-D.	31
Figure 3.20. Multi-dimensional scaling plot (MDS) of the sediment data, also coded for acoustic class. The four main cluster subgroups, identified in Figure 3.17, have been circled (Groups A-D).	31
Figure 3.21. Lough Hyne Marine Reserve located on the south coast of Ireland (courtesy of John Rowlands, University of Wales, Bangor).	35
Figure 3.22. Biotope distribution of Lough Hyne as (a) observed, and as (b) continuous coverage generated by Kitching et al. (1976). See table for biotope descriptions and depth ranges observed by Kitching et al. (1976) in the lough.	36
Figure 3.23. A track plot of the ECHOplus survey (minus the anomalies removed) performed at Lough Hyne during August 2003.	38
Figure 3.24. Results of the ECHOplus survey of Lough Hyne in August 2003 (a) E1-Roughness and (b) E2-Hardness. Values interpolated using Kriging with a 2m grid and the coastline blanked (black).	39
Figure 3.25. Unsupervised classification of sublittoral habitats of Lough Hyne using (a) subjective box clusters placed on the scatterplot of E2 against E1 obtained from an ECHOplus survey in August 2003; giving (b) the resulting distribution of "acoustic classes" interpolated using the nearest neighbour algorithm in Surfer™. The 5 acoustic classes produced are assigned habitat complexes that they cover (the principle ones in bold) using the codes listed in Table 3.1.	39
Figure 3.26. Unsupervised classification of sublittoral habitats of Lough Hyne using cluster analysis of a False Colour Image composed of E1 and E2 values obtained from an ECHOplus survey performed in August 2003. The 6	

acoustic classes produced are assigned habitat complexes that they cover (the principle ones in bold) using the codes listed in Table 3.1.....	41
Figure 3.27. The 6 acoustic classes from Figure 3.26 are reduced to 4 'habitat' complexes that they cover using the codes listed in Table 3.1.....	41
Figure 3.28. Unsupervised classification with contextual editing of sublittoral habitats of Lough Hyne.....	42
Figure 4.1. Comparison of coverage between acoustic mapping technologies.....	45
Figure 4.2. Example raw 'waterfall' sidescan record.....	46
Figure 4.3. Typical sidescan sonar fish.....	47
Figure 4.4. Sidescan sonar thermal paper recorder.....	48
Figure 4.5. Display from sidescan digital acquisition system.....	48
Figure 4.6. Beam pattern of sidescan sonar.....	50
Figure 4.7. Sidescan sonar image of seagrass hummocks exhibiting beam spread in far ranges.....	50
Figure 4.8. Processing of sidescan sonar and video data into a classified map of the seabed a) sidescan sonar mosaic, b) raw waterfall image c) classified video track d) timestamped and georeferenced frame of video e) classified map.....	54
Figure 5.1. Typical geometry of the transmit and receive beams of MBSS.....	60
Figure 5.2. Bathymetry images before (left panel) and after (right panel) compensation for ship's motion (from the results of the Coastal Water Habitat Mapping project of the Coastal CRC).....	61
Figure 5.3. Slope (left panel) and TVI (right panel) draped over a 3-D bathymetry over the Morinda Shoal region in the Bowling Green Bay, Queensland, Australia (from the results of the Coastal CRC CWHM project).....	62
Figure 5.4. Sand-ripple roughness of seafloor surface modelled by an anisotropic fractal spectrum with a fractal dimension of 2.5.....	63
Figure 5.5. Backscatter intensity image of the seafloor build from five overlapping swath lines, before correction for the angular dependence (left panel) and after (central panel). The right panel demonstrates the mean slope of angular dependence within a 5-40° measured at the central points of each section of swath lines, superimposed on the grey-scale backscatter image. The seafloor in the surveyed area consisted mainly of sand. Note seagrass patches of various sizes clearly visible as yellow and red coloured (dark) spots at the bottom and at the upper right corner of the area.....	65
Figure 5.6. Measured histograms and statistical distribution fitting for two different types of the seafloor cover: rock – left panel; sand – right panel. Gray-scale images on the left of each graph are backscatter intensity images of the respective seafloor types (from Hellequin et al., 2003).....	66
Figure 5.7. Variations of the statistical estimates of shape factor $1/\alpha_{\text{eff}}$ versus the average incidence angle (from Hellequin et al., 2003).....	66

Figure 5.8. Angular dependence of backscattering strength from seagrass (1) and sand (2) measured in Cockburn Sound, Western Australia within the CWHM project [Gavrilov et al., 2005].	67
Figure 5.9. Three main domains (D1, D2, D3) of angular response curves and the parameters extracted to describe each domain (from Hughes Clarke et al., 1997).	68
Figure 5.10. Frequency of textural classes plotted against grain size determined from core samples (from Diaz, 1999).	69
Figure 5.11. AD classes plotted against grain size from core samples (from Diaz, 1999).	69
Figure 5.12. 3-D views of the seafloor across a coral reef in Morinda Shoal, Bowling Green Bay, Queensland.. The images show four colour-coded attributes extracted from the MBSS data: bathymetry (upper-left), slope (upper-right), TVI (bottom-left), and backscatter intensity (bottom-right). All of them are draped over the 3-D bathymetric map. Colour spots indicate the location of sampling stations for assessing fish abundance.	70
Figure 6.1. Deployment of various shallow-water sub-bottom profiling systems. After Stoker et al. (1997).	71
Figure 6.2. Frequency, depth of penetration, and approximate system vertical resolution (R), with typical sonar system ranges (depicted by horizontal bars). After Stoker et al. (1997).	73
Figure 6.3. Boomer sub-bottom profiles of the seafloor around the Whitsunday Islands, Great Barrier Reef platform, Australia (after Heap, 2000). The system used was an EG & G TM Uniboom sounder, triggered every 0.5 s at 200 J, and towed 0.3 m below the surface 11 m behind an 8 element hydrophone array. (A) The reflectors reveal a range of recent, Holocene, and pre-Holocene features, showing an exposure of bedrock surrounded by recent sand accumulations. (B) Steeply NE dipping bedding structures (clinoforms) and surficial dune bedforms record the accumulation and present-day movement of sand into a depocentre.	78
Figure 6.4. Acoustic impedance as a function of both sediment porosity and wet bulk density (after LeBlanc et al., 1992a).	81
Figure 6.5. Sediment acoustic attenuation measurements, or relaxation time values plotted as a function of mean grain size in phi units (after LeBlanc et al., 1992b).	81
Figure 7.1. Polygons representing the marine parks to be mapped. The remote locations and long transit times between sites imposed some constraints on the project.	82
Figure 7.2. Primary area for habitat mapping trials. A 2km by 0.5km detailed site survey over ecologically sensitive seabed of coastal habitat mapping significance within the Marmion Marine Park. Surveyed with Reson 8101, Reson 8125 and GeoAcoustics GeoSwath Multibeam systems, and EG&G 272, C-Max and Klein 5500 Sidescan sonar systems, this data provides an excellent proving ground.	83

Figure 7.3. A single line of data was acquired for deep water trials west of Rottnest Island with a GeoAcoustics GeoSwath interferometric sonar.....	83
Figure 7.4. The M/V Mirage – A photo of the Mirage showing the GPS antennas and the bow installation to mount the acoustic sensors.	85
Figure 7.5. Offset diagram of the M/V Mirage – showing the three dimensional offsets of the equipment installed on the vessel.....	85
Figure 7.6. Surface navigation equipment.	86
Figure 7.7. Bow pole arrangement for fixing the hydro acoustic transducers. All systems were mounted to this common flange. This ensured no additional error sources were introduced in the systematic comparison. In this case, the freestanding section is less than 300mm in length.....	87
Figure 7.8. The GeoSwath transducer mounted on MV Mirage bow mount.	88
Figure 7.9. The 8101 transducer and the topside 81P processor.	89
Figure 7.10. The Reson 8125 transducer on the bow mount of the MV Mirage. Note the requirement for the SVP probe alongside the head. The flat acoustic transducer face requires an instant and accurate value for the velocity of sound at the head. This is used for determination of direction of acoustic reception.....	89
Figure 7.11. The tow fish and its descendant, the GeoAcoustics 159D, are the real workhorses of the shallow geophysical industry. Simple to operate and maintain, they are well understood, robust and reliable.	90
Figure 7.12. The Klein 5500 installed on the bow of MV Mirage. Although this is not a standard operating mode, it provided excellent geo-referencing of the data, and was the safest option in such shallow water.....	91
Figure 7.13. Klein 5500 beam pattern. With the five simultaneous beams, 100% coverage at a high survey speed is possible.....	91
Figure 7.14. The CM2 digital tow fish off the stern of MV Mirage. As the fish has no fixed mounting point, it had to be towed behind the vessel. Also shown is the “CM2 C-Case” all in one acquisition and logging unit.	91
Figure 7.15. The UWA towed video system. The underwater lights in this photo were not used in these trials.	92
Figure 7.16. Survey line plan in Marmion Marine Park. Double density line spacing was used to provide excellent overlapped Multibeam bathymetry. This assisted in the analysis and comparison of the various systems.	93
Figure 7.17. Data processing pipeline for the Reson Seabat systems. Both Reson data sets were processed without any difficulties. Processing rates exceeding real time capture rates were easily achieved.....	94
Figure 7.18. Data processing pipeline for the GeoAcoustics GeoSwath system.....	95
Figure 7.19. Data processing pipeline for the EG&G 272 Sidescan sonar.....	96
Figure 7.20. Data processing pipeline for the Klein 5500 Sidescan sonar.	96
Figure 7.21. Data processing pipeline for the C-Max Sidescan sonar.....	96

Figure 7.22. GeoSwath swath width examples. The green soundings above indicate the soundings that fall within eight times the water depth. The red soundings are those that fall between the eight and twelve time's water depth.....	98
Figure 7.23. GeoSwath single beam maximum operational depth was not as good as expected.	99
Figure 7.24. GeoSwath cross profile in 82m water depths. This cross profile is indicative of the data collected off Rottnest.	99
Figure 7.25. Reson 8101 survey weather conditions were less than ideal. Credit should be given to the F180 GPS system which performed admirably underwater!	100
Figure 7.26. A cross profile of a single swath of filtered GeoSwath data. The soundings here are all considered good.	100
Figure 7.27. A single swath of de-spiked GeoSwath data.	101
Figure 7.28. Gridded Reson 8125 bathymetry over a shallow reef. Note how clearly the features are defined. Grid axes spacing is 50m.	102
Figure 7.29. Gridded 8101 bathymetry over the same shallow reef. Note the small artefacts in the data due to adverse weather conditions.	103
Figure 7.30. Gridded GeoSwath bathymetry data over the same shallow reef. Whilst all the features are still in place, and have similar depths, there is smearing of the features. This is caused by the higher variance in the point cloud. Note the artefacts due to the time stamping issue.	103
Figure 7.31. Surface of seafloor depth from the Reson 8101. A simple transform of depth to colour provides useful of information. It is widely understood that habitats change with depth. As such, seafloor depth is a significant factor in automated classification algorithms.....	105
Figure 7.32. Surface of seafloor slope from the Reson 8101. Depiction of relief via the use of shaded relief maps provides immediate visual cues to the location and spatial extents of potential habitats.	105
Figure 7.33. The combination of shaded relief and colour depth surfaces provides a primary presentation mechanism for the bathymetric data component of any Multibeam survey. It is easily understood by a casual observer and skilled technician alike.....	106
Figure 7.34a. Bathymetry quality surface provides a useful metadata layer. This can be used as a masking layer to omit noisy or unreliable data from classification systems.....	106
Figure 7.34b. NSamples surface provides a metadata surface indicating how many bathymetric observations were utilised in order to determine the depth for each pixel. This surface is very useful when analysing the survey to determine how efficiently it was undertaken.	106
Figure 7.35. Snippet backscatter data from the 8101 using the UNB1 processing algorithm. All major features are identified within the backscatter data, and co-location of adjacent swaths is correct. It should be noted that the “uniform snippet” backscatter was used in this trial (Reson 2000). Subsequent to these	

trials it is suggested that “FlatBottom snippets” is more appropriate (Gavrilov, personal communication).	107
Figure 7.36. Snippet backscatter data from the 8101 using a Per Beam Variance processing algorithm. All major features are identified within the backscatter data, and co-location of adjacent swaths is correct. It should be noted that the “uniform snippet” backscatter was used in this trial. Subsequent to these trials it is suggested that “FlatBottom snippets” is more appropriate (Gavrilov, personal communication).	108
Figure 7.37. Backscatter data from the GeoSwath. All major features are identified within the backscatter data, and co-location of adjacent swaths is correct. Nadir effects in the data possibly caused by interferometric bottom tracking problems can clearly be seen. Overall, the GeoSwath provided the highest resolution backscatter of all the Multibeam systems used.	108
Figure 7.38. Snippet backscatter data from the 8125 using the UNB1 processing algorithm. All major features are identified within the backscatter data, and co-location of adjacent swaths is correct. Minor features were not as clearly identifiable as the GeoSwath. Reef structure was not as clearly defined in the 8125 backscatter. Nadir effects are not as pronounced as the GeoSwath data.	109
Figure 7.39. Snippet backscatter data from the 8125 using the Per Beam Variance processing algorithm. All major features are identified within the backscatter data, and co-location of adjacent swaths is correct. Minor features were as clearly identifiable as the GeoSwath. Reef structure was well defined in the 8125 backscatter. Nadir effects are not as pronounced as the GeoSwath data, but still a serious impediment to automated classification.	109
Figure 7.40. EG&G 272 Sidescan sonar. Good across track resolution and a high degree of discrimination make this an invaluable tool. Poor geo-referencing of the towed fish caused by lack of accurate navigation, pitch, roll and heading reduce the absolute accuracy of the resulting mosaic, but relative positions of features are maintained.	112
Figure 7.41. C-Max Sidescan sonar suffered from bottom tracking problems. This caused significant AVG artefacts in the across track direction. The bottom tracking algorithm built into the C-Max is still under development.	112
Figure 7.42. The Klein 5500 has the best along track and across track resolution. Together with the accurate co-registration via the bow mount, this provided the highest backscatter from the Sidescan sonar’s in the trial.	113
Figure 7.43. An ISO unsupervised classification based on the bathymetric surface and its derivatives (Holmes, personal communication). The region has been classified into areas of low reef, high reef, deep sand and sand inundated. Correlation to the bathymetry and backscatter surfaces can clearly be seen. ...	113
Figure 8.1 Outline of object detection ability vs cost of operation for several acoustic systems.....	117

LIST OF TABLES

Table 3.1. Habitat complexes observed in Lough Hyne as described by the JNCC Biotope Marine Classification System (Conner et al., 1997), with their assigned habitat/biotope code and the depth ranges in which they are generally found according to Kitching et al. (1976). *Fluidised fine sediment is an additional habitat complex not found in the JNCC classification system. .	37
Table 6.1. System characteristics of various classes of sub-bottom profilers.	74
Table 6.2. Description and examples of echo character types (after Damuth, 1980, Whitmore and Belton, 1997, Rollet et al., 2001).	79

1. INTRODUCTION

This document has emerged from the Coastal Water Habitat Mapping (CWHM) Project of the Cooperative Research Centre for Coastal Zone, Estuary and Waterway Management. Material from the three year CWHM Project, together with selected information from other sources, is included in the document. The document also incorporates much of a report (Penrose and Siwabessy 2001) commissioned in 2001 by the Marine Conservation Branch of the Western Australia Department of Conservation and Land Management (CALM). Contributing authors to the present document have, in most cases, focussed on one aspect of the acoustic techniques reviewed, as outlined below. There has also been, however, considerable interaction between contributing authors during its development, and most chapters have had inputs from several of the author team. The final compilation and editing has been carried out by J. Penrose assisted by J. Siwabessy.

A valuable companion document to this review is an extensive bibliography of acoustic seabed classification prepared by Hamilton (2005) and, as with this document, listed as a Technical Report of the Coastal CRC.

The document reviews the use of acoustic techniques for the identification, classification and mapping of benthic habitats. It is intended for readers with an interest or background in the science and technology of acoustic techniques for seabed classification. The utility of acoustic techniques in benthic assessment lies in the ability to provide relatively rapid coverage of large seabed areas, compared to conventional photographic and direct sampling methods. Acoustic techniques should be seen as complementary to aerial and satellite based systems, being of greatest value where factors such as water depth or turbidity limit the scope of optical sensing.

The extensive use of acoustics in marine science and technology reflects the relatively low absorption experienced by acoustic waves in seawater, compared to electromagnetic waves at frequencies of interest. A very substantial literature in marine acoustics is associated with defence and seismic exploration activities, and also with biomass assessment applicable to pelagic fisheries. Acoustical techniques to provide indicators of seabed habitat type are now emerging and are the subject of this review. Only a small amount of the extensive defence and seismic literature concerned with seabed structures would appear to be of value for this review, although some techniques from such activities are informing current efforts in habitat assessment. This is because defence and seismic research has normally used relatively low frequencies and involved interactions at considerable depths below the seabed interface, with the exception of some work concerned with the detection of buried munitions. Habitat classification necessarily has a primary focus on the optically discerned water/seabed interface and short distances above and below this boundary. In general this leads to the use of relatively high acoustic frequencies and most examples and discussion below concerns acoustic frequencies at tens of kilohertz or above, essentially the ranges used in fisheries acoustics generally.

Seabed classification is of interest to defence and some engineering tasks. Much defence work has involved comparatively low frequencies, and is not often applicable to benthic assessment. Thus the very extensive literature concerning the development of geoaoustic models for low frequency propagation prediction is not represented

here, as the seabed regime of interest for such work extends well below depths of biological importance. Defence concerns for the detection of surface deployed or shallow buried munitions do however overlap to some extent with the issues arising from the classification of benthos, and use relatively high frequencies. A number of extensive defence research programs of this kind have been reported in the open literature, a useful example being provided in the Special Issue on High Frequency Acoustics of the Journal of Oceanic Engineering of January 2001. Simmen *et al.* (2001) provide an overview of the work covered in this journal. For the purposes of the present review, though, direct defence related programs are not reported, as at this time a significant amount of more directly applicable fisheries and environment oriented acoustic systems exist.

Similarly, the need for information about the first metre or so of the seabed, in the context of cable and pipeline burial has led to engineering techniques with some potential for application to broader benthic classification. In Western Australia, Fugro Survey Pty. Ltd. have pioneered a short range, shallow penetration seismic refraction system which provides assessment of the compressional sound speed in the upper few metres of the seabed, a parameter linked to other seabed properties such as compressive strength. At this time, however, this system is unlikely to be competitive with the techniques outlined below and is therefore not further reported here.

Acoustic techniques for seabed classification need to be considered in the context of broader ecological and other considerations. Chapter 2 deals briefly with some aspects of the benthic environment which have relevance to the use of acoustical techniques.

As with some other techniques, acoustic methods for benthic assessment yield information on surrogate measures of habitat. Acoustic reflection and scattering from the seabed itself and from biota extending above the seabed are central to benthic assessment. Acoustic returns from biota below the seabed surface are not easily distinguished in most acoustic signals. This review is being compiled at a time when considerable value is seen in mapping seabed habitats such that bottom topography data and acoustic backscatter can be spatially co-located. Such conjoint data sets, informed by periodic towed video information, in particular, are currently seen as providing a workable basis for many seabed habitat requirements. Issues of spatial scales and coverage, of needed and possible spatial resolution, of the choice of classification systems and of survey costs remain as ongoing topics for consideration.

Spatial coverage limitations associated with acoustic systems are particularly significant for, in this respect, the least satisfactory of these systems, those based on single beam echosounders. The relatively low cost of such systems, has nonetheless led to significant use of echosounders in benthic classification. Such single beam systems have been the earliest developed and applied technology in the field. For successful implementation of echo sounding based benthic assessment, a high dynamic range sounder linked with suitable data acquisition and navigation technology is needed. A processing package is called for and several commercial and non-commercial variants exist. Attention needs to be given to several effects arising from varying water depth and to the influence of the host vessel. J. Siwabessy, L.Hamilton and I. Parnum have been lead authors for Chapter 3, on single beam techniques and B. Brooke and D.Ryan have contributed additional material. This chapter includes some comment on acoustic backscatter from benthic biota, rather than solely from the water – sediment/reef interface itself, a topic of emerging

significance. Chapter 3 includes discussion on several topics of relevance to the sidescan and multibeam material covered in later chapters.

Sidescan sonar provides extensive spatial coverage and in some cases immediately useful information on bottom type. In general, however, the interpretation of sidescan records is limited in terms of bottom biota and this technology is often seen as providing a preliminary tool to guide a suite of more detailed studies on small areas. Further work using a range of acoustic frequencies and involving texture analysis of sidescan images is warranted to seek maximum value from this technology. The advent of sidescan systems using interferometric techniques to provide linked bathymetry and backscatter information represents, at the time of writing, a developing pathway to the provision of such conjoint information. A. Bickers has been lead author for Chapter 4, which concentrates on sidescan. Chapter 7 also contains material on sidescan and interferometric sidescan systems.

The multibeam swath systems now available offer high performance in the provision of topographical information and are also beginning to yield linked backscatter data. The present review focuses on shallow water examples and applications. One deep water project investigating this potential has however been completed in Australian waters and further deep water swath projects are currently underway. In Chapter 5, concerned with multibeam and swath systems, A. Gavrilov has been lead author for this chapter, which focuses on high frequency, shallow water swath applications. Chapter 7 also revisits a number of multibeam related topics.

B. Brooke and D. Ryan are lead authors for Chapter 6, concerned with sub-surface sensing technologies. Their contribution points to the opportunity to explore linkages between shallow sub-surface geology and the seabed benthic environment. Their material also highlights the issues of sediment classification and mobility in the assessment of benthic habitat.

P. Kennedy is lead author for Chapter 7, which provides a valuable case study involving the comparison of a number of acoustic systems in a selected test area off the Western Australian coast and information on an extensive survey program off the Victorian coast, which was begun as the current document was being completed. This chapter contains material on data processing methods applicable to the acoustic systems used.

Chapter 8 comprises a number of conclusions and comments, drawn from the contributions of the author team, and representing a snapshot of issues associated with the use of acoustic techniques in seabed habitat assessment as of July 2005, in the experience of the authors.

2. BASIC CONSIDERATIONS

2.1. Habitat and Habitat Surrogates

One of the many definitions of habitat is given by the Shorter Oxford English Dictionary and cited in Harden-Jones (1994) as; “The locality in which a plant or animal naturally grows or lives; habitation. Applied (a) to the geographical area over which it extends; (b) to the particular station in which a specimen is found; (c) but chiefly used to indicate the kind of locality, as the sea-shore, chalk hills, or the like”. In some usages, the term habitat is extended to include the biological communities associated with a given locality. In such cases, description of a marine habitat may involve consideration of the total biomass in an area and its biodiversity. Some commentators make use of the term “biotope” to represent the seabed physical habitat and its associated biological communities. Acoustic assessment of the seabed has commonly been employed essentially as a sediment classification technique. Considerable attention has been given (see Sternlicht (1999) for a review of this issue) to the linked parameters of sediment grain size, density, porosity, compressional and shear sound speeds and absorptions and surface roughness. This work has informed the discussion below and in part underlies the method of operation of the commercially available systems which use acoustics for seabed classification. As discussed in Chapter 3, the concepts of seabed acoustic “roughness” and “hardness” are used as seabed descriptors. Here and later in this review “acoustic hardness” is used as a descriptor of the acoustic impedance of the substrate type and hence of the impedance contrast offered to an acoustic wave by the water-seabed interface. The physical roughness of a surface influences the amount of sound backscattered to a receiver, so that measured backscatter or “acoustic roughness” are often proxies for physical sediment roughness. (Backscattered sound is that part of the total scattered sound that goes back towards the source) For sedimentary seabeds “hardness” in particular can sometimes be linked to sediment density and compressional sound speed, which in turn link to other sediment parameters. A difficulty is that these acoustic descriptors “hardness” and “roughness” need not necessarily describe the actual physical hardness or geometrical roughness properties of the seabed. The roughness of sedimentary seabeds is seen as a consequence of the sources and sinks of sediment and of the kinetic energy delivered to the seabed by waves, tides and currents. However, high reflectivity and high backscatter from even a small shell content in sediments can degrade the use of acoustic “roughness” and “hardness” parameters for inference of geometrical seabed roughness. Additionally, epibenthic biota, particularly seagrasses and macroalgae of sufficient density can dominate acoustic returns and mask signals from the seabed itself.

A recent UK Government study discusses an approach to marine and coastal environments, listing seven areas of coherent action which are in turn linked to 12 guiding principles of the Ecosystem Approach as defined by the Convention on Biological Diversity. One such area of coherent action is concerned with the environment and includes a priority action item “Using surrogate information sources”. This appears to be a response to the need to access information on benthic habitat structure and function, amongst other factors, which can guide management and usage of the marine environment under conditions of limited understanding of ecosystem dynamics and usually, limited spatial and temporal data coverage.

As currently employed acoustic techniques provide several surrogate descriptors of habitat. These descriptors are usually linked to more direct habitat parameters by a variety of techniques, including photography and spot sampling of sediments and biota.

In recent decades, a number of studies have linked sediment grain size with infaunal invertebrate distributions. This issue has been reviewed by Snelgrove and Butman (1994) who conclude however that “the complexity of soft-sediment communities may defy any simple paradigm relating to a single factor, and we propose a shift in focus towards understanding relationships between organism distributions and the dynamic sedimentary and hydrodynamic environment”. In the context however of a broader range of seabed types, including harder sediments and exposed reef structures, some generalisations appear to be justified. Thus Siwabessy (2001), as discussed below in Section 3.3.1, has shown that certain groupings of near bottom fish species can be related to acoustically determined seabed type.

2.2. Vertical Extent of Bottom Habitat

Most discussion of acoustic interaction with the seabed does not consider that benthos above the sediment or reef surface contributes to measurable backscatter. Thus most commonly, biota such as macroalgae and sea grass are treated as “invisible” to acoustic sensing. This simplification appears to be a usable first approximation where low frequencies are used, and where only the dominant seabed surface return is sought. However, as shown by Hundley, Zaboudil and Norall (undated), seabed plant assemblies may be detected by appropriate acoustic techniques. Such detection may well provide a more direct surrogate measure of relevance to habitat classification than the measures currently employed, at least where substantial plant biomass areal density exists. A system known as SAVEWS (Submerged Aquatic Vegetation Early Warning System) has been developed by the U.S. Army Engineer Waterways Experiment Station to characterise vegetation in shallow water environments. SAVEWS uses a BioSonics DT4000 digital hydroacoustic sounder with a narrow-beam transducer (Sabol and Burczynski 1998). The system records the depths of the tops of vegetation, usually appearing as “a jagged pattern”. The pattern is interpreted visually or automatically. Koniwinski *et al.* (1999) have used this system.

Discussion of sub-surface contributions to acoustic backscatter are much more common. At the high frequencies relevant to the present work, such sub-surface scattering can be expected from targets such as shell material, sediment grains, biological matter such as rhizomes, and gas bubbles. Sub-surface scattering necessarily follows in time what is usually a dominant seabed reflection/scattering signal and is mixed with off-axis acoustic returns from the major interface. Thus, for most acoustic geometries information about sub-surface scatterers is not retrievable from signals such as echosounder returns, although sub-surface scattering contributes to the received echo return. Sternlicht (1999) reviews this issue, which has received considerable attention at a somewhat deeper depth scale than is of importance for habitat description, in the context of sensing for buried munitions. However, the acoustic systems are usually very good detectors of shell beds, as these have high acoustic reflectivity and backscatter e.g. Smith *et al.* (2001), and organisms such as horseshoe crabs and brittle stars (Magorrian *et al.*, 1995). Tseng *et al.* (2005) have

described a technique for distinguishing several classes of seabed biotic cover using a Genetic programming technique for processing single beam return signals.

In discussing acoustic techniques applied to seabed habitat description, it is important to note that the “seabed” extends both above and below the sediment or reef interface with the water column. Biotic material above the direct interface is susceptible to acoustic detection, while that below is difficult to distinguish from signals derived from the direct interface itself.

2.3. Non-acoustic Techniques for Habitat Classification

This review has as its focus the use of acoustics in seabed assessment. Most work in seabed assessment to date has made use of underwater photography, point geological sampling and benthic trawls to inform and evaluate acoustic data. Commonly, such non-acoustic techniques, which are relatively slow and labour intensive are combined with the comparatively rapid data acquisition capability, albeit yielding surrogate measures, provided by acoustic instrumentation. Thus acoustic techniques might be favoured in water depths or conditions where, for example aerial photography, or satellite data products are not suitable. It would also be of value to allow for some overlap between areas covered by acoustic and other techniques for purposes of comparison and evaluation. A recent overview of the roles of video techniques in fisheries, including benthic examples is provided by Harvey and Cappo (2000).

Aerial photography, under optimum conditions of wind/seastate, water clarity and sun position appears to allow e.g. macroalgae and seagrass communities to be distinguished in water of up to approximately ten metres depth (Kendrick¹, personal communication). Similarly, detailed spectral analysis, from airborne or satellite sensors may allow classification of substrate type in suitable conditions. It is understood that DSTO Sydney has had some involvement with satellite based multispectral and hyperspectral techniques, in conjunction with Ball AIMS and CSIRO Land and Water (Held *et al.*, 2000).

A variety of other sensor techniques are under development for seabed assessment. One such technique uses comparatively low frequency electromagnetic waves to estimate bathymetry and to provide some information on sediment properties (Vrbanich *et al.*, 2001a, 2001b). This technique appears to be directed more to geophysical exploration requirements than investigation of benthos. The Laser Airborne Depth Sounder (LADS) system, (see e.g. Sinclair *et al.*, 1999) which has shown significant successes in providing rapid bathymetry information in shallow water, does not seem to be configured to provide benthos information. Airborne lidar has similarly been employed for depth determination, and although providing some evidence of reef structures (West and Lilleycrop, 1999) does not appear to have been greatly employed for benthic classification.

¹Dr. G. Kendrick is a Senior Lecturer at the School of Plant Biology in the University of Western Australia, Perth, Australia.

2.4. Sampling Statistics and Coverage

Many, if not most, oceanographic measuring and sampling tasks must be carried out under costs and effort constraints which allow for only under-sampled data sets to be gained. The task of adequately assessing and classifying seabed regimes in the many areas of interest highlights this issue. Acoustic techniques are attracting considerable interest because they offer the potential to provide comparatively rapid assessment of some seabed properties. Nonetheless, the techniques described in the body of this report, involving as they do the use of boats as operating platforms, are also subject to their own cost and effort constraints on coverage. This is particularly so in the case of the earliest developed classification techniques, which use single beam echosounder technology. Such systems allow for data acquisition at slow to medium vessel speeds and from a strip of the seabed of cross-track width which depends on sounder beamwidth and water depth. Such track widths are a function of beamwidth, and may approach the water depth for beam widths of 50-60°, common in fish finding sounders, but are usually somewhat less than this figure. The sampled area provided from echosounder systems thus provides good along-track coverage and across-track coverage linked to the spacing between tracks. Interpolation between tracks, needed if a full 2D representation of the area surveyed is to be attempted, thus calls for some assumptions concerning the spatial variability of the seabed and benthic types. Siwabessy (2001) has approached this problem on the North West Shelf of Western Australia by firstly assessing, from a variety of track directions, whether or not spatial variability shows a clear distinction between tracks at constant depth, i.e. from tracks which follow depth contours, and tracks which follow maximum gradients in the area. In both cases an estimate of the autocorrelation characteristic length of roughness/hardness, i.e. lengths in which attributes of roughness/hardness data are self correlated, is made from the time/space sounder records. In his example, no evident contrast was seen between the along-track and cross-track runs. These autocorrelation characteristic lengths are then used as a basis for interpolating between tracks.

A further statistical consideration concerns the “patch size” provided by an acoustic system incident on the sea floor. An example of patch size is provided by the seabed area insonified by an echosounder. Commonly this is approximated as the projection of the central beam on the seabed interface at the depth of interest; the angular limits of the beam being represented by the 3dB points of the transmit beam pattern. In shallow water such a patch size is necessarily small and may be less than the horizontal roughness scale lengths of the surface. A succession of returns gained as the sounder is translated across such an environment will provide a distribution of reflected/scattered signal amplitudes. At greater depths a larger patch size is insonified and may now exceed the roughness length scales. This will provide a different form of signal amplitude distribution. This issue has been addressed by, amongst others, Dugelay *et al.* (2000) who also report on the effect of grazing angle on echo ensemble distribution form.

3. SOUNDER BASED SYSTEMS

3.1. Available Systems

Echosounder, single beam acoustic techniques for seabed classification using measures associated with substrate type have been widely applied, especially on continental shelves. Three commercial systems are noted below which use an extension of the technique employed by some Western Australian bottom fishing operators, probably amongst others, in earlier times. The approach is essentially to use some measure of acoustic backscatter signal magnitude to provide an estimate of the “hardness” of the seabed, and some measure of the length of the echo return to provide an estimate of seabed roughness. In the experience of the authors, one method, used to infer the presence of reef structures, was to run parallel to the depth contours with the sounder set over what was assessed to be a sandy bottom, at a gain setting which was just less than sufficient to provide a second bottom return. When second returns were observed, with or without sudden changes in depth, it was inferred that the substrate contained hard, reef dominated structures. Given the limited dynamic range of the sounder displays in use at the time, it was not clear how well this interpretation system functioned. The process did, however, contain the essence of several systems later developed commercially, in using the magnitude of the second echo as a measure of bottom hardness. Here and later in this review “hardness” is used as a descriptor of the acoustic impedance of the substrate type and hence of the impedance contrast offered to an acoustic wave by the water-seabed interface.

The three existing commercial systems, and a number of variants not marketed commercially apply signal processing technology to nominal normal incidence single beam echosounders. Such systems will be referred to here as single beam systems to distinguish them from the multibeam systems to be discussed in Chapter 5. The Tasmanian company SonarData hosts a valuable web site which covers the echosounder based systems discussed here and some related variants from other companies and institutions. These additional entries include the CSIRO developed ECHO software which the Division of Marine Research use on their Simrad scientific echosounder systems installed on RV Southern Surveyor. The SonarData web site has the address www.sonardata.com. This describes the Echoview software produced by that company and, through the sequence “Support and Download” and “Useful Links” connects to a variety of useful sites and publications, including material on benthic classification.

Single beam echosounders may be used to obtain a variety of information about the reflective characteristics of the seabed. They send a pulse of sound at a particular frequency (usually between 30kHz and 200kHz) that reflects from the seabed and the echo is picked up by the transducer. Three commercial bottom classifiers available in the market are the RoxAnn system, the QTC View system and the more recent ECHOplus system. The ECHOplus system is marketed by the United Kingdom company SEA (Advanced Products) Ltd. which appears to use similar techniques to RoxAnn. ECHOplus and RoxAnn are presented as similar in concept and function, although ECHOplus is advertised as being suited to dual-frequency sounder systems. In addition, ECHOplus is a digital system whereas RoxAnn is an analogue system.

3.2. Principles of Operation for Single Beam Acoustic Bottom Classification Systems

The general empirical basis for acoustic bottom seabed classification is well established, although a full theoretical basis to describe interaction of the incident ping with the bottom is not. Acoustic bottom classification systems use wide beam echosounders (beamwidth typically 12-55°) to obtain information on seabed acoustic "hardness" (acoustic reflection coefficient) and acoustic "roughness" (as a backscatter coefficient). Pace *et al.* (1998) discuss inversion approaches which could enable seabed geoacoustic parameters to be estimated from normal incidence data. SACLANTCEN have developed the BORIS model to return the time series response of the seafloor similar to the signal received by echosounders. However, it is doubtful whether inversions will allow reliable estimates of bottom type for the complicated and variegated seabed types experienced in the real world. Shell components in particular can cause unpredictable returns, and particular echo shapes need not have a unique cause.

3.2.1. Wavefront curvature and echo shape

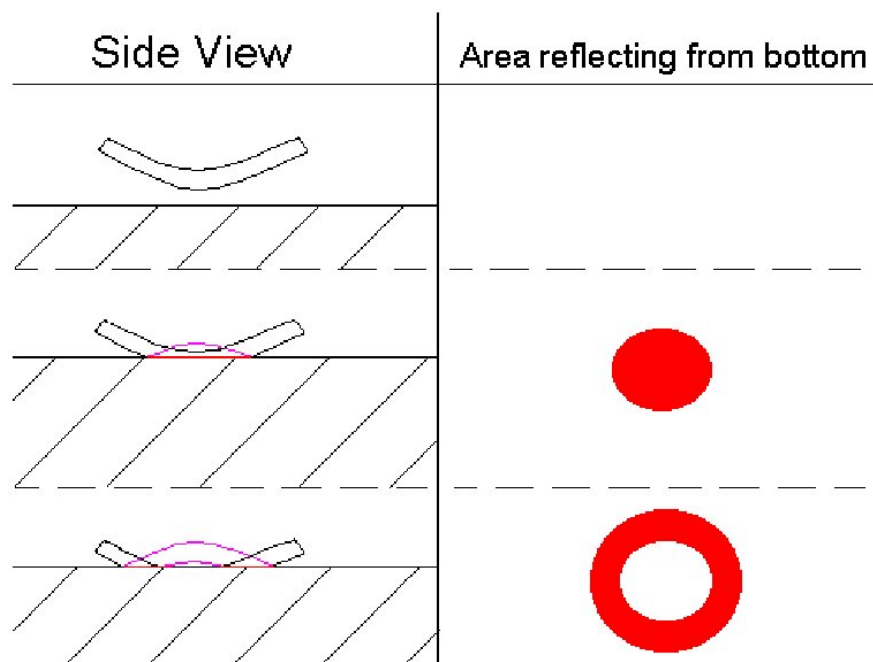


Figure 3.1. Interaction of an echosounder ping with the seabed (figure supplied by Andrew Balkin). The left hand side of the figure depicts the energy of the ping as it reflects from a horizontal seabed, and the right hand side shows the cross-section of the ping that is in contact with the seabed at the particular instant. In the centre frames, the back edge of the ping has not reached the seafloor, and a circle is ensonified. In the bottom frames, the back edge of the ping has already reached the seafloor, and an annulus is ensonified.

Because of wavefront curvature a ping from an echosounder with a wide angle beam ensonifies first a circle on the seabed, then progressively ensonifies annuli of increasing radii and lower grazing angles (Figure 3.1). If an amplitude envelope detector is used, then the signal recorded over a sampling interval is the total specular and backscatter return from some particular annulus. Echo shapes and energies

depend on bottom acoustic hardness and roughness. The first part of the resulting echo shape (Figure 3.2) is a peak dominantly from specular return, and the second part is a decaying tail principally from incoherent backscatter contributions. A smooth flat bottom returns the incident ping with its shape largely unchanged, but greater penetration into softer sediments attenuates the signal strength more than acoustically harder sediments. Rougher sediment surfaces provide more backscattered energy from the outer parts of the beam than smoother surfaces (which simply reflect the energy away from the direction of the transducer), so that a rougher surface is expected to have a lower peak and a longer tail than a smoother surface of the same composition. The length and energy of the tail provide a direct measure of acoustic roughness of the sediment surface. The echo shape is also a function of echosounder characteristics such as frequency, ping length, ping shape, and beam width. Acoustic penetration into the bottom and presence of subsurface reflectors can also affect echo shape through volume reverberation. Acquisition and classification of echo envelopes allows the bottom type to be inferred from the energy and/or shape characteristics of the echoes.

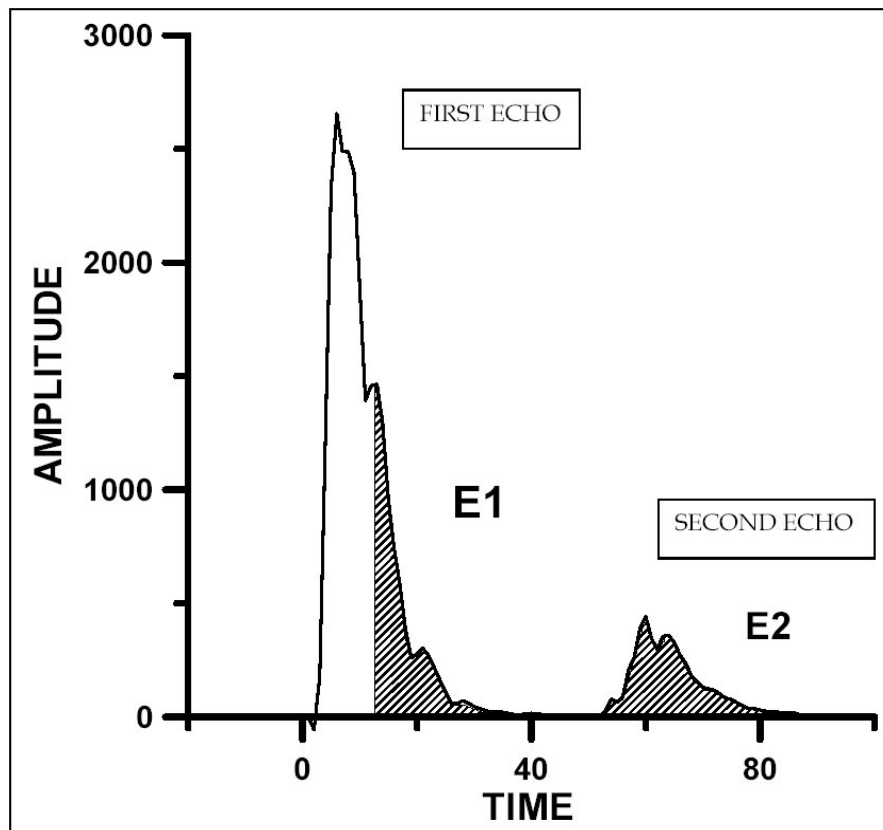


Figure 3.2. The parts of the first and second bottom returns used by the RoxAnn system. Energy of the shaded regions is integrated to form two indices - E1 (for the tail of the first echo – summation begins one pulse length from the echo start) and E2 (for all the second echo). From Hamilton (2001).

In reality the situation is more complicated as harder surfaces such as rock tend to have greater roughness and more random orientation of seabed facets than other sediments, resulting in widely varying return shapes and energies which can have an average signal strength resembling that of mud, if suitable averaging techniques are not used (Hamilton *et al.*, 1999). This phenomenon was noted many years ago in deep sea work, and has been “rediscovered” for acoustic bottom applications. “Regarding the reflection of sound by the ocean bottom, experimental studies ... have shown that

sound reflection is determined by the parameters of the sediment only at comparatively low frequencies. At frequencies above a few kilohertz, bottom relief plays a dominating role. Reflection from a very rough rocky bottom may appear to be less than that from a muddy sediment” (Brekhovskikh and Lysanov 1982; section 1.9). Similarly, losses due to roughness effects can cause sand with ripples, sandwaves, holes, and scours to appear to some acoustic measures to have the same properties as mud. Suitable averaging of echoes can overcome much of this variability, however acoustic bottom classification results are sometimes ambiguous, a point which must always be remembered.

3.2.2. The need for a reference depth

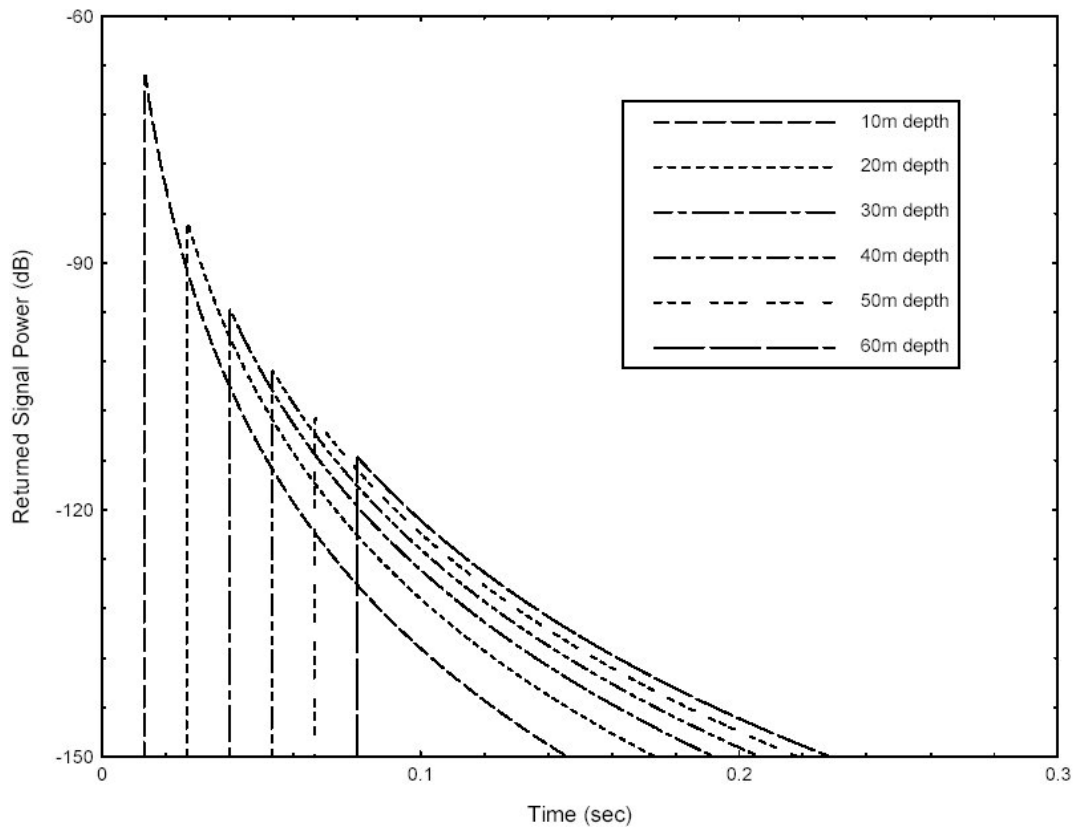


Figure 3.3. Effect of depth on echo shape for a very short ping. From Clarke and Hamilton (1999).

The shape and power of the returned signal can change significantly with depth, even if the bottom type remains the same. Examples are given in Caughey *et al.* (1994), Caughey and Kirilin (1996), and Figure 3.3. The returns for a particular bottom type are expanded (dilated) along the time axis for a deeper bottom, and compressed in time for a shallower bottom, so that returns from the same bottom sediment type lying at different depths do not have the same shape. This occurs because signals are sampled or digitised at equal time intervals rather than at equal angles (Caughey *et al.*, 1994). More samples are obtained from one particular angle to another for a deeper bottom compared to a shallower bottom. Before the echoes can be processed they must be transformed to a reference depth e.g. average survey depth. Normalising echosounder waveforms to a reference depth allows signal sampling to correspond to a standard set of incidence angles, as opposed to a set of linearly spaced times

(Caughey *et al.*, 1994). For a particular echosounder this conveniently removes the need to allow for beam patterns, and for the backscatter function changing with angle of incidence. Spherical spreading corrections are also applied. Absorption can usually be neglected for short ranges for lower frequencies e.g. 50 kHz, but becomes increasingly significant at higher frequencies. Since the signal to noise ratio decreases with increasing depth, large depth variations over an area could influence these corrections adversely.

To transform a returned signal to a reference depth, time and power corrections need to be made. The time correction is first made to adjust the length of the returned ping. The power correction then corrects the effect of spherical spreading. These corrections are required because signals are sampled or digitised at equal time intervals rather than at equal angles (Caughey *et al.*, 1994). Figure 3.3 shows the effect of depth changes on a short rectangular ping. Normalising echosounder waveforms to a reference depth followed by resampling allows signal sampling to correspond to a standard set of incidence angles, as opposed to a set of linearly spaced times (Caughey *et al.*, 1994).

The time correction employed enables returns from the actual depth d and the reference depth d_0 to maintain the same time/angle relationship (Caughey *et al.*, 1994). Sampling at the same angles for different depths removes the need to allow for beam patterns, and the need to allow for the bottom backscatter function changing with incidence angle.

The time correction is $\gamma = \frac{d}{d_0}$ (Caughey *et al.*, 1994)

where d = the actual depth; d_0 = the reference depth.

Therefore $t' = \frac{t}{\gamma} = \frac{d_0 t}{d}$

where t' = the corrected time; t = the time from the uncorrected signal.

Interpolation is then performed at times corresponding to reference depth sample times.

3.2.3. Averaging of returns

Return echo shapes can vary markedly over a small time interval, even for the same bottom type. As a result of ship and sensor movements and natural variability the returns from any particular angle are of a random nature, sometimes adding and sometimes subtracting as bottom facets lying at slightly different angles and depths are encountered. Echoes are also subject to noise, natural variability, and echosounder instability. To obtain acoustic signal stability ten pings are usually averaged. Over rougher terrain simple averaging may not help ping stability, and can act to reduce overall ping levels from their 'true' value, causing rocky surfaces to be classed as muds, a drawback of some commercial systems (Hamilton *et al.*, 1999). In this circumstance a smaller number of pings could be averaged or a different averaging method used e.g. Hamilton *et al.* (1999) suggested using the average of the one-third

highest values in a ping set, under the assumption that higher energy returns are least affected by roughness effects. A system developed by BioSonics allows selection of the highest value in a ping set, or averaging of values over a selected threshold (Burczynski 1999). However the current version v1.9 of the BioSonics system does not have depth normalisation.

3.2.4. Allowance for slope effects

Particularly for multiecho methods, it is necessary to scan for successive points, or for sets of points, with 'large' depth changes. Very large apparent depth changes are often indicative of errors e.g. due to crossing bubble wakes, and should be removed at early stages of the processing. Other changes due to bottom slope must also either be removed or checked for acoustic data stability and reliability. For vessel speeds of about 4 to 5 knots, and a classification about every five seconds, 'large' changes may be 0.8 m or less, according to RoxAnn data from Sydney Harbour obtained at beamwidths of 50°. This equates to a bottom slope of 4.5 degrees, quite a low value. Some confirmation is provided by a detailed analysis of slope effects on the QTC View system (von Szalay and McConnaughey 2001). They found slopes above only 5-8° caused misclassifications for two 38 kHz QTC View systems with beamwidths of 7°x7° and 9°x13°.

Acoustic bottom classification systems ensonify different areas at different depths, so depth changes may change results even for the same bottom types. A postulated example from Rukavina (1997) is as follows: "it is important to note that where the bottom variability is at a smaller scale than the footprint, because RoxAnn integrates over the footprint it cannot distinguish e.g. ... clay and boulders from a uniform gravel with the same average acoustic properties. Also the footprint size varies with depth".

Signal to noise ratio decreases with increasing depth, so that a wide range of depths in an area may cause poor classifications. A wide depth range can also affect the reference depth corrections.

Acoustic bottom classification systems are subject to bottom slope effects, especially for second echo methods. They may not provide reliable results near the sides of channels, over deep holes, or outcrops.

3.2.5. Calibration

For classification the systems rely on establishing empirical relations between ad hoc acoustic parameters and sediment sample properties. System calibration and classification then become a function of the bottom sampling strategy, a key point which cannot be over-emphasised. Classification can also depend on the purpose of the user e.g. a mapping of fish habitat could produce a different classification from a mapping allied to grain size. Video or similar groundtruthing is of central importance notwithstanding the restricted field of view associated with such techniques.

Acoustic systems are subject to noise and variability. Because of their empirical nature, classifications made using different acoustic bottom classification systems have an unknown relation to each other. Even for the same system and vessel,

classifications could differ over time with changes in transducer characteristics with age or fouling, or in background noise, regardless of any changes to the environment.

Calibration methods may be classed as direct or indirect. Direct methods are applied by classing particular portions of the acoustic bottom classification parameter space, and generally seek quantitative calibrations: explicit correlations of portions of the parameter space are sought with bottom properties such as grainsize bounds or vegetation indices obtained at calibration sites. Indirect methods may classify in parameter or geographical space e.g. the RoxAnn space may simply be arbitrarily classed by rectangles of equal size, and the geographical class distributions so formed are then examined for obvious trends. A second example of an indirect method is that of applying image processing methods to RoxAnn data in geographical space, and then using groundtruth to assign meaning to the geographical classes (Greenstreet *et al.*, 1997; Fox *et al.*, 1998). The geographical classes so formed should be transferred back to RoxAnn space to check for outliers and errors. Indirect methods may be more appropriate for habitat assessments, where explicit separation of classes or groundtruth might not exist. For indirect methods Geographic Information Systems (GIS) could be used to overlay acoustic classes and groundtruth to check for correspondences or otherwise.

3.3. The RoxAnn System

The RoxAnn system is manufactured by Marine Micro Systems of Aberdeen, Scotland, UK. The system uses the first and second acoustic bottom returns in order to perform bottom sediment classification. The first acoustic bottom return is reflected directly from the seabed and the second acoustic bottom return is reflected twice off of the seabed and once off of the sea surface (and the vessel hull). This method was earlier used by experienced fishers using regular echosounders (Chivers *et al.*, 1990). The double bottom interaction of the second echo causes it to be strongly affected by the acoustic bottom hardness, with roughness effects becoming secondary. Figure 3.4 shows the voltage trace of typical echosounder output for a single ping. Normally, this output is not available to the user because the system processes the data and stacks up a number of pings prior to display.

Shown on the left of Figure 3.4 is the tail end of the transmission, which may be ringing in the transducer, or reflections from close in structure or from entrained air bubbles beneath a hull-mounted transducer. In the middle of Figure 3.4, the first acoustic bottom return from the seabed is shown. In general, where epibenthos does not provide significant scattering, the first acoustic bottom return from the seabed is composed of at least three components: (1) the initial reflection from the seabed immediately beneath the transducer, (2) backscatter from an area surrounding the point on the seabed below the transducer and (3) possibly reflections from the sub-bottom (sub-bottom reverberation). Shown on the right of Figure 3.4 is the second acoustic bottom return from the seabed which has undergone an additional trip to and from the sea surface. The arrival time of the second acoustic bottom return is approximately twice that of the first acoustic bottom return. The second acoustic bottom return, however, is not just a scaled and delayed version of the first echo. It indeed carries further information (see below).

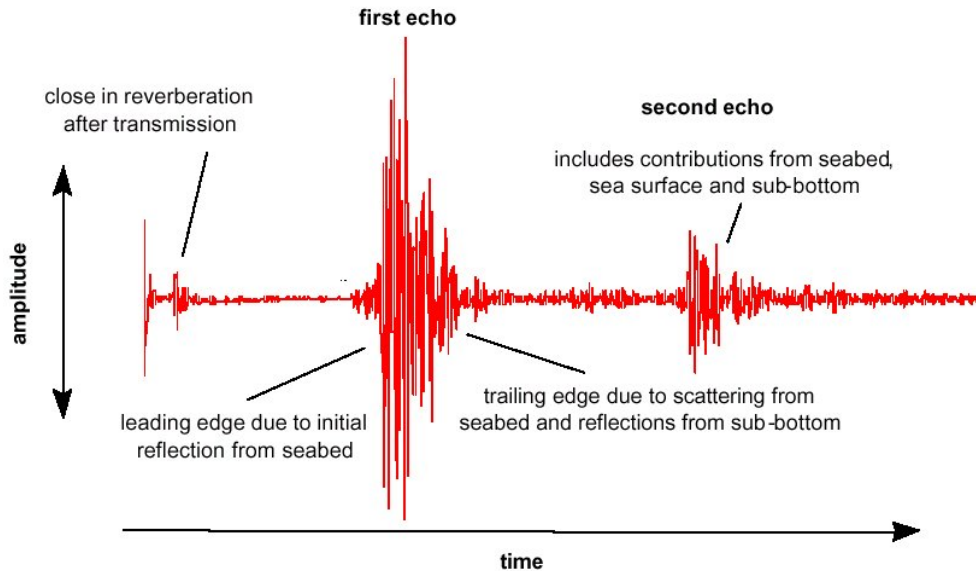


Figure 3.4. Typical echosounder output.

The RoxAnn system uses echo-integration methodology to derive values for an electronically gated tail part of the first return echo (E1) and the whole of the first multiple return echo (E2). While E2 is primarily a function of the gross reflectivity of the sediment and therefore hardness, E1 is influenced by the small to meso-scale backscatter from the seabed and is used to describe the roughness of the bottom. By plotting E1 against E2 various acoustically different seabed types can be discriminated (Chivers *et al.*, 1990; Heald and Pace, 1996). In principle E1 and E2 are related dominantly to acoustic roughness and hardness respectively, although each contains components of both.

The scattering geometries, along with parts of interest of bottom returns in the transducer response, are shown in Figure 3.5. An echosounder transducer transmits over a broad range of angles. If the seabed were perfectly smooth all the energy transmitted normally to the seabed would return to the transducer and energy at other angles would be reflected away. The seabed is not completely flat and a fraction of the energy transmitted at other angles is returned to the transducer. This backscatter mechanism is illustrated in Figure 3.5(a). The rougher the seabed, the more energy is scattered back to the transducer and the more energy appears in the tail of the echo, which also lengthens.

To avoid contamination of the backscattered energy with energy that has been directly reflected from below the transducer only the tail of the first echo is used in the analysis as shown by the dark curve in Figure 3.5(b).

The characteristics of the second echo are not as simple as the first and there are at least two rationales for the underlying physical mechanisms.

In the first rationale by Chivers *et al.*, (1990), the dominant ray paths for the second echo undergo two reflections at the seabed and a single scattering at the sea surface as shown in Figure 3.5(c). The amount of reflection is related to the difference in acoustic impedance between seawater and the sea bottom. Therefore, the harder the

seafloor the more energy is reflected forward to the surface and back to the transducer and the more energy appears in the dark curve in Figure 3.5(d).

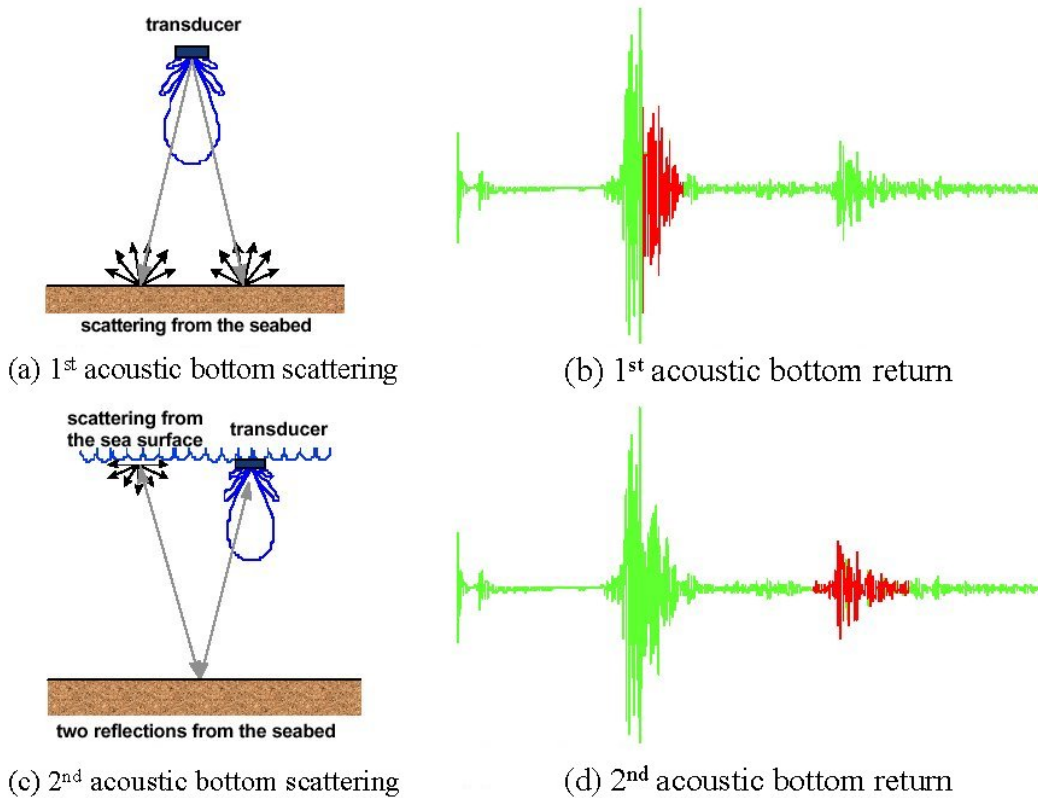


Figure 3.5. Scattering geometry and parts of interest of 1st and 2nd bottom returns.

In the second rationale by Heald and Pace (1996), the important observation is that because of the presence of the sea surface, the configuration is really a bistatic one with the transmitter and the receivers vertically displaced by twice the water depth. The impact of this is that the receiving transducer is in the near field scattering zone of the seabed and the scattered energy is therefore driven by the reflection and hence hardness properties of the seabed.

Both rationales, however, support the concept that the harder the seabed the more energy appears in the dark curve in Figure 3.5(d). However, a very rough, hard surface can scatter so much energy that it appears acoustically softer than expected. In deep sea applications “Reflection from a very rough rocky bottom may appear to be less than that from a muddy sediment” (Brekhovskikh and Lysanov 1982; section 1.9). Similarly, losses due to roughness effects can cause sand with ripples, sandwaves, holes, and scours to appear to some acoustic measures to have the same properties as mud. Suitable averaging of echoes can overcome much of this variability, however acoustic bottom classification results are sometimes ambiguous, a point which must always be remembered.

The parameters E1 and E2 are plotted against each other, and different pairings of the two are expected to be related to different bottom types. The user must determine which parameter combinations are related to particular bottom types by taking bottom samples. The approach is purely empirical, but works very well for flatter bottoms (Hamilton *et al.*, 1999). Some rationale is given for this approach by noting that

smaller scale sediment roughness may be physically related to grainsize (McKinney and Anderson 1964). McKinney and Anderson (1964) expected backscatter to be a function of particle size and bottom relief, and proposed sediment particle size influenced the size of bottom relief. Burns *et al.* (1989) state this as “harder ground has a greater capability of exhibiting roughness”, effectively the rationale assumed for RoxAnn operation. However these relations are lost over rougher topographies (Hamilton *et al.*, 1999). E2 and E1 are often referred to as “hardness” and “roughness”, implying measures of mechanical hardness and geometrical or physical roughness, but they are simply acoustic indices with some unknown relation to seabed conditions. E1 is a bottom backscatter index, and E2 is related to acoustic reflectivity.

Over rougher bottoms e.g. those with ripples, the energy lost to the second echo by backscatter can lead to lower than expected values of RoxAnn acoustical “hardness” for a particular sediment type, so that careful calibration against sediment samples is needed to obtain inferences of bottom type from the acoustics. See Hamilton *et al.* (1999) for more details. Depending on beam angle, unreliable E2 values are returned even for small slope values, a problem not widely appreciated. Voulgaris and Collins (1990) quote Jagodzinski (1960) as follows: “the second echo cannot be received unless the inclination of the bottom is smaller than the half beam width of the receiving oscillator. As a result the second echo may in some cases not be recorded, especially in the case of rocky bottoms or features such as sandwaves where the inclination changes rapidly on either side of the sand wave”.

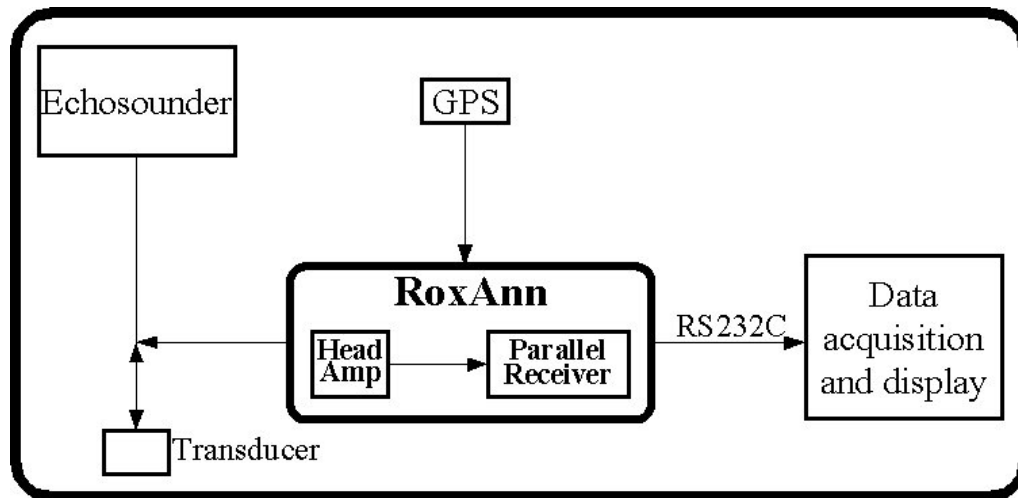


Figure 3.6. RoxAnn system configuration.

The RoxAnn system consists of a head amplifier, which is connected across an existing echosounder transducer in parallel with the existing echosounder transmitter (Figure 3.6), and tuned to the transmitter frequency. The parallel receiver accepts the echo train from the head amplifier (Schlagintweit, 1993). The installation requires no extra hull fittings, simply room for the processing equipment. The required processing equipment includes an IBM compatible computer together with a monitor. Software, specifically written to handle RoxAnn data, must then be installed on the computer for processing analysis.

Papers describing the RoxAnn type system include Kloser *et al.* (2001b), Hamilton *et al.* (1999), Siwabessy *et al.* (1999, 2000), Bax *et al.* (1999), Sorensen *et al.* (1998),

Greenstreet *et al.* (1997), Davies *et al.* (1997), Ryan *et al.* (1997), Magorrian *et al.* (1995), Schlagintweit (1993) and Voulgaris and Collins (1990).

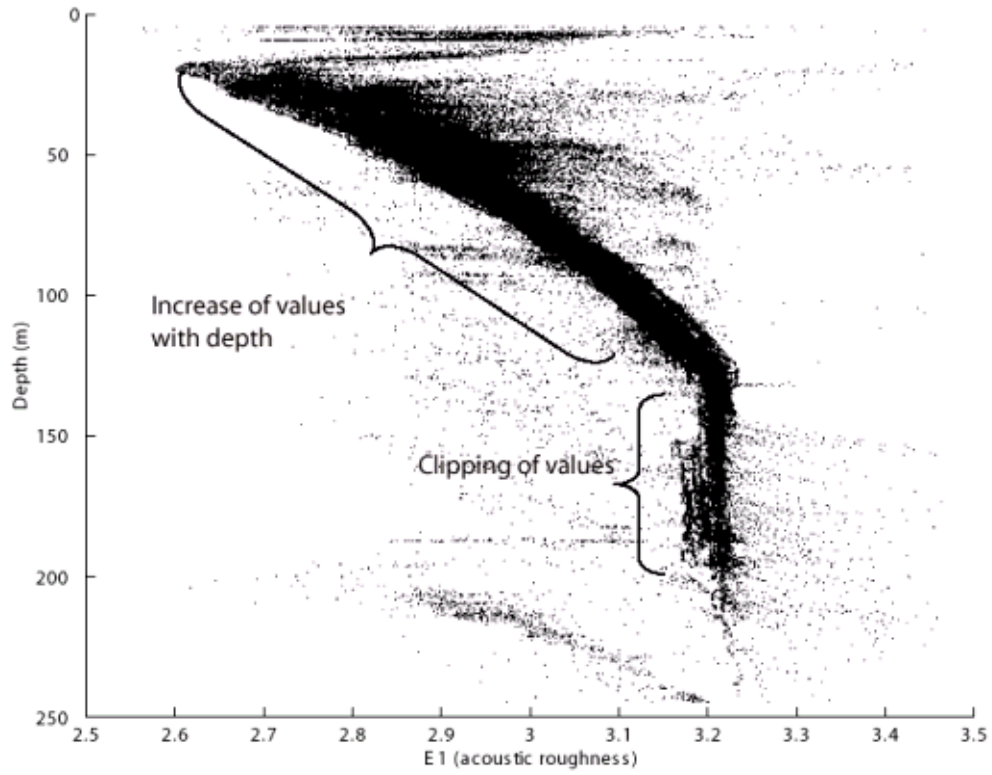
Kloser *et al.* (2001b) and Voulgaris and Collins (1990) experienced a depth dependence in their RoxAnn data that could not be explained by differences in bottom type as determined from sediment and photographic samples (Figure 3.7). When the depth trend prior to data clipping was removed from the E1 and E2 results, the resulting data compared favourably with the data derived from a CSIRO developed processing algorithm (Kloser *et al.*, 2001b). Although Hamilton *et al.* (1999) did not observe depth dependence in their RoxAnn data, they have warned that RoxAnn data might vary with depth and water column properties because water column absorption and scattering are not allowed for by the RoxAnn system. The depth dependence reported by Kloser has also been experienced in RoxAnn data gained in Antarctica (Pauly¹, personal communication). In addition, Hamilton *et al.* (1999) noticed that the RoxAnn system when sampling seabed with great slopes or depth changes could have problems detecting the second echo and part of it could be included in the first echo.

Despite the claim by the manufacturer that the RoxAnn system is not dependent on vessel speed, Hamilton *et al.* (1999) found that E2 was inversely related to vessel speed. They also found that E1 sometimes experienced change in synchronisation with E2. Similarly, Schlagintweit (1993) observed a consistent seabed classification by the RoxAnn system only at constant speed. He suggested that this might be related to changes in aeration and engine noise. Hamilton *et al.* (1999) also found that the occasional engine noise as the vessel was held on station or manoeuvred gave an unexpected result i.e. the RoxAnn system did not function well when the vessel was essentially stationary where it was expected to be more reliable. Wilding *et al.* (2003) have also reported RoxAnn classification results that vary with vessel speed, amongst other factors.

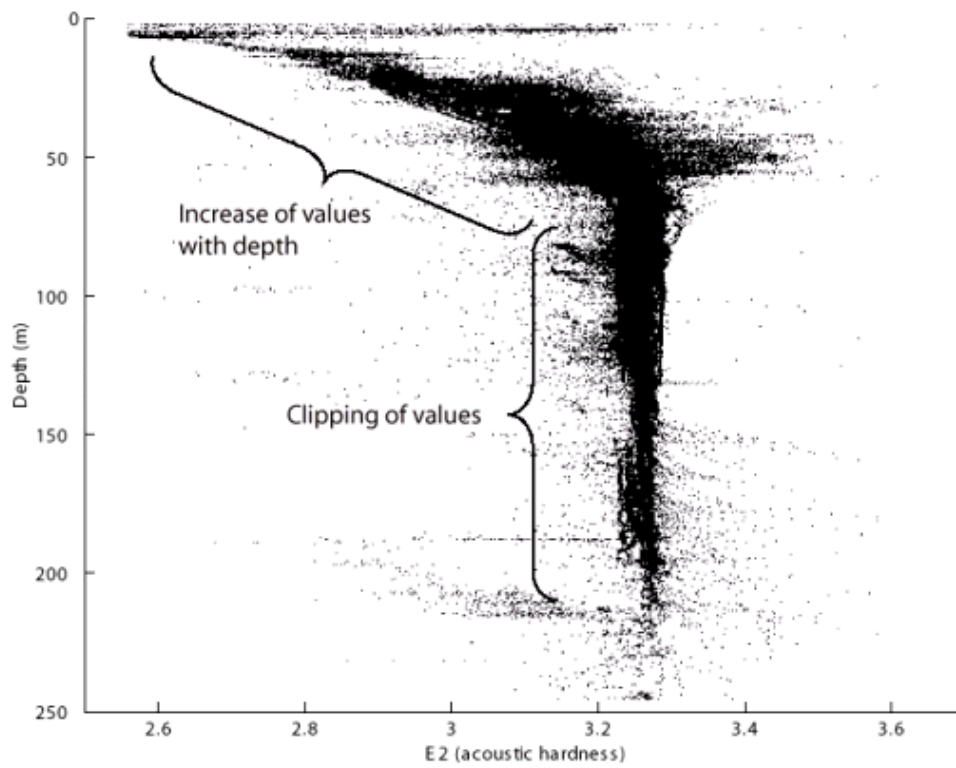
The RoxAnn manufacturer recommends the use of RoxAnn squares, introduced by Burns *et al.* (1989), to assess seabed classifications and encourages users to adopt it. A typical scatterplot of E2 versus E1 together with the RoxAnn squares is shown in Figure 3.8. Each of the squares represents one particular seabed type and is determined arbitrarily based upon ground truth. A number of problems in using the RoxAnn squares, however, have been notified by Voulgaris and Collins (1990), Greenstreet *et al.* (1997) and Hamilton *et al.* (1999).

While Greenstreet *et al.* (1997) observed inconsistency in the allocation system of the RoxAnn squares in boundaries between different seabed types, Voulgaris and Collins (1990), Greenstreet *et al.* (1997) and Hamilton *et al.* (1999) found that E1 and E2 parameters were not independent but linearly related such that data form an elongated roughly elliptical envelope inclined to E1 and E2 axes (Hamilton *et al.*, 1999). Since E1 and E2 are not orthogonal in RoxAnn space, Hamilton *et al.* (1999) argued that the RoxAnn squares cut across the data trend. In addition, Schlagintweit (1993) believed that an unsupervised classification method would be the best alternative, i.e., let the system select the natural groupings and then look at ground truthing.

¹Dr. T. Pauly is a Director for Business Development for SonarData and the Verdant Group, Hobart, Tasmania. He spent ten years as a Research Scientist and Hydroacoustician with the Antarctic Marine Living Resources Group of the Australian Antarctic Division.

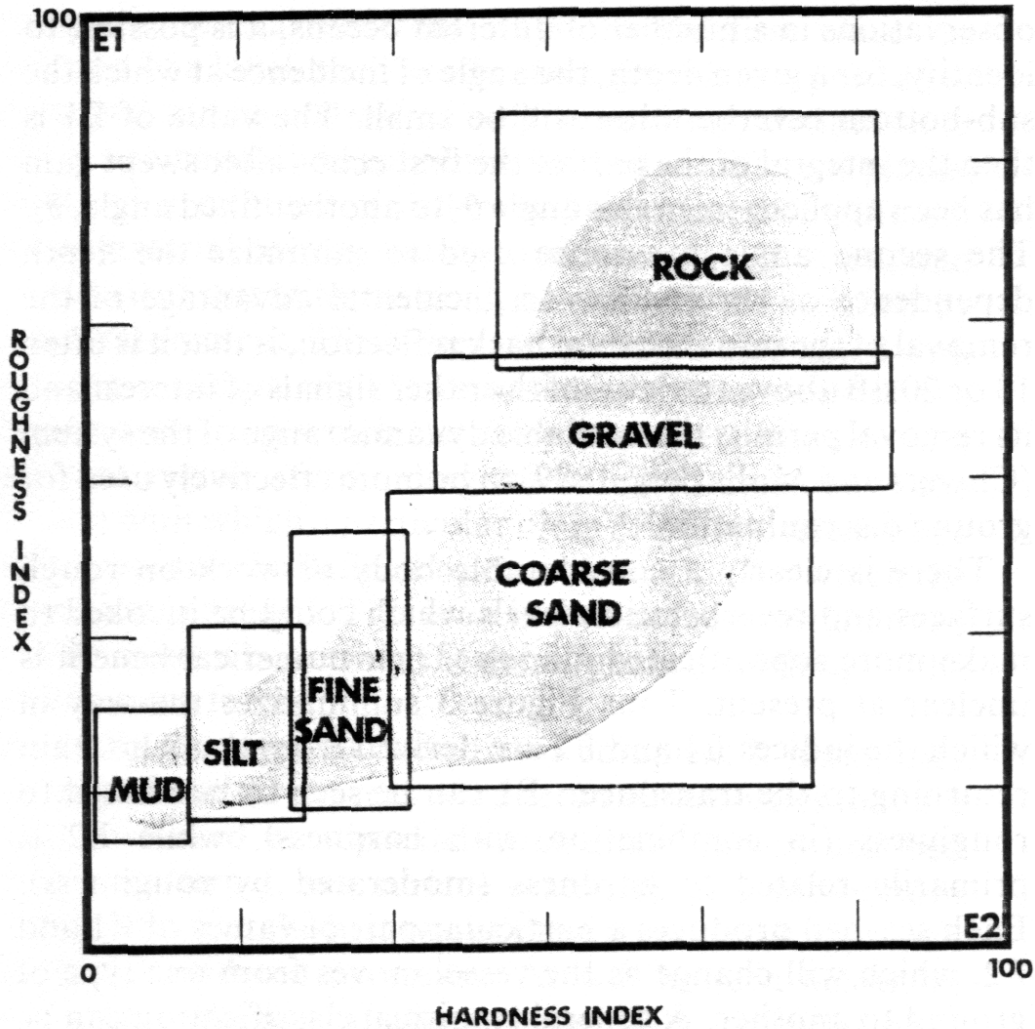


(a)



(b)

Figure 3.7. Scatterplot of RoxAnn E1 (roughness) and E2 (hardness) indices with depth collected in the South East Fisheries region (After Kloser et al., 2001b).



 TYPICAL SPREAD OF E1 E2 DATA

Figure 3.8. Typical plot of E2 versus E1 together with the RoxAnn Squares, each of which represents one particular seabed type (After Chivers et al., 1990).

Kloser *et al.* (2001b) and Schlagintweit (1993) observed the dependency of seabed classification on acoustic frequency. For the same seabed feature, different roughness indices were observed for two different frequencies they used. Schlagintweit (1993) found that the differences arising from 40 and 208 kHz data were due to the different seabed penetration depths of these frequencies on various sea floor types. That is, the frequency dependent penetration factor into the sea floor depended on the local sea floor itself. Schlagintweit (1993) felt that the frequency should be chosen according to the application.

At low frequencies where acoustic wavelengths are larger than the scale of seabed roughness, the seabed surface will appear acoustically smooth. In this case, seabed reflection will dominate seabed scattering. On the other hand at high frequencies such that acoustic wavelengths are smaller than the scale of seabed roughness scattering can dominate the returning signal and the seabed may be considered to be acoustically rough. In addition, as the seabed absorbs less energy at low frequency than it does at

high frequency, layers underneath the seabed surface might be acoustically visible. As such, seabed backscatter and sub bottom reflection at low frequency may arrive at the same time from different angles.

Hamilton *et al.* (1999) and Kloser *et al.* (2001b) noticed a bias due to slope or a sudden rise or drop of the seabed in their RoxAnn data. High slopes or sudden rises or drops of the seabed normally produce long tails in the first bottom echo which thus provide large acoustic roughness index estimates. For a sudden rise or drop of the seabed, this bias can be easily noticed in the echograms. Similarly, this bias can be picked up easily in the echograms if the vessel steams normal to the high slopes. If on the other the vessel is transecting parallel to the slope, this bias can only be interpreted once seabed types are plotted on the corresponding bathymetric map. This bias however can be used as a unique indication to identify such seabed types or areas (Greenstreet *et al.*, 1997; Hamilton *et al.*, 1999; Kloser *et al.*, 2001b). In addition, Kloser *et al.* (2001b) found that a narrow beamwidth was more sensitive to slopes than a wider one.

3.3.1. Results from North West Shelf and Southeast Fisheries Regions

CSIRO Marine Research has developed its own system using the first and second echo technique. Using a SIMRAD EK 500 scientific echosounder operating three frequencies (12, 38 and 120 kHz), acoustic volume reverberation (s_v) data are continuously logged using ECHO, a software package developed by CSIRO Marine Research (Waring *et al.*, 1994; Kloser *et al.*, 1998). The quality control and the derivation of E1 and E2 indices are conducted by using the ECHO software as well. The ECHO software provides several algorithms to derive E1 and E2 indices including a constant depth and a constant angular algorithm. This system has been tested in at least two Australian areas, namely the North West Shelf and the Southeast Fishery regions.

Making use the system developed by CSIRO just mentioned, Siwabessy *et al.* (1999, 2000) developed a procedure for seabed classification using a multi-frequency technique. The procedure of seabed classification involves multivariate analysis, in particular Principal Component Analysis and Cluster Analysis (the iterative relocation (k-means) technique). This procedure has been tested in the two regions studied.

It is assumed that the linearly increasing trend of E1 with depth shown in much of Figure 3.7 is likely to be an artefact of beam geometry and choice, and reliability, of TVG. Despite the fact that there is no law of nature which requires that $\partial E1/\partial R_0$ must equal to 0, as his working hypothesis, Siwabessy (2001) assumed that on average $\partial E1/\partial R_0 = 0$ where E1 is the acoustic roughness index and R_0 is the depth. To implement the above assumption, he used the constant angular integration interval algorithm within ECHO software developed by CSIRO Marine Research (Kloser, *et al.*, 1998). This algorithm ensures that the proportion of the tail sector being integrated is similar regardless of depth.

In his study, Siwabessy developed an alternative approach to the use of echosounder returns for bottom classification. The approach used, while similar to that used in the commercial RoxAnn system, involves several further developments. In grouping

bottom types, multivariate analysis (Principal Component Analysis and Cluster Analysis) was used instead of the RoxAnn squares mentioned previously. In addition, the approach adopted allowed for quality control over acoustic data before further analysis was undertaken, an issue of considerable importance in handling many real data sets. Three different frequencies, i.e. 12, 38 and 120 kHz, were operated. Principal Component Analysis was used in his study to reduce the dimensionality of the roughness indices from 3 to 1. The same was done for the hardness indices. The k-means technique was applied to cluster the resulting E1-E2 pairs formed for each set of six parameters to see if this would produce separable seabed types. This produced four separable seabed types, namely soft-smooth, soft-rough, hard-smooth and hard-rough seabeds (Figure 3.9). Principal Component Analysis was also used to reduce the dimensionality of the area backscattering coefficient s_A , widely accepted in fisheries acoustics as a relative measure of biomass of benthic biota, here assumed to be mobile.

There are some possible drawbacks to this technique, in that what is being done may merely be density clustering of a continuous data cloud (see Figure 3.12) without physical meaning. A seabed type which is sampled less often than another type may be lost (absorbed into another type), even if it is dramatically different from other types, unless it appears as extreme outliers. This seems to be an unrealised problem in acoustic bottom classification. Greenstreet *et al.* (1997) noted this problem for their bottom grab samples, these being evenly spaced throughout their study area, rather than there being the same number of samples for each bottom type. A similar problem exists with acoustic data (Hamilton 2001).

The bottom classification described above appeared to be robust in that, where independent ground truthing was found, acoustic classification was consistent (Figures 3.10 and 3.11). When investigating the relationship between the derived bottom type and acoustically assessed total biomass of benthic mobile biota, no trend linking the two parameters, however, appears. Figures 3.12 and 3.13, however, reveal some patterns between seabed types and derived fish communities formed from key species according to Sainsbury (1991) for the NWS region and to Bax *et al.* (1999) for the South East Fisheries (SEF) region. In addition, using the hierarchical agglomerative technique applied to a set of variables containing the:

- average and centroids of first principal component of roughness and hardness indices associated with the four seabed types;
- average first principal component of the area backscattering coefficient (s_A);
- species composition of fish community;

from which two main groups of acoustic population were observed in the North West Shelf (NWS) study area and three groups were observed in the SEF study area.

The two main groups of acoustic population in the NWS study area and the three main groups of acoustic population in the SEF study area were associated with the derived seabed types and fish communities of the key species.

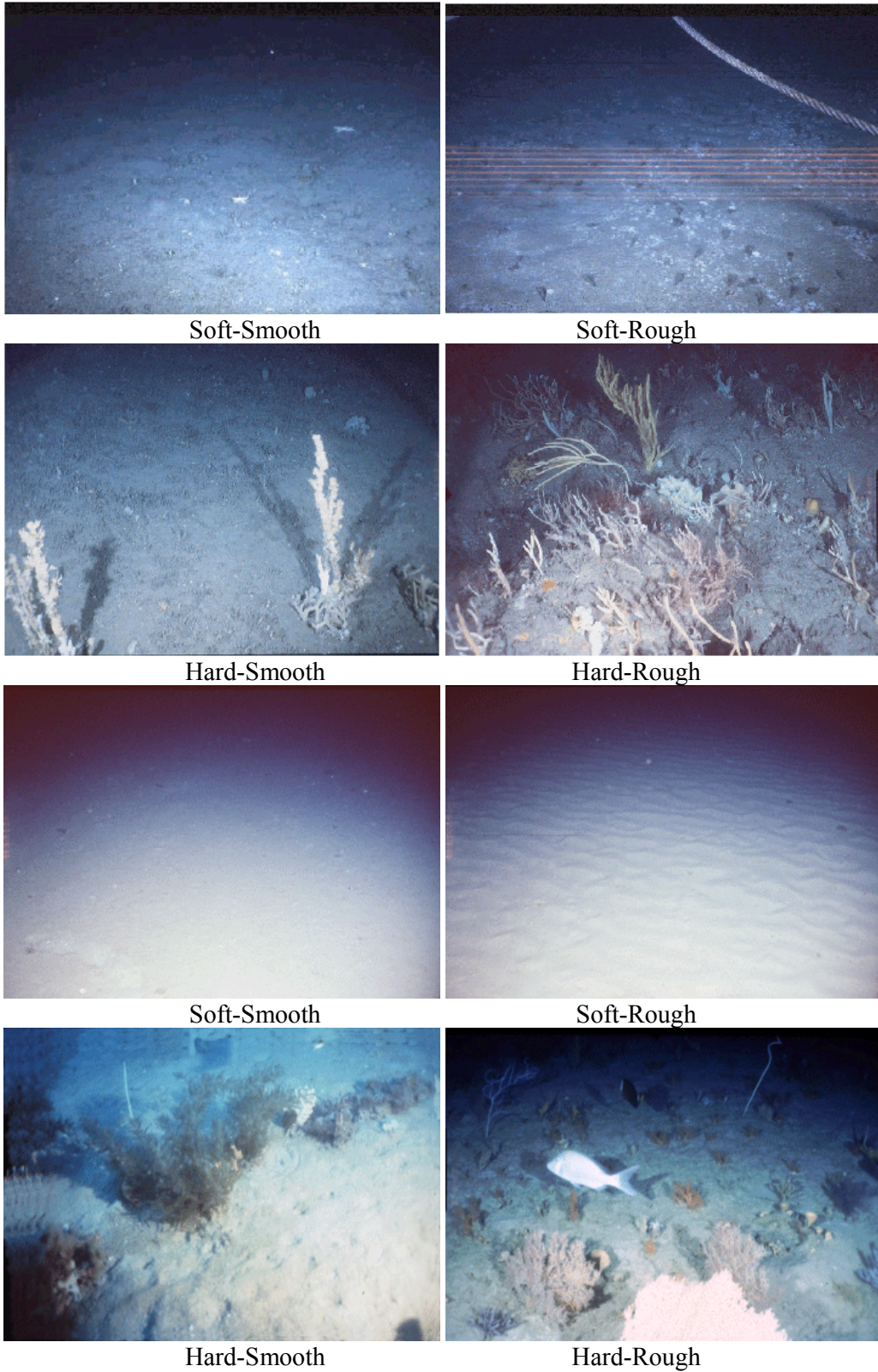


Figure 3.9. Representative examples of seabed images taken by a 35 mm PhotoSEA 1000 camera system in the SEF area - upper 4 images (after Kloser et al., 2001b) and the NWS study area – lower 4 images (after Siwabessy et al., 1999).

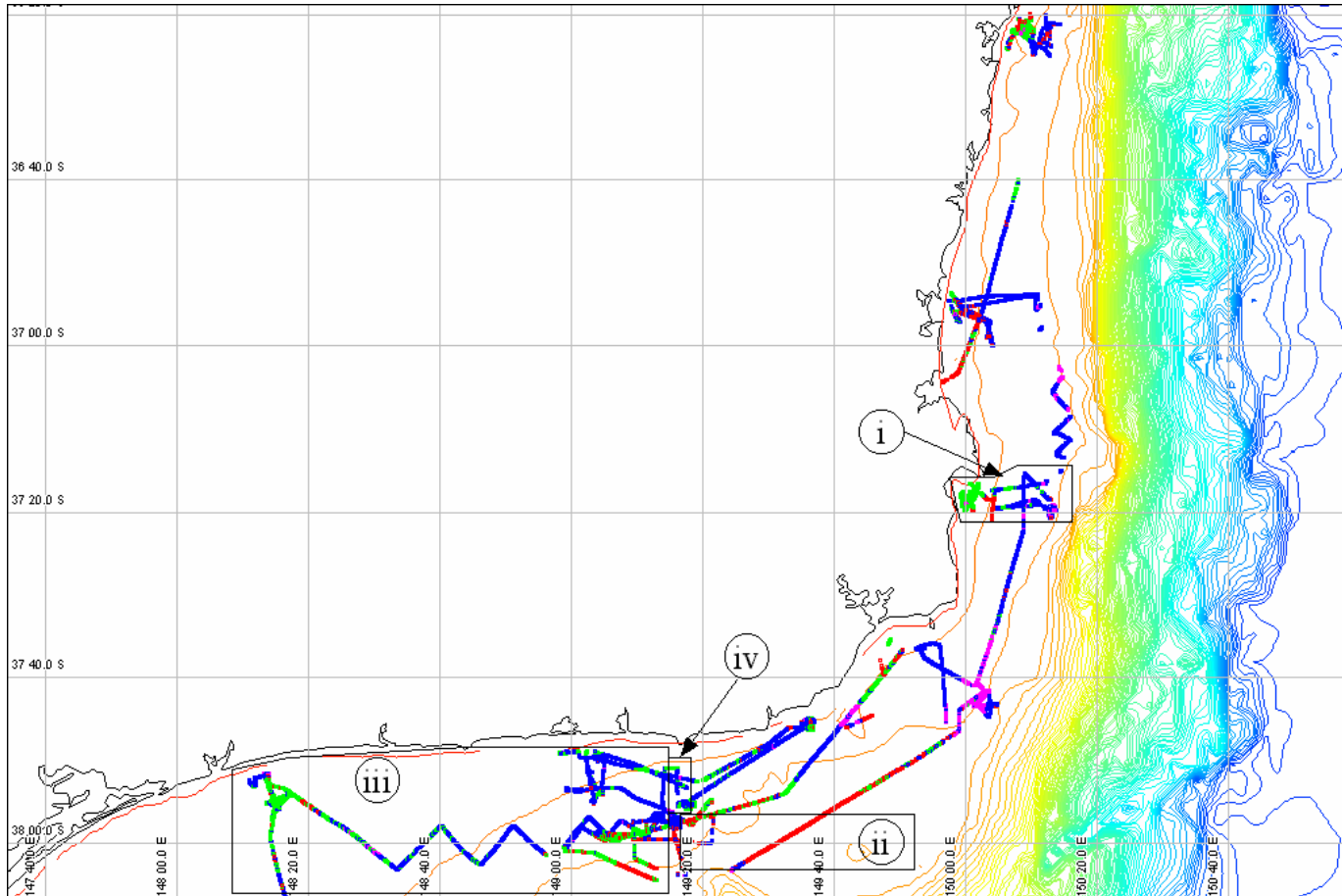


Figure 3.10. Map of acoustically derived seabed types along the track, bathymetry and coastline for the SEF study area. ● = soft-smooth (SoSm); ● = soft-rough (SoRg); ● = hard-smooth (HdSm); ● = hard-rough (HdRg).

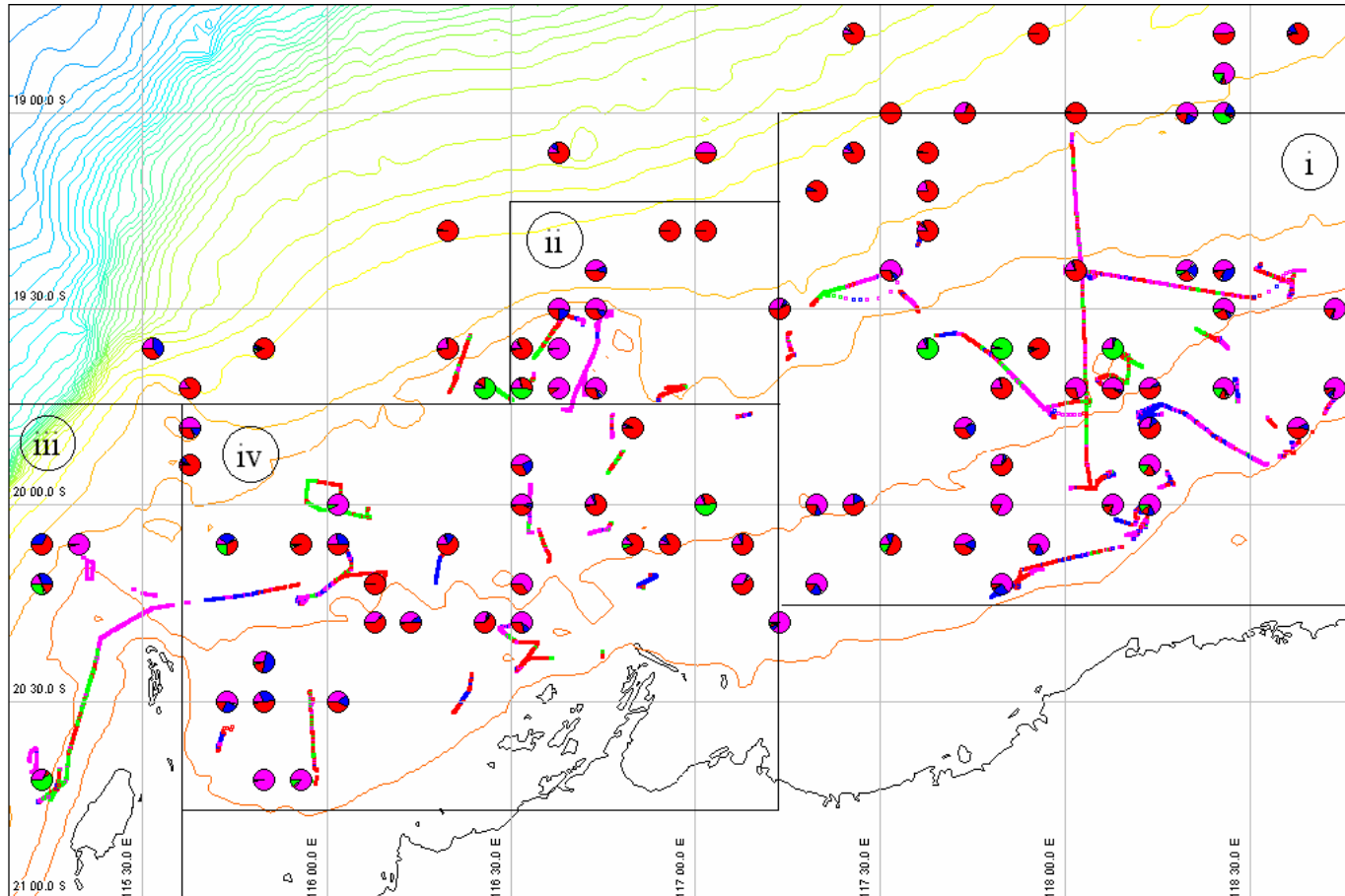


Figure 3.11. Map of acoustically derived seabed types along the track, bathymetry, coastline and benthic habitat types (pie charts) from Althaus et al. (in prep) for the NWS study area. ● = soft-smooth (SoSm) = habitat 4 (H4); ● = soft-rough (SoRg) = habitat 5 (H5); ● = hard-smooth (HdSm) = habitat 3 (H3); ● = hard-rough (HdRg) = habitats 1 & 2 (H12).

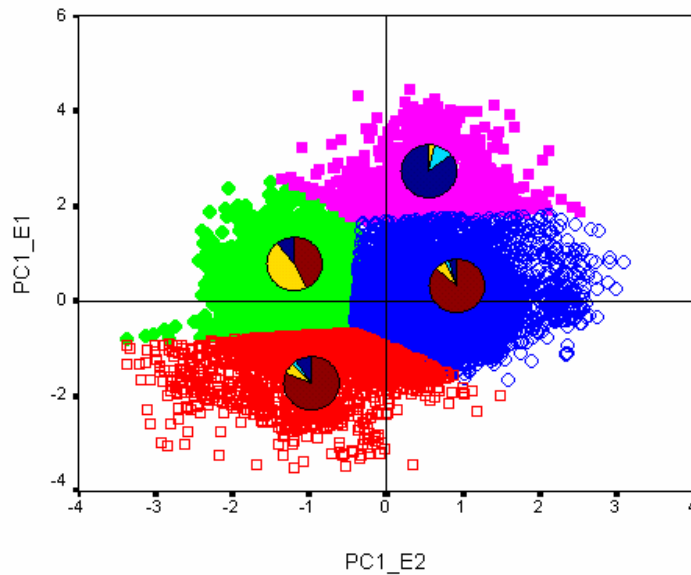


Figure 3.12. Pictorial plot of four derived fish communities given as pie charts overlaid into four seabed types given as a Cartesian plot of $PC1_E1$ versus $PC1_E2$ for the SEF study area. Colour definition for seabed types remains the same with that given previously. ■, ■, ■ and ■ are communities 1, 2, 3 and 4, respectively.

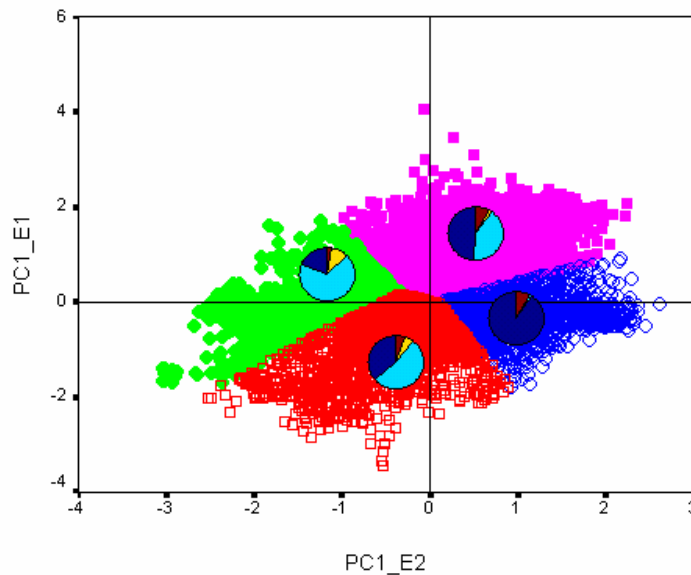


Figure 3.13. Pictorial plot of four derived fish communities given as pie charts overlaid into four seabed types given as a Cartesian plot of $PC1_E2$ versus $PC1_E1$ for the NWS study area. Colour definition for seabed types remains the same with that given previously. ■, ■, ■ and ■ are communities 1, 2, 3 and 4, respectively.

3.4. The QTC View System

The QTC View system is manufactured and distributed by Quester Tangent Corporation of Sidney, BC, Canada. Like the RoxAnn system, the QTC View system uses the existing echosounder transducer; however, the QTC View system uses only the first echo. The QTC View system operates in the following manner:

First, both the transmitted echosounder signal and return signals are captured and digitised by the QTC View system as a continuous time series. Second, the seabed echo is located (bottom pick), and an averaged echo from several consecutive returns is computed. This reduces the effects of acoustic and environmental variability. Next, the effects of the water column and beam spreading are removed such that the remaining waveform represents the seabed and the immediate subsurface (Collins *et al.*, 1996). Quester Tangent's echo shape analysis works on the principle that different seabeds result in characteristic waveforms. Through principal component analysis, complex echo shapes are reduced into common characteristics. Each waveform is processed by a series of algorithms which characterise it by a cited 166 shape parameters (Collins *et al.*, 1996). A covariance matrix of dimension 166 x 166 is produced and the eigenvectors and eigenvalues are calculated. In general, three of the 166 eigenvectors account for more than 95 per cent of the covariance found in all the waveforms. The 166 (full-feature) elements of the original eigenvector are reduced to three elements ("Q values"). These reduced feature elements will cluster around locations in reduced feature space, which may correspond to a seabed type.

The QTC View system was designed to operate in either the supervised or unsupervised classification mode. In the unsupervised classification mode, class assignment is based solely on the statistical nature of the data (the distribution of data) without knowledge of the spread of data of any seabed types. This can only be done in post processing. In the supervised classification mode, however, the classification is based on the knowledge of the spread of data of each seabed type revealed from ground truthing encountered in a particular survey. Classification then becomes a function of bottom sampling.

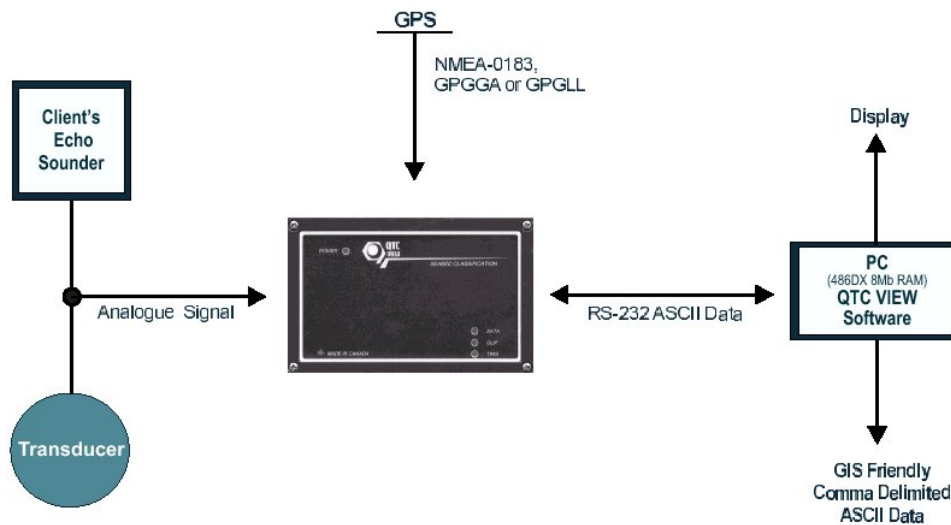


Figure 3.14. QTC View system configuration.

The QTC View system is comprised of a head amplifier and PC (see Figure 3.14). The head amplifier is connected in parallel across the existing transducer and to the PC via an RS232 cable. The PC also accepts GPS data in NMEA-0183 standard GGA or GGL format for georeferencing of data (Collins *et al.*, 1996). The PC displays three windows: one for the reduced vector space, one for the track plot and classification and the third for seabed profile and classification.

Papers on the performance of the QTC View system include Hamilton *et al.* (1999), Bornhold *et al.* (1999), Collins and McConnaughey (1998), Galloway and Collins (1998), Collins and Rhynas (1998), Tsemahman *et al.* (1997), Collins and Lacroix (1997). The first paper is the only one without authors from Quester Tangent Corporation.

Tsemahman *et al.* (1997) used the QTC View system in selected areas near Vancouver Island. They found that the system was able to discriminate between four different acoustic classes. After a calibration, QTC View was found to agree with each ground truthed area and showed good transition from seabed type to seabed type (Tsemahman *et al.*, 1997). Preston *et al.* (2000) recently have described the use of a modified QTC system in very shallow waters, with depths as small as one metre.

Unlike the RoxAnn system, the depth dependency of the QTC View system has not been reported in any papers on the performance of the system. Hamilton *et al.* (1999), nonetheless, have warned that QTC data might vary with depth and water column properties because water column absorption and scattering are not allowed for by the system. In addition, they observed that the QTC data were not obviously dependent on vessel speed. They also found that classification was consistent and did not change regardless of speed or even when the vessel was stationary or manoeuvred. They, however, noticed a bias due to slope or a sudden rise or drop of the seabed in their QTC data. This bias however can be used as a unique indication to identify such seabed types or areas (Hamilton *et al.*, 1999).

3.4.1. Results from Wallis Lake, NSW

This section summaries results of acoustic mapping of estuarine benthic habitats in Wallis Lake, NSW, fully reported in Ryan *et al.* (2004). A collaborative field trial of the Quester-Tangent View Series 5 single beam acoustic benthic mapping system was conducted in Wallis Lake by Geoscience Australia and Quester Tangent Corporation, with the assistance of NSW Department of Infrastructure, Planning and Natural Resources, Great Lakes Council and Curtin University. The survey, in June 2002, involved acquisition of the acoustic backscatter data from the northern channels and basins of Wallis Lake. Quester-Tangent software (IMPACT v3) was used to classify acoustic signals (echograms) that returned from the lake bottom into statistically different acoustic classes. The classification was based on characteristics of the echograms, which were further reduced using a principal component analysis (PCA) algorithm. An algorithm then divided the data into logical clusters, each cluster representing a unique acoustic class. Six acoustically different substrate types were identified in the Wallis Lake survey area (Figures 3.15 and 3.16).

In conjunction with the acoustic survey, ground-truthing was undertaken to identify the sedimentological and biological features of the lake floor that influenced the shape of the return echograms. Samples of lake-bottom sediment were collected from over 100 sites (located by DGPS) by snorkel divers, and pole-coring. For each sample, laboratory measurements were made of grain size, wet bulk density, total organic carbon, CaCO₃ content. Mass of coarse fraction (mainly shell) material was recorded for samples taken in December. At most sampling sites, diver observations provided information about the morphology of the lake bed, such as density of animal burrows, and seagrass species and coverage; and at several sites photographs of the substrate

were taken. A scheme of simple ranked indices was developed to reflect the relative density of each of these site features.

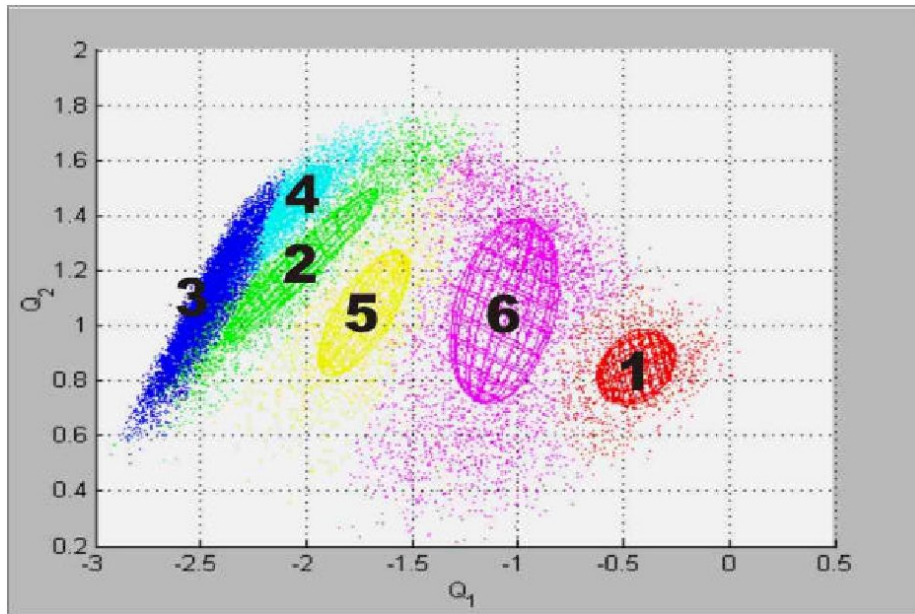


Figure 3.15. Clusters identified in the Wallis Lake acoustic dataset, based upon a Principal Components Analysis (using QTC Impact software). The ellipsoidal shapes (representing 95% confidence limits) include data points that make up the six acoustic classes (Class 1 = Red, Class 2 = Green, Class 3 = Blue, Class 4 = Cyan, Class 5 = Yellow, Class 6 = Pink).

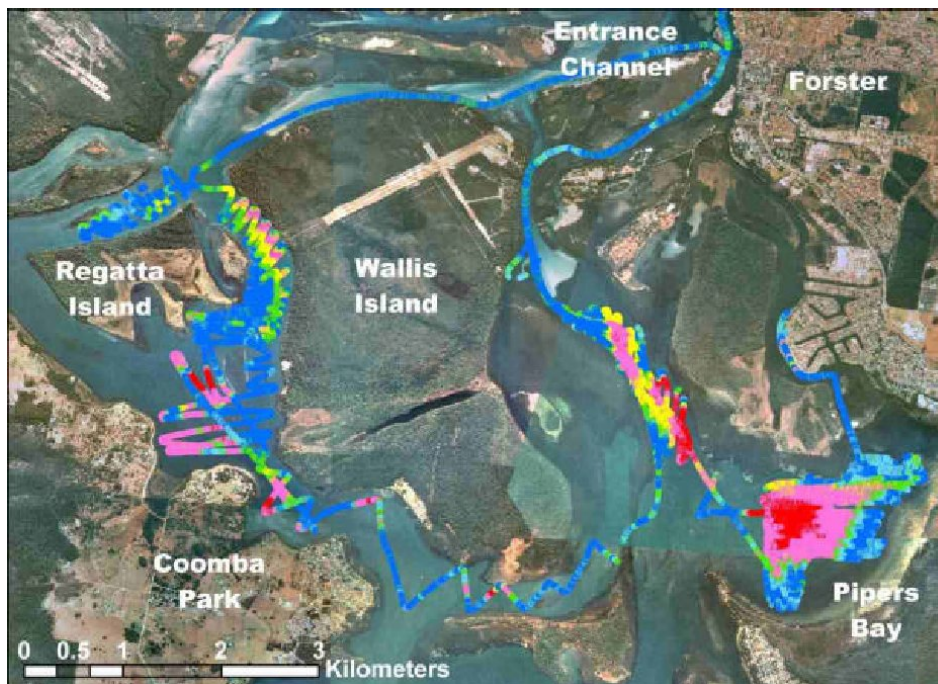


Figure 3.16. Spatial representation of the acoustic data, coded for acoustic class, and plotted on a digital aerial photograph. Aerial photographs courtesy of Land and Property Information, NSW.

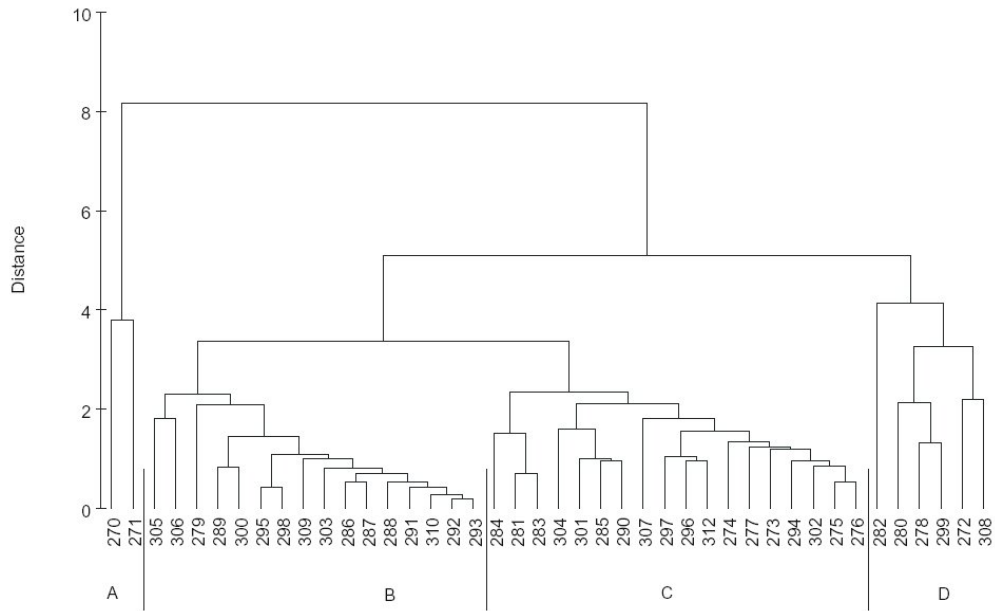


Figure 3.17. Cluster analysis dendrogram of the sediment data. Ground-truthing sample site numbers are shown on the x-axis. The four main cluster subgroups have been labelled Groups A-D.

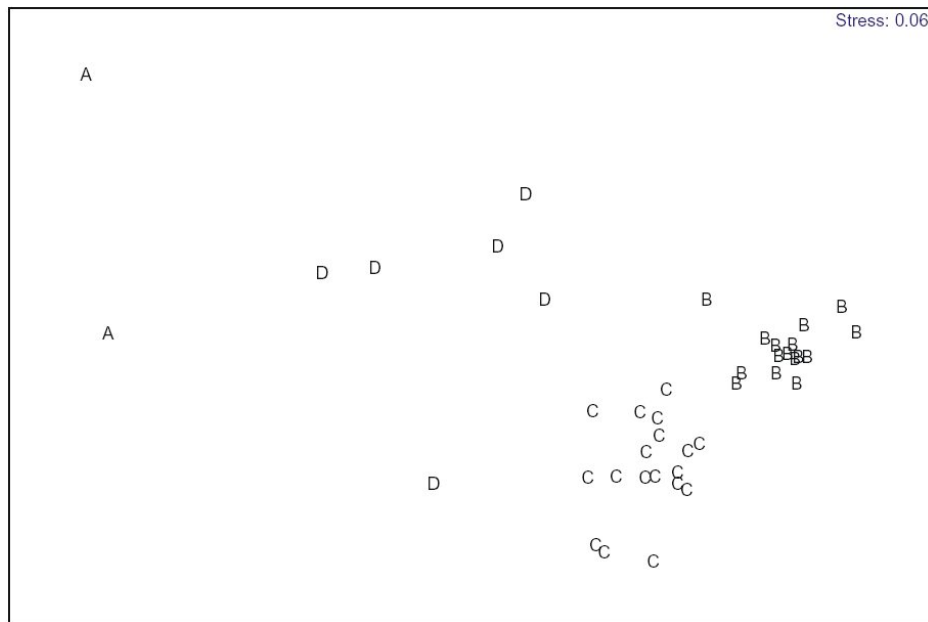


Figure 3.18. Multi-dimensional scaling plot (MDS) of the sediment data. The four main cluster subgroups, identified in Figure 3.17, have been labelled Groups A-D.

Statistical cluster analysis and multi-dimensional scaling were utilised to identify any physical similarities between groups of ground-truthing sites (Figures 3.17 and 3.18). The analysis revealed four distinct and mappable substrate types in the study area. These comprised dense, shelly sands, low density mud without shells, low density shelly mud, and poorly sorted muddy sand. Very little relationship between seagrass distribution and sediment type was detected. Cluster analyses and multi-dimensional scaling were also used to indicate the degree of association between acoustic classes and both sediment parameters and observed biophysical features (Figures 3.19 and 3.20). Groundtruthing sample sites were coded for acoustic class, based on their

proximity to the acoustic survey track lines. The analysis revealed that, based on the parameters measured, not all of the six acoustic classes were uniquely linked to distinct sedimentological facies, indicating that factors other than the sediment parameters influence the return acoustic signal. However, the well recognised estuarine sedimentary environments, such as marine sands and muddy basin sediments, are clearly delineated.

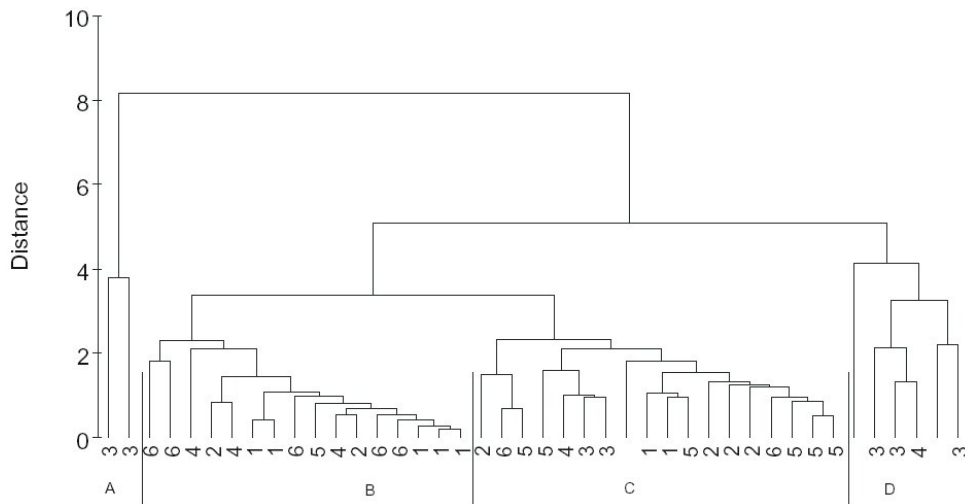


Figure 3.19. Cluster analysis dendrogram of the sediment data. Each sample is coded for acoustic class (Figure 3.15) on the x-axis. The four main cluster subgroups have been labelled Groups A-D.

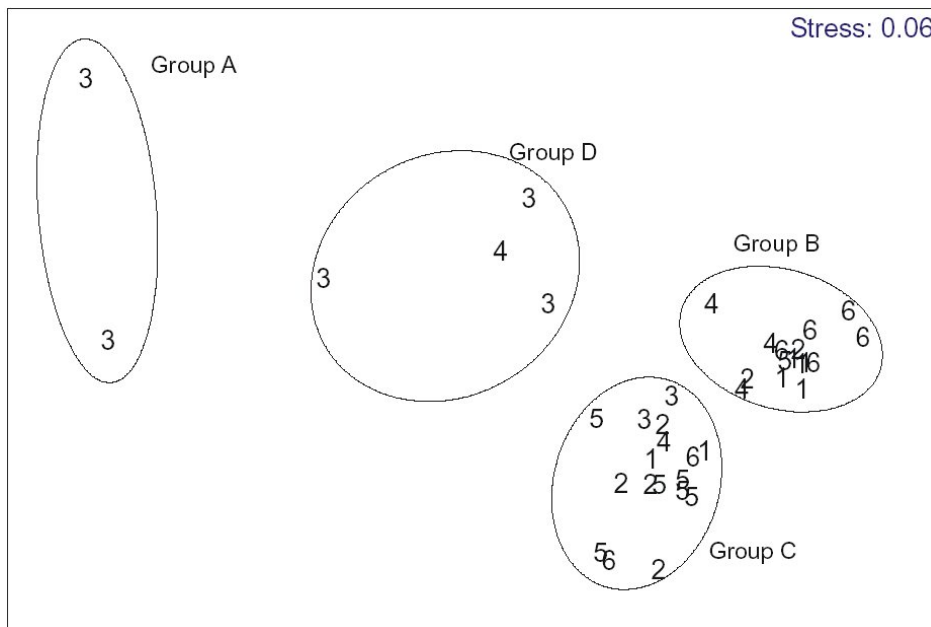


Figure 3.20. Multi-dimensional scaling plot (MDS) of the sediment data, also coded for acoustic class. The four main cluster subgroups, identified in Figure 3.17, have been circled (Groups A-D).

Much of the seagrass-dominated environments are limited to the shallow-water margins of the basin and channel areas. The wide central basin areas, such as Pipers Bay and the area west of Wallis Island, were dominated by very fine sediments with varying concentrations of shell material, and densely populated by various infaunal organisms. The channel areas, which form intricate networks in northern Wallis Lake,

were the deepest areas in the lake, and comprised relatively dense sandy muds and muddy sands, and also featured a high concentration of shell material. The marine tidal delta was also a distinct and mappable habitat, with clean well sorted sand, and dense seagrass beds.

The Quester-Tangent View Series 5 system demonstrated the ability to rapidly survey a relatively large and diverse area, to produce a coherent map of spatially homogenous acoustic classes. Although not all of the acoustic substrate classes could be identified in sedimentological terms, useful linkages were made between the acoustic classes and known estuarine sedimentary environments, illustrating that the Quester-Tangent acoustic mapping system is a useful tool for coastal management and research. The spatial interpretation of the Wallis Lake Quester-Tangent data represents the first quantification of non-seagrass habitats in the deeper areas of the lake, and provides a useful indication of benthic habitat diversity and abundance. For future studies, a more quantitative measure of faunal burrow size and density, and also other sedimentary bedforms, is recommended. Other unmeasured features of the lake bed may also have influenced the echograms, for example gas bubbles produced by plants or evolved from within surficial organic-rich muds.

3.5. The ECHO*plus* System

The ECHO*plus* (Bates and Whitehead, 2001a, 2001b) system appears to utilise a similar approach to that of the RoxAnn system, but is digital not analogue. It is noteworthy that the authors report a similar approach to coping with the apparent depth dependence exhibited by data from a number of RoxAnn implementations as had been adopted by CSIRO and Siwabessy (2001).

3.5.1. Principles of operation

A detailed description of the ECHO*plus* system is given by SEA personnel (Bates and Whitehead, 2001a; Bates and Whitehead, 2001b), below is a summary of this work.

ECHO*plus* is a digital version of RoxAnn (described in Section 3.3) produced by SEA (Advanced Products) Ltd. (Aberdeen, Scotland). Like RoxAnn, ECHO*plus* does not record the complete waveform, but instead measures the parameters E1 and E2 to characterise the acoustic roughness and hardness of the seafloor (see Section 3.3 for definitions). An advantage of ECHO*plus* over other acoustic ground discrimination systems (AGDS) available (e.g. RoxAnn, QTC View) is its capability of undertaking simultaneous dual frequency analysis. Moreover, the ECHO*plus* system attempts to compensate for common problems in single-beam surveys (identified in earlier sections), namely:

- Depth;
- Frequency;
- Power level; and,
- Pulse length.

Depth

If no compensating action were taken the ECHO*plus* outputs would depend on depth as both the echo return levels and the total absorption losses are depth dependent. In

order to compensate for the former a time varying gain is applied to the digitised voltages within the system. Because of the underlying geometry of the system, in particular the constant beam width of the transducer, this gain factor is a linear function of depth.

Frequency

Unlike other systems (e.g. QTC), ECHOplus automatically detects and operates with any echosounder within its operating range. In addition, ECHOplus has the facility to input and process two frequencies simultaneously. There is no requirement for user intervention to tune the system to a particular frequency. This is achieved by using wideband low loss front-end analogue hardware together with frequency estimation software. The centre frequency of the transmitter is estimated directly from the pulse waveform and used to control the analogue data acquisition and the digital base-banding when listening to receive echoes.

Power level

To compensate for power level, the pulse amplitude is measured by the system on every transmission and the estimated amplitude is used to scale the outputs accordingly. ECHOplus measures the *electrical* power at the output of the echosounder transmitter. This does not automatically relate to the *acoustic* power delivered by the transducer into the water column, as there are a number of sources of variation that cannot be compensated for including losses within the transducer cable, efficiency changes between different transducers and efficiency changes for the same transducer as a function of age. Apart from the final one, however, these will be constant for a particular installation.

Pulse length

The pulse length is measured and used to adjust the outputs accordingly. There are separate and independent corrections for roughness (E1) and hardness (E2) values. The measured pulse length is also used to tune the filtering process so that the signal to noise ratio and hence overall performance and reliability are optimised.

A potential drawback for scientific use is that the various compensations made by the ECHOplus system may unwittingly affect the parameters being measured. There is also no justification for assuming linearity between acoustic parameters measured with different frequencies or echosounder characteristics (Hamilton, 2001). In addition, there are other factors that may influence the output levels:

- Beam pattern and direction,
- Feed losses and impedance,
- Transducer transmit and receive efficiencies,
- Surface scatter.

ECHOplus, therefore, provides a reference calibration facility which can be set by the user post installation. These factors can be compensated for either by using this reference calibration facility on ECHOplus or via a similar function in the analysis software, if it has this capability. However, there is no work available that assesses this calibration facility.

3.5.2. Examples of using ECHOplus

ECHOplus was first trialled by SEA personnel (Bates and Whitehead 2001a; Bates and Whitehead, 2001b) in the sediment dominated Hopavågen Bay, Norway, from which it was concluded: “The results exhibit excellent correlation between acoustic bottom classes and ground truth data”. Although the hardness and roughness values obtained from the surveyed area indicated that ECHOplus can possibly distinguish between different grades of sediment, the study lacked a rigorous accuracy assessment. A better appraisal of the discrimination ability of ECHOplus can be seen in Riegl *et al.* (in press), which compares macroalgae surveys in the Indian River Lagoon in Florida using both QTC View and ECHOplus. Both systems were able to distinguish between seagrass-algae-bare substratum. A three-class confusion matrix based on QTC View surveys, suggested a total accuracy of around 60%. However, both systems showed high confusion when trying to discriminate two algae classes (sparse versus dense). When comparing the two systems, Riegl *et al.* (in press) conclude that: “ECHOplus appeared to give a somewhat clearer distinction, which could, however, largely be due to the way classes were assigned as binned intervals of the digital numbers provided by the ECHOplus, while in the QTC View system classes are assigned based on the position of signals in pseudo- 3-dimensional space after PCA”. To support this observation, the study would have benefited from producing a confusion matrix for the ECHOplus results as well.

Based on trials in 2000 (Anonymous, 2001a), the Archaeological Diving Unit based at the University of St. Andrews has purchased ECHOplus as a means of monitoring underwater sites to complement other methods including sidescan. An initial study by Lawrence and Bates (2001) showed statistically distinct clusters of E1-E2 data that were associated with the exposed archaeological material, which distinguished the wreck site from the surrounding seabed. However, it might be expected that a ground discrimination system can differentiate between artifacts and seabed, since their acoustic properties are likely to be very different.

3.5.3. Results from Lough Hyne, Ireland

This section summarises results of mapping sublittoral habitats of an Irish sea lough using ECHOplus, fully reported in Parnum (2003). The aim of this summary is to indicate the ability ECHOplus to distinguish between visually different habitats and the comparison of using subjective box classification with image processing techniques to classify the E1/E2 data.

Lough Hyne

Located on the south coast of Ireland, Lough Hyne Marine Reserve (Figure 3.21) is of great conservation, scientific and historic importance. It has been extensively studied and is known to have a very high species diversity and species richness for such a small area (Kitching, 1990). As part of a study to investigate the role acoustic techniques can play in mapping and monitoring the sublittoral habitats of Lough Hyne, an ECHOplus survey was performed in August 2003.

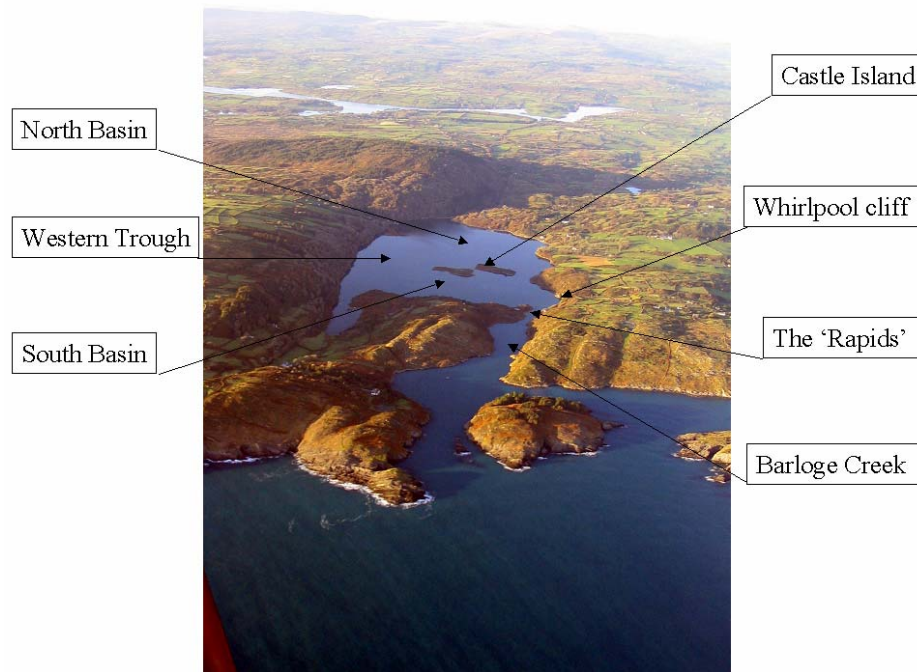
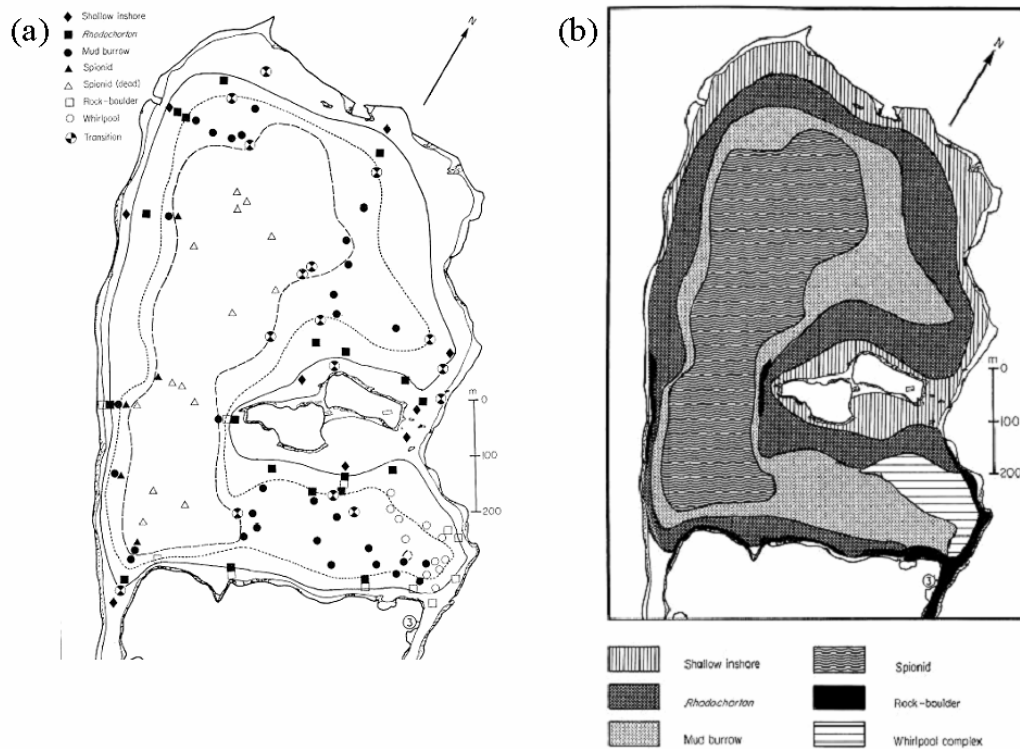


Figure 3.21. Lough Hyne Marine Reserve located on the south coast of Ireland (courtesy of John Rowlands, University of Wales, Bangor).

Lough Hyne is a deep landlocked bay or ‘marine lake’ joined by a narrow channel (Barloge Creek) to the sea. The actual embayment area (shown in Figure 3.21) is around 50 ha; Castle Island separates the two shallower (North and South) basins (20m), with the deepest area in the Western trough (50m). Lough Hyne's sublittoral habitats were first classified by Kitching *et al.* (1976) through a series of diver observations and grab sampling throughout the Lough. There were a total of 6 biotopes identified by Kitching *et al.* (1976), their descriptions, depth ranges, and maps of the point observations and subsequent contoured map of the biotope distribution can be found in Figure 3.22. From the work done by Kitching *et al.* (1976), it is evident that Lough Hyne is dominated by soft sediments. According to the authors, these soft sediment biotopes are depth-dependant, starting at just below the surface (3m) with a zone of the red algae *Rhodochorton floridulum* covering soft sediment down to 17m. Below the photoreceptive region is a characteristic *mud-burrow zone* between 17 and 25m. Below 25m the soft sediment becomes distinctly finer (clay/silt), and also contains large numbers of spionid tubes projecting from the surface. Soft sediment was only found to be replaced by coarse or hard substrate in areas of fast moving current such as the Rapids and Whirlpool area, or on underwater cliffs or in very shallow water. Although Lough Hyne is relatively small and despite the authors’ extensive experience surveying the lough over a number of years, it is hard to give great confidence to the actual position of the point observations as there was no form of geo-referencing in the data. Furthermore, although depth is an important factor on the distribution of biotopes, in reality patchiness of the ground and occurrence of intermediate biotopes due to overlapping, means the contoured map generated by Kitching *et al.* (1976) is unlikely to be precise. Therefore, the results from Kitching *et al.* (1976) have to be taken as a broad distribution of biotopes present at the time of study.



Biotope	Description	Depth range
Shallow inshore	Boulder slopes, either bare or covered in green algae such as <i>Enteromorpha</i> spp. And <i>Stilophora rhizodes</i> .	< 5m
Rhodochorton	A blanket of the filamentous red algae <i>Rhodochorton floridulum</i> covering soft sediment (mud).	3-17m
Mud burrow	A zone of bare mud with many burrows, believed to be the work of various organisms, for example: the decapods <i>Nephrops norvegicus</i> and <i>Calocaris macandreae</i> .	17-25m
Spionid	Large numbers of spionid tubes protruded from the very fine sediment (clay/silt) found in this region.	>25m
Whirlpool complex	Coarse sediment found near Whirlpool cliff resulting from transport from the nearby rapids.	<25m
Rock boulder	Solid bedrock	<20m

Figure 3.22. Biotope distribution of Lough Hyne as (a) observed, and as (b) continuous coverage generated by Kitching et al. (1976). See table for biotope descriptions and depth ranges observed by Kitching et al. (1976) in the lough.

Other ground truth information available includes diver transects performed across the South Basin by Thrush and Townsend (1986), which confirms the distinctly different habitats found in the middle of the South Basin (soft sediment) compared to near to the entrance to the Rapids and Whirlpool cliff (coarse gravel-like sediment). Also, an alternative substratum map of Lough Hyne was presented by Wilkins and Myers (1990) as part of their study on the distribution of gobies in the lough. Again this was constructed through diver observations, however, there was no raw point data to assess the accuracy and confidence that can be given to the map. Another source of

information, for this study, on the distribution of benthic habitats in Lough Hyne came from diver observations by Turner¹ (personal communication).

Classification of sublittoral habitats

Marine biotopes for the northeast Atlantic have been described and classified as part of the Joint Nature Conservation Committee (JNCC) Marine Nature Conservation Review (MNCR) by Connor *et al.* (1997). This classification system has been adopted by both the British and Irish conservation agencies. Therefore, it was appropriate to adopt this system to classify the different sublittoral habitats found in Lough Hyne. From the diver observations and grab sample records in previous studies (as mentioned above), Lough Hyne's sublittoral habitats were separated into 5 'Habitat Complexes' described by Conner *et al.* (1997). These habitat complexes were fine sediment (mud), mixed sediment (predominately shell and mud), macrophyte dominated sediment (e.g. *Rhodochorton floridulum* on mud), coarse sediment (i.e. gravel) and rock. In addition, a further habitat complex was added to accommodate the observations of Kitching *et al.* (1976) and Turner (personal communication) that in the centre of the Western Trough below 25m there is distinct transition from fine cohesive sediment (mud) to much finer fluid-like sediment. This fluidised fine sediment, which is commonly found in some ports, was given the code SFluid. Table 3.1 details these 6 habitat complexes with their biotope code and depth ranges observed by Kitching *et al.* (1976).

Table 3.1. Habitat complexes observed in Lough Hyne as described by the JNCC Biotope Marine Classification System (Conner *et al.*, 1997), with their assigned habitat/biotope code and the depth ranges in which they are generally found according to Kitching *et al.* (1976). *Fluidised fine sediment is an additional habitat complex not found in the JNCC classification system.

Substrate	Sublittoral (S) Habitat/Biotope code	Depth Range (m)
Rock (including boulders)	SR	<25
Coarse sediment (gravel)	SCs	<25
Mixed sediment (predominantly a shell-mud complex)	SMx	<17
Macrophyte dominated sediment (predominantly <i>Rhodochorton floridulum</i> on mud)	SMp	<17
Soft sediment (cohesive mud)	SMu	17-25
Fluidised fine sediment*	SFluid	>25

ECHOpus data acquisition & processing

The ECHOpus system utilised a Raytheon DE-719B echosounder operating at 210kHz, with a sampling rate of 9Hz and 8° beam width. The ECHOpus survey took place on the 3rd August 2003. As the area was well known (by the navigator) the track spacing and navigation employed aimed to record the extent of the different biotopes. A track plot of the ECHOpus survey can be found in Figure 3.23 (only data used in classification shown). There were a limited number of useable acoustic returns obtained from deeper areas (>25m), in particular, in and around the Western Trough. This was due to a combination of the high frequency of the sounder, the limited sounder power available, the presence of steep slopes leading into deeper areas, and

¹Dr. J.R. Turner is a Senior Lecturer in Marine Ecology at the School of Ocean Sciences in the University of Wales, Bangor and has dived Lough Hyne extensively over a 20 year period.

the low reflection coefficient of the very soft bottom sediments found in the deeper areas. Also, strong water currents coming in from the rapids generating bubbles by Whirlpool Cliff prevented the ECHOpus system working effectively. Similar problems were encountered from a different sounder in a separate single-beam bathymetric survey performed the previous day.

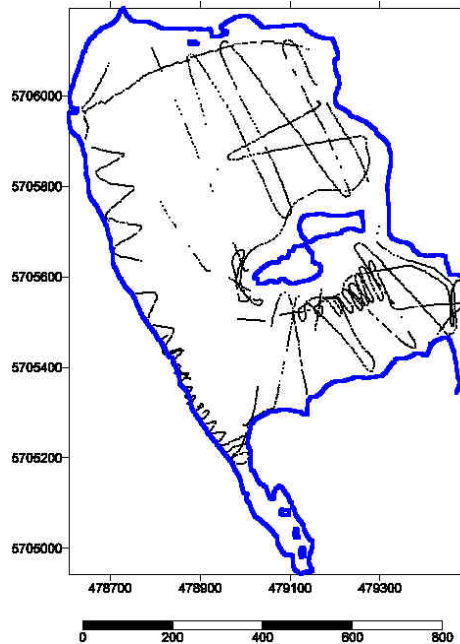


Figure 3.23. A track plot of the ECHOpus survey (minus the anomalies removed) performed at Lough Hyne during August 2003.

After the survey, ECHOpus data was imported into a spreadsheet, where all erroneous data possibly due to: hardware failure, bad bottom-pick, steep slope or strong water current were removed. These were usually indicated by incorrect depth values (e.g. 500m), or where large deviations (>10%) occurred outside the general run of observations. Also, where the seabed had not been detected a default readings for the depth, E1 or E2 were given, and these were removed. The "clean" data was corrected to standard datum using a tidal correction over the same time period from a tidal gauge deployed in the lough. Then data was converted into Easting and Northing (UTM WGS84 northern region 29). The clean and edited E1 and E2 data were independently interpolated using the Kriging algorithm in *Surfer*, both with a 2m grid size, and using a blanking file added to distinguish Lough Hyne's coastline, shown in Figure 3.24.

Classification of ECHOpus data

The objective of the classification of sublittoral habitats of Lough Hyne was to provide a broad scale distribution of habitat complexes found in the lough. The lack of geo-reference ground-truth points limited any attempt to carry out supervised classification of ECHOpus data. Therefore, unsupervised classification was used. The individual E1 and E2 distribution maps (Figure 3.24) indicated that neither 'hardness' nor 'roughness' independently would be suitable for classifying the seabed. Thus, it was optimal to use both E1 and E2 together to classify Lough Hyne's sublittoral habitats. The two methods used were:

1. Subjective box classification
2. Cluster analysis of False Colour Imagery (FCI)

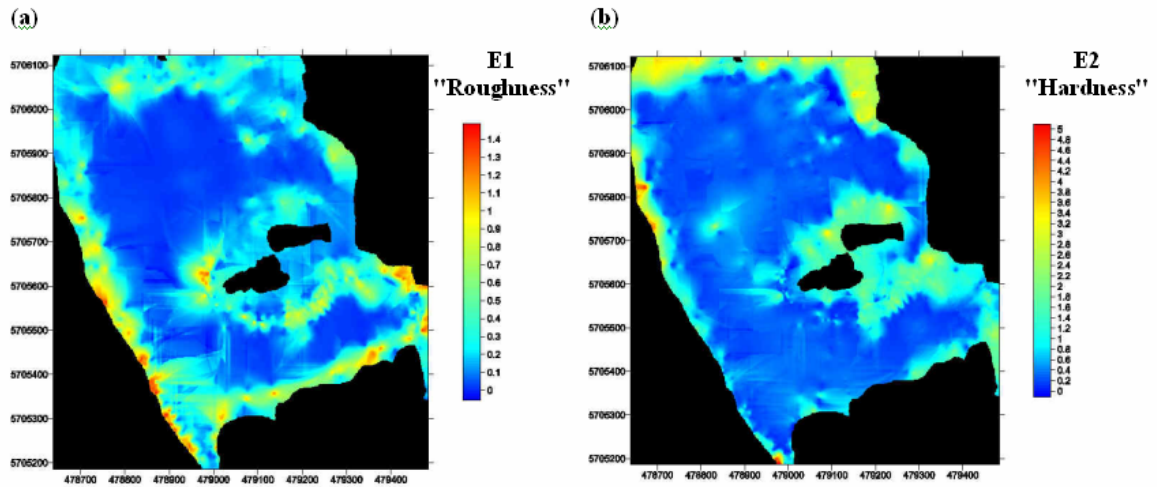


Figure 3.24. Results of the ECHOpus survey of Lough Hyne in August 2003 (a) E1-Roughness and (b) E2-Hardness. Values interpolated using Kriging with a 2m grid and the coastline blanked (black).

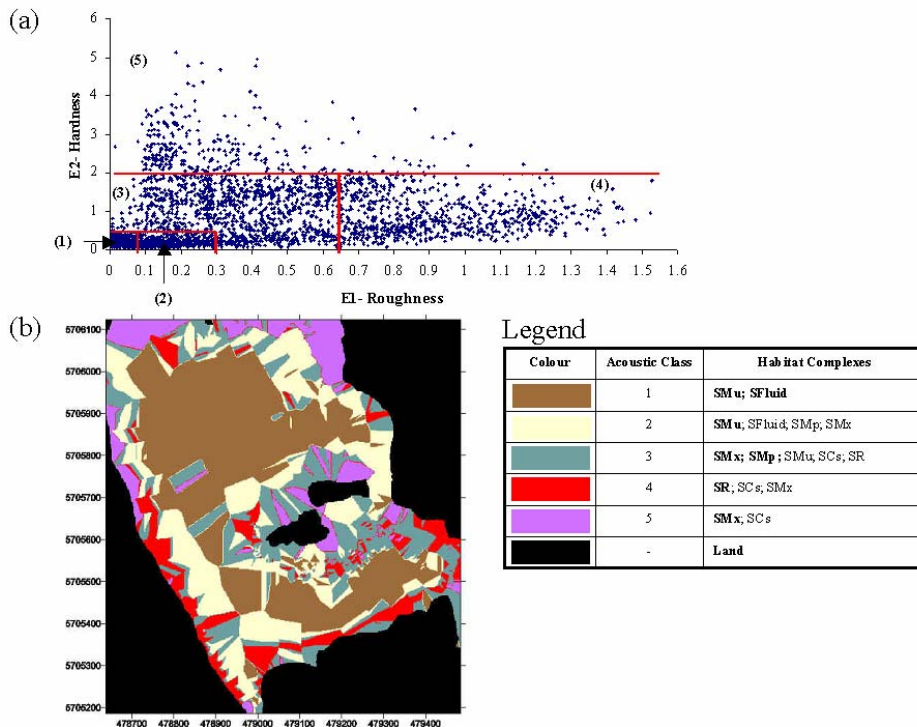


Figure 3.25. Unsupervised classification of sublittoral habitats of Lough Hyne using (a) subjective box clusters placed on the scatterplot of E2 against E1 obtained from an ECHOpus survey in August 2003; giving (b) the resulting distribution of "acoustic classes" interpolated using the nearest neighbour algorithm in Surfer™. The 5 acoustic classes produced are assigned habitat complexes that they cover (the principle ones in bold) using the codes listed in Table 3.1.

Subjective box classification of ECHOpus data

The unsupervised classification of Lough Hyne's sublittoral habitats using subjective box classification, is presented in Figure 3.25, which shows the scatter plot of E1 and

E2 obtained from the ECHOplus survey of Lough Hyne with the subjective boxes placed over 'clusters' of points, and the classified points interpolated using nearest neighbour to produce the classified map. There are an infinite number of combinations of boxes, and the final version represents a compromise between the number of habitats present and the number of 'clusters' that can be successfully represented by using boxes. Thus, the classified map produced in Figure 3.25, is better thought of as the distribution of acoustic classes rather than habitat complexes. Nevertheless, acoustic classes 1, 4 and 5 appear to represent the soft sediment, rock and mixed sediment habitats reasonably well. However, acoustic classes 2 and 3 cover most habitat complexes present in the lough. Although through an iterative process these classes could be refined, the inappropriate nature of using boxes to cluster points would eventually limit any discrimination of habitats present.

Cluster analysis of False Colour Imagery (FCI)

Cluster analysis of False Colour Imagery based on the methods used by Sotheran *et al.* (1997) (given in more detail in Foster-Smith *et al.* (1999) and Greenstreet *et al.* (1997)), was also used to classify the ECHOplus data. Using image processing software (ERDAS™) the interpolated E1 and E2 raster images (Figure 3.24) were stacked into one False Colour Image (retaining the 2m grid size). Then unsupervised classification using the ISODATA algorithm was performed, data were first clustered into 6 acoustic classes in an attempt to match the number of sublittoral habitat complexes that are known to be present (Figure 3.26). As for the box classification above, the fine sediment, rock, and mixed sediment appear to be well represented, here, in acoustic classes 1, 4 and 6 respectively. In addition, acoustic class 3 appears to represent the macrophyte dominated regions found from sample points by Kitching *et al.* (1976), however, there are a few misclassified regions in deeper areas where there will be an absence of algae. Despite acoustic class 5 representing some areas of known coarse sediment, in particular, in the Rapids/Whirlpool area and adjacent to cliffs sections, it also indicates areas of mixed sediment, e.g. around Castle Island and in the shallower regions of the North Basin. Furthermore, there is no distinction between cohesive soft sediment (mud) and the fluid fine sediment found in the Western Trough, with class 2 representing the same habitats as class 1. It is worth noting, that the inclusion of depth as a third layer in the FCI was tried in the classification procedure, however, this produced a classified image that related more to depth contours than to biotope distributions.

Overall, the classification of habitats using cluster analysis of FCI appears to be more representative and plausible than the subjective box classification method. Consequently, Figure 3.26 was chosen to be further enhanced, first by combining class 1 with 2, and class 5 with 6 to produce a new map shown in Figure 3.27. Despite this improvement to the accuracy by combining classes, contextual editing was required. In particular, known areas of soft sediment found in deeper water were misclassified as mixed sediment, macrophyte dominated sediment or rock. Misclassification in deeper water has occurred in other surveys using AGDSs (Hamilton, 2001; Kenny, 2000). The nature of sound scattering from steep slopes and the low acoustic impedance of the fluidised fine sediment found in the deeper water of Lough Hyne are the most likely source of misleading E1 and E2 values. After contextual editing, the final classified image of the distribution of sublittoral habitat complexes in Lough Hyne and can be seen in Figure 3.27.

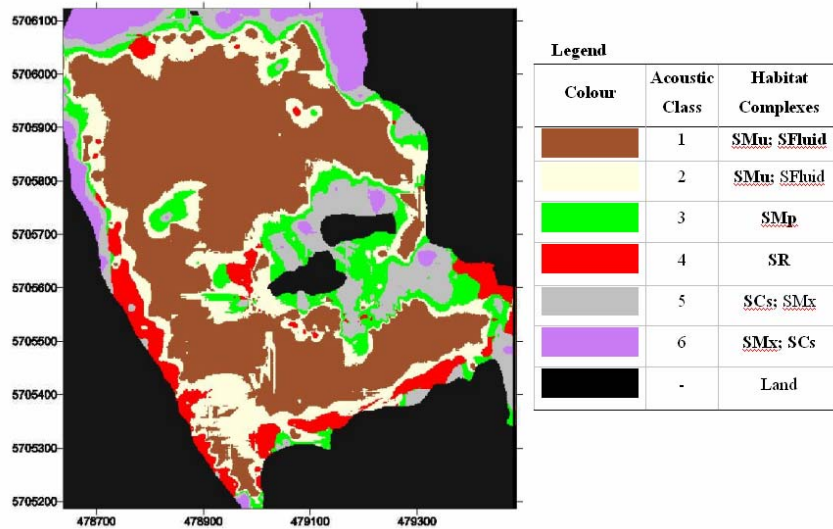


Figure 3.26. Unsupervised classification of sublittoral habitats of Lough Hyne using cluster analysis of a False Colour Image composed of E1 and E2 values obtained from an ECHOpus survey performed in August 2003. The 6 acoustic classes produced are assigned habitat complexes that they cover (the principle ones in bold) using the codes listed in Table 3.1.

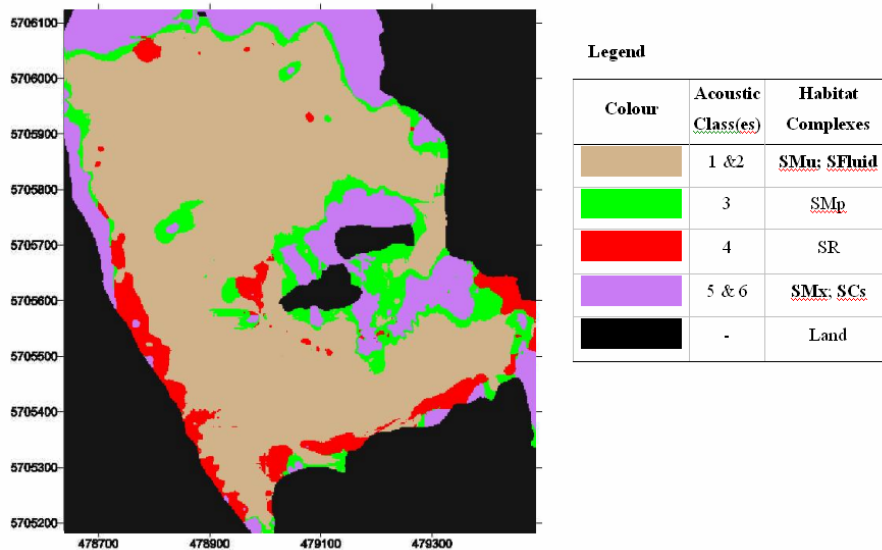
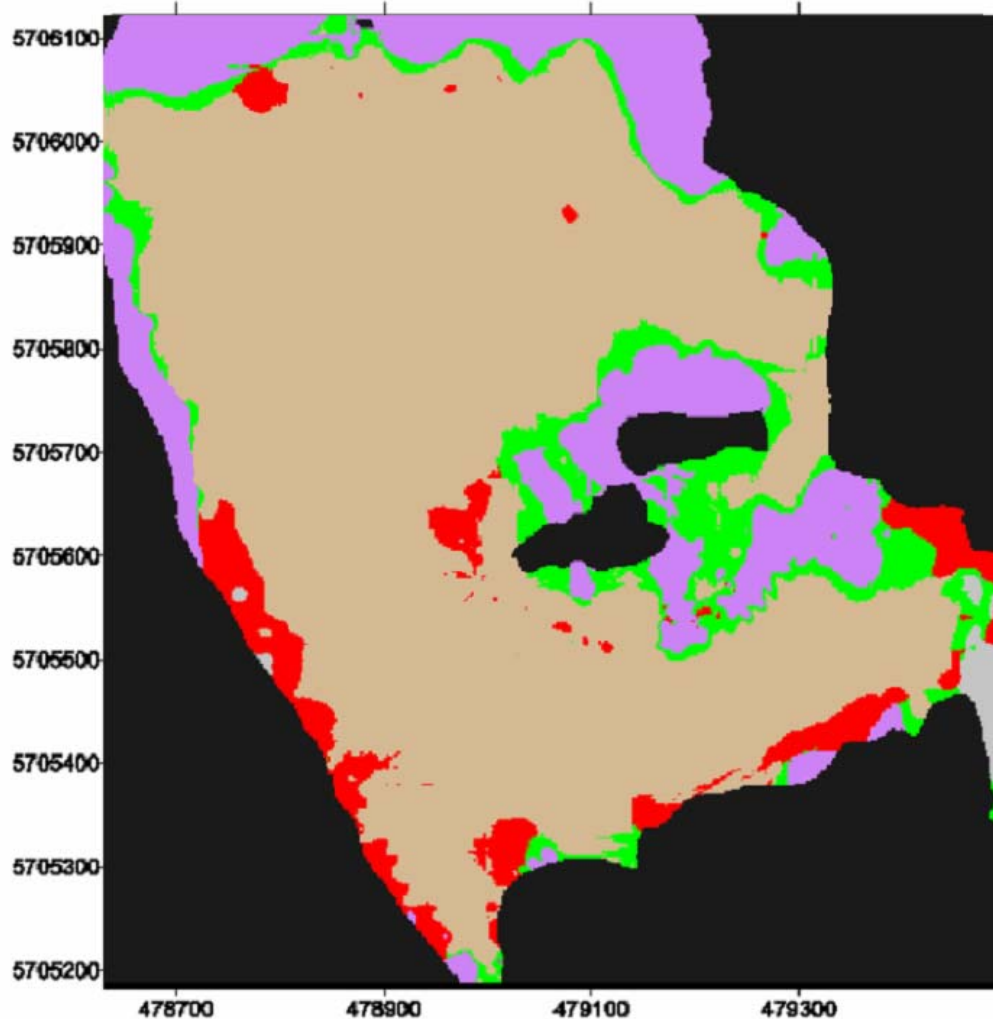


Figure 3.27. The 6 acoustic classes from Figure 3.26 are reduced to 4 'habitat' complexes that they cover using the codes listed in Table 3.1.

The final classified image of the sublittoral habitat complexes found at Lough Hyne (Figure 3.27) agrees well with previous studies (Kitching *et al.*, 1976; Thrush and Townsend, 1986; Wilkins and Myers, 1990; and Turner, personal communication), which is maybe to be expected as these studies were used to classify and help in contextual editing. However, as the point data in this study was interpolated using more sophisticated geo-statistics than subjective contouring round diver observations (as in previous maps), the map's distribution of habitats has a more natural look and is less contrived than previous maps produced. Nevertheless, without a formal accuracy assessment (which was not possible) the habitat map produced in this study (Figure 3.27) cannot be shown or concluded to be more accurate than any previous efforts. Moreover, as the habitat maps have been produced from unsupervised classification

of interpolated remotely sensed data, they are not definitive like a road map, but are predictive distributions of habitats known to occur there. Therefore, there will always be a large degree of uncertainty associated with these types of habitat maps.



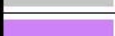
Colour	Acoustic Class(es)	Habitat Complex(es)
	1 & 2	Soft sediment (SMu) or Fluidised fine sediment (SFluid)
	3	Macrophyte dominated sediment (SMp)
	4	Rock including boulders (SR)
	5	Coarse sediment (SCs)
	5 & 6	Mixed sediment (SMx)
	-	Land

Figure 3.28. Unsupervised classification with contextual editing of sublittoral habitats of Lough Hyne.

Despite these concerns over accuracy and misclassification of the classified image produced, the study does conclude that using cluster analysis within image processing software is a more robust and repeatable method than using subjective box clusters to classify AGDS data. A conclusion that is shared by other authors (Foster-Smith *et al.*,

1999; Fox *et al.*, 1998; Greenstreet *et al.*, 1997). However, a drawback of this technique is that the original data is not preserved, furthermore, spatial interpolation between tracks (as done for both methods here) implies a knowledge of bottom type there which does not exist, while along track smoothing to achieve regular pixel sizes may remove real changes (Hamilton, 2001). Finally, as this study had to employ unsupervised classification, future work that obtains geo-referenced ground truth data from Lough Hyne, could develop signatures of E1 and E2 (and possibly depth) to perform supervised classification on the ECHOplus data to produce a more reliable habitat map and a better appraisal of ECHOplus.

3.5.4. Conclusions

The limited examples of the use of ECHOplus hinder a thorough assessment of the system's performance in seabed discrimination. In particular, more comparisons of ECHOplus with other systems (e.g. RoxAnn and QTC) would be beneficial. Also of value would be studies that utilise its dual frequency capability, which is an advantage of the system. Siwabessy (2001) showed that having multiple frequencies increases the discrimination ability, as different scales of seafloor roughness and levels of seafloor volume contributions are being examined simultaneously, thus, exploitation of this feature could optimise the use of ECHOplus. Nevertheless, from the limited examples available, ECHOplus does seem to provide good discrimination between noticeably different seafloor types (e.g. rock, algae and sand). However, more subtle changes in seafloor habitat (e.g. sparse versus dense algae cover) are perhaps not picked up. Furthermore, misclassification can occur in deeper water (as with RoxAnn), this is can be mainly attributed to the nature of the scattering of sound from rougher bottoms and its effect on the E1/E2 parameters (Hamilton, 2001). The biggest shortcoming of ECHOplus (and other systems) is that the raw waveform is not recorded. As useful as E1 and E2 parameters are, they are no substitute for the complete echogram, which can be used to identify bad bottom-picks (e.g. due to mid-water reflectors) and perhaps to derive other acoustic parameters from either the seafloor (e.g. rise time) or water column (e.g. fish).

3.6. Comparisons of Systems

Hamilton *et al.* (1999) compared performance of the RoxAnn and QTC View systems in the Cairns area of the Great Barrier Reef lagoon. QTC outperformed RoxAnn, but one outcome of the resulting analysis was that RoxAnn results were consistent only when obtained at constant speed. This was contrary to the manufacturer's prescriptions which specify that any speed can be used. However any system may be subject to ship noise and aeration. QTC results did not appear to be speed affected, but insufficient data was obtained for RoxAnn within any particular speed band to draw any real conclusions. One interesting result was that Hamilton *et al.* (1999) were able to obtain a direct mapping of QTC classes to RoxAnn space.

Smith *et al.* (2001) did not find much difference between QTC View and RoxAnn when searching for oyster beds. Both systems performed well, although tests were not comprehensive.

In 2001, a report describing a comparison of the RoxAnn and QTC View systems appeared (Foster-Smith *et al.*, 2001). This work emerged from an extensive multi-year

British program funded by the UK Department for Environment, Food and Rural Affairs and the Crown Estate. The report, and its companion document Brown *et al.* (2001) describe acoustic biotope assessment in four areas off the southeast coast of England. A significant component of the motivation for the work was to facilitate mapping of gravel sites. Three study regions were of 48 sq km area and one had area of 336 sq km. The two lengthy reports arising from this work constitute a valuable resource for the conduct of echosounder based benthic classification, both for location of gravels and related substrate types and for more general classification requirements.

Foster-Smith *et al.* (2001) concluded that there was little difference between the performance of RoxAnn and QTC View, although the detailed conclusions throughout the report favoured RoxAnn. It is noteworthy that the authors do not report the depth dependent parameter variation discussed in Section 3.3 above. It appears that the depth ranges involved always enabled a second return to be gained, as no reference exists in the reports to the loss of the second echo. The availability of a second echo is central to the RoxAnn technique and not relevant to QTC View. In this regard, QTC View does not offer an advantage over RoxAnn in relatively shallow water operation.

4. SIDESCAN SONAR

4.1. Introduction

When considering the range of acoustic techniques available for seabed mapping and classification, there is a significant step between technologies that provide information about discrete points along a line below the vessel such as single beam sounders and sub bottom profilers and swath type technologies such as sidescan sonar and multibeam systems.

In the operation of a single beam sounder, the time to first return is used to provide the depth below the vessel and from analysis of the subsequent backscatter, parameters relating to the nature of the seafloor can be derived. No matter how large the footprint of the acoustic beam is however (which is a function of depth and transducer angle), only a single set of parameters for each acoustic transmission can be obtained, as discussed above. In the case of backscatter analysis, often the return from a number of 'pings' are averaged to derive a value for the 'roughness' and 'hardness' of the seabed. The values obtained are taken as being for a single position below the vessel and surveys therefore provide a line of discrete points along the vessels track for which a number of parameters such as depth, hardness and roughness have been derived for each point. The spacing of these points is a function of the depth, vessel speed and number of pings used to calculate the required parameters. The situation is similar for sub bottom profilers that use a combination of power and low frequency to penetrate the seabed to provide information about the structure and nature of the substrate below the surface. The returns from each ping from a sub bottom profiler are also used to generate information about a single point below the vessel and are built up into a continuous track line. Swath technologies differ fundamentally from single beam sounders and sub bottom profilers in footprint shape and in that they provide spatially referenced information about the variability of recorded parameters from within the footprint (Figure 4.1).

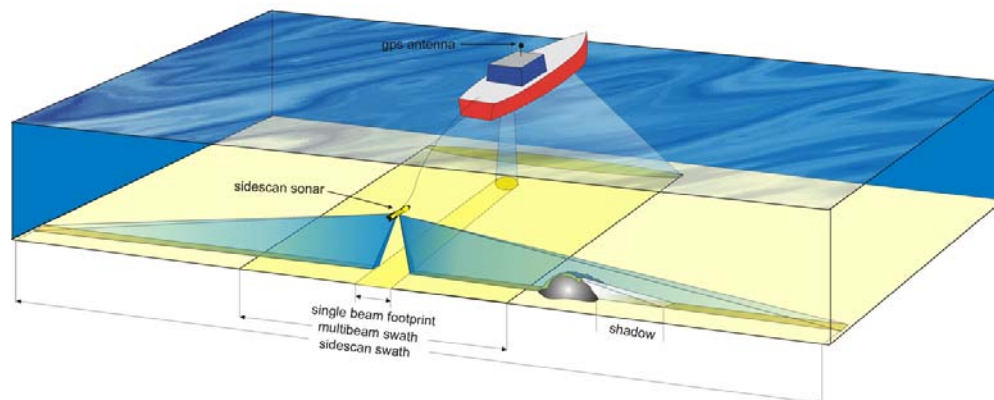


Figure 4.1. Comparison of coverage between acoustic mapping technologies.

The two fundamental products of bathymetry and backscatter produced by single beam systems are also however the basic products of swath technologies. Swath technologies are typically divided into two main types of equipment; sidescan sonars and multibeam sonars. Although this chapter is dedicated to a review of activities

relating to sidescan sonars some comparisons and discussion of their relative merits are necessary. Sidescan sonars and multibeam systems are often used in unison to gain complementary data sets, but recently the uses and types of information provided by multibeam and newer interferometric sidescan equipment have converged. To briefly introduce a comparison of swath systems it can be said that traditionally sidescan sonars provide only backscatter data and little information about depth forming a wide, often almost photo realistic image of the seabed (Figure 4.2).

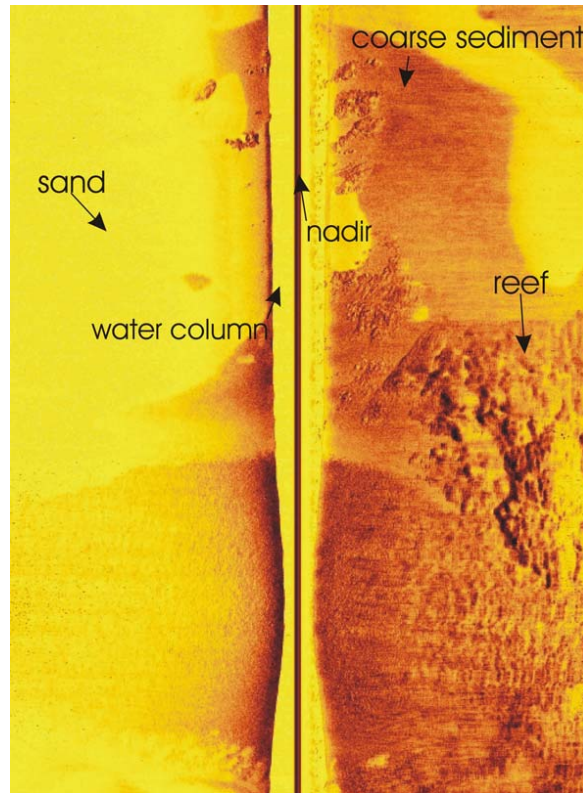


Figure 4.2. Example raw 'waterfall' sidescan record.

The primary product of multibeam sonars however is bathymetry and although backscatter is also recorded, the imagery acquired is generally accepted to be of a lower quality than that recorded from sidescan sonars. Recently however, sidescan sonars known collectively as 'interferometric sonars' that can provide depth information are becoming more popular. The crux of the comparison between multibeam systems and sidescan sonars was recently eloquently stated by Lloyd Huff at a 2004 University of New Hampshire workshop attended by Australian researchers, "Multibeam manufacturers are trying to provide better quality backscatter and sidescan manufacturers are trying to provide bathymetry".

As the subject of this review document is 'seabed classification', the means of processing and classification of the information acquired is also addressed, although it should be noted that sidescan sonars are rarely used as a single technique for this purpose. At minimum the acoustic records of sidescan sonars are validated using direct sampling techniques such as video or still photography or direct geophysical and biological sampling by grab, but are often used in conjunction with multibeam or single beam sonars and sub bottom profilers.

The following sections describe the two types of sidescan systems available with reference to selected manufacturers, specific models and published literature. Software used for processing, classification and visualisation is discussed. The choice of examples used and any omissions does not necessarily reflect any bias in the choice of equipment or preferences of the author. It is outside the scope of this document to compare all the equipment available and to provide an exhaustive list of all the work and research that has been carried out and published. The discussion is also generally limited to that relevant to surveys of continental shelf type depths, with a bias towards ‘habitat mapping’ type work carried out in Australian coastal waters.

4.2. Basic Sidescan Sonar Operation

Basic sidescan principles are covered well in Blondel and Murton (1997), and Fish and Carr (1991), although there have been many recent advances in personal computer based digital acquisition and processing packages since their publication. Sidescan sonars typically consists of two transducers mounted either side of a vessel, ROV, AUV or more commonly, a towed body or ‘fish’ (Figure 4.3).



Figure 4.3. Typical sidescan sonar fish.

Each transducer produces a thin fan shaped beam that is concentrated on a thin line that runs from below the fish perpendicular to the direction of travel out to a maximum range that is restricted by frequency, power and transducer design (Figure 4.1). As the pulse of sound emitted by the transducers interacts with the seafloor at angles off normal, most of the energy is reflected away from the transducer. The acoustic backscatter that is reflected back to the transducer from the seabed is recorded for an extended period of time for each ping forming a time series of amplitudes. Using the vessels position, speed of sound in water, and the height off the bottom, the position on the seabed can be predicted for any point on this time series and a line of instantaneous backscatter amplitudes can be created that is referenced to positions along the beam footprint on the seabed. This short statement however belies the range and complexity of corrections that are made to the image at this stage to compensate for various geometric and radiometric distortion.

As the transducers move through the water, the lines of data recorded from each subsequent ping are formed into an acoustic image of the area. An example of a typical raw ‘waterfall sidescan image is shown in Figure 4.2.

This image is a record of the instantaneous intensity of the backscatter and is affected by the following factors, in decreasing order of importance (after Kvitek *et al.*, 1999).

- Sonar frequency (higher frequencies give higher resolution but attenuate more quickly with range than lower frequencies)
- The geometric relationship between the transducer and the target object (slope)
- Physical characteristics of the surface (texture)
- Nature of the surface (composition, density)

The vessel can then be manoeuvred to obtain the desired coverage of the seafloor from successive tracks. Although historically sidescan sonar records have been recorded on thermal paper printouts (Figure 4.4), most manufacturers (and a number of aftermarket equipment suppliers) offer sophisticated digital acquisition systems with advanced features.



Figure 4.4. Sidescan sonar thermal paper recorder.

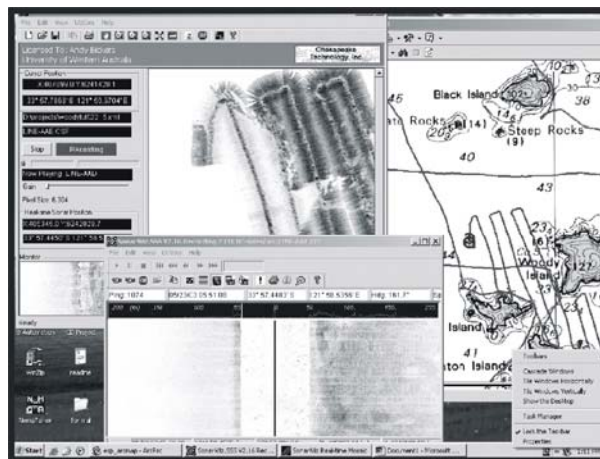


Figure 4.5. Display from sidescan digital acquisition system.

Whilst surveying, these systems offer a number of ways to view the acoustic imagery live whilst surveying. The raw data obtained is displayed as a ping by ping record known as a waterfall. Using an input from a GPS, this raw data is positioned correctly in geographic space and live ‘mosaics’ can also be produced building a composite image of the seabed superimposed on charts as the survey is underway (Figure 4.5).

The current generation of digital acquisition software therefore function as navigation aids for the survey assisting the vessel in following defined survey lines, ensuring the required coverage is obtained and avoiding obstacles.

Sidescan systems are available from a number of manufacturers. These units vary in terms of frequency or combination of frequency and configuration (towed or vessel mounted, digital or analogue). High end systems also provide special features such as focussed beams, high tow speeds, chirp technology (wide frequency range), synthetic apertures or in the case of interferometric systems, the ability to obtain bathymetry. The latter are considered here as a special case and are described in a later section.

4.3. Considerations in Sidescan Sonar Operation

Before discussing available equipment, it would be prudent to introduce some concepts, compromises and drawbacks relating to the use of sidescan sonar. A good introduction to the practicalities of using sidescan sonar can be found in Bennell (2001) and Kenny *et al.* (2003).

4.3.1. Frequency, range and resolution

Typical frequencies of sidescan sonars used in nearshore mapping range between 100 and 500kHz. Although higher frequencies can provide maximum resolution of approaching a few cm, their ranges are significantly more limited than that at lower frequencies. At 100kHz maximum ranges are typically around 200 to 300m per transducer, forming total swaths widths of up to 600m, with a typical maximum resolution of 0.15m. At 500kHz ranges would be reduced to 75m per side, but with increased resolution. The choice of frequency has obvious ramifications for survey planning.

4.3.2. Survey planning

The great utility of sidescan sonar is the wide swath and surveys may attempt to exploit this to provide the fastest coverage of an area. There are however a number of considerations that must be made that depend on a trade off between the financial resources available and the quality and coverage of data that is required. The resolution vs range compromise is discussed above, but as the beam angles of the transducers are typically fixed there are also a range of geometric considerations affecting coverage that must also be considered. The first of these is that the transducers are angled so that the fish is effectively blind to an area each side of the 'nadir, the centre line of the direction of travel (Figure 4.6).

Theroretically this means that if full coverage of the seabed is required swaths must be overlapped by at least 50% to achieve 100% coverage. Often however full coverage is not necessary to gain the required information relating to boundaries on the seabed and swaths are typically overlapped by 20 to 30%. The second is that to achieve the maximum coverage possible, the transducers must be a suitable height above the seabed (between 10 to 20% of the swath width). Should this height off the bottom not be able to be achieved, for instance where the water is too shallow, the swath width will be reduced from maximum and will be typically a multiple of water depth. For most 100kHz systems this multiple is about 10 per side with swaths widths

maximized at 200m per side with the fish traveling 20m from the seabed. There are therefore water depths at which the use of higher frequencies will not compromise range.

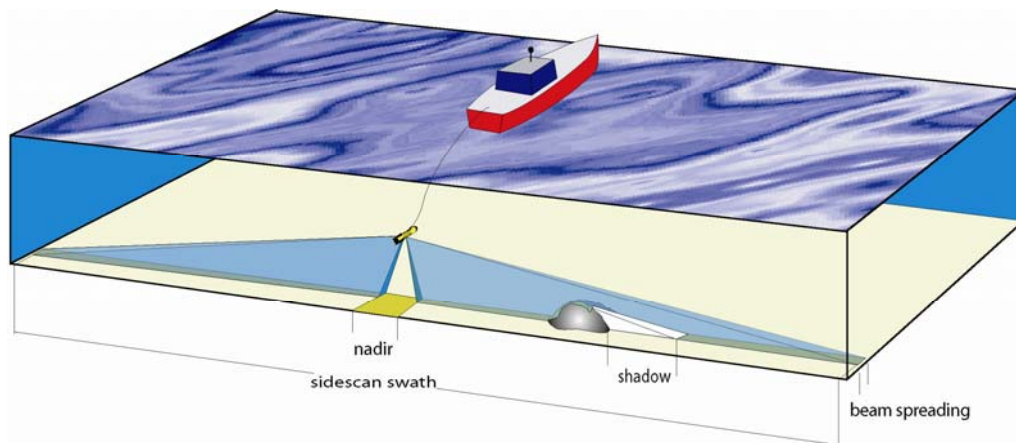


Figure 4.6. Beam pattern of sidescan sonar.

Unsurveyed blind spots are also caused by acoustic shadows behind high relief terrain (Figure 4.6). These shadows become larger at larger ranges. To obtain full coverage the seabed must be ensonified in two directions and overlaps between subsequent swaths must be 100%. A further consideration when planning survey tracks must be made which relates to the spread of the beam with range (Figure 4.6). This has the effect that imagery of similar features obtained at far ranges appears quite different than that obtained at near ranges. Because of this effect, the requirement for high quality imagery often limits the range that can be used in a survey. This effect is exacerbated when the fish is subject to movement. A bad example of this effect is shown in Figure 4.7 where seagrass hummocks appear quite different in the near range than the far range of a raw sidescan record.

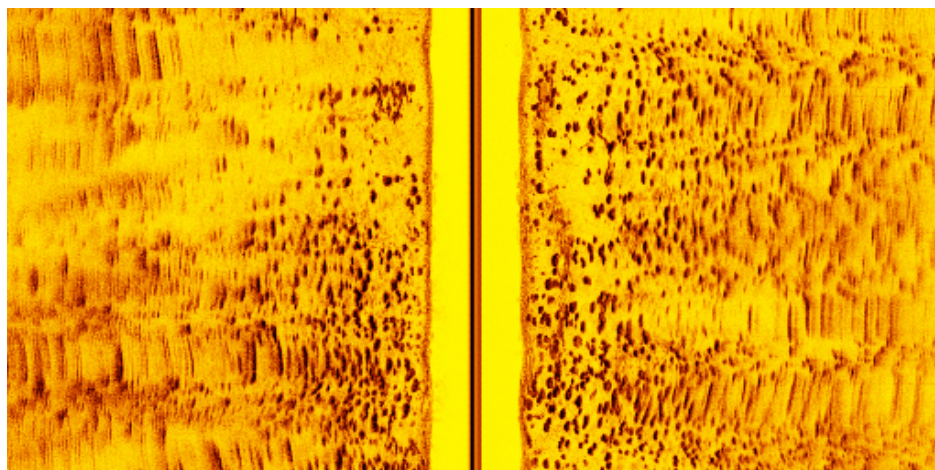


Figure 4.7. Sidescan sonar image of seagrass hummocks exhibiting beam spread in far ranges.

4.3.3. Survey speed and ping rates

The survey speed is also a consideration when planning surveys. The ping rates of equipment are selected by the operator and are generally limited by the range in use. For longer ranges, the backscatter signals will take longer to be received and the

delays between pings will be greater. This also means that along track resolution of data will be less than for data obtained at similar speeds with lower ranges. A compromise must be reached where the survey speed is maximized but the required data quality is achieved. Sidescan sonars are normally towed at 4 to 6 knots, but more modern high end equipment is now available that can be towed at up to 14 knots. As an example, on a 200m range setting, a sidescan sonar will typically ping no more than three times in a second. At 6 knots this gives an along track resolution of approximately 1m.

4.3.4. Positioning, sidescan deployment and sea conditions

Although sidescan sonar is normally thought of as being deployed as a towed body, it can also be mounted on the hull of a vessel, or on the body of an ROV or AUV. The great advantage of towing is that the fish and therefore the transducers can be maintained at an optimum depth above the bottom in deeper and varying depths of water, maintaining footprint, resolution and geometry. Towed bodies are also less susceptible to movement due to sea state, although for most vessel mounted systems this issue has been overcome with the use of accurate motion reference units and heading gyrocompasses. Sophisticated software can then use the records of pitch, roll, yaw, heave and heading to compensate for the motion of the vessel due to sea and weather conditions. It should also be noted however that a number of more expensive towed sidescan sonars also have these features helping in monitoring the attitude of the towed body.

Towing has a further disadvantage that it is difficult to predict the horizontal position of the fish with reference to the GPS antenna on the surface. This really relates to attempts to predict the horizontal distance the fish is behind the vessel known as the 'layback'. Accurate acoustic positioning systems for towed bodies are available at varying cost which can help position the fish (see Chapter 7 below). Estimates of layback can also be made by performing a patch test where overlapping tracks in opposite directions are performed over a distinct feature on the seabed and the layback is adjusted during processing until the features on both tracks line up.

Sea condition also affects the operation of sidescan sonar. Even vessel mounted systems with sophisticated positioning have a limit of conditions that they can operate in and the records from and ability to position towed systems quickly deteriorate in poor conditions. Often the survey set up will have to be made with reference to the weather conditions so the vessel is running into and away from the prevailing sea or wind. The limits that can be worked are specific to the vessel, conditions and area, but typically larger vessels can operate in poorer conditions.

4.4. Examples of Current Sidescan Sonar Systems

Older style analogue systems such as the Edgetech 272TD have been used in the offshore industry since the late 1970's, but are still in production (Figure 4.3). A towed fish providing 105kHz or 390kHz operation, it has a reputation for producing high quality imagery with ease of support in the field. Ranges from 105kHz operation are up to 200m per side, reduced to 75m per side at 390kHz. The standard 260 surface unit and paper chart reader (Figure 4.4) can be replaced with aftermarket systems from CodaOctopus or Edgetech and a range of configurations of personal computer

based digital acquisition software from manufacturers such as Chesapeake Technologies are available. Whilst still being robust and supportable units, analogue sidescans such as the 272 have the disadvantage of having an expensive multicore cable. The move to digital sidescan systems has reduced the number of cores to two assisting in improvements in weight, drag, cost and times to repair. Lying between analogue and digital systems, the GeoAcoustics 159D (114/410kHz) is a common workhorse unit that uses two cores to transmit analogue data to the SS981 surface unit.

More modern dual frequency digital systems are available in the form of the Edgetech DF1000 (105/390kHz), C-MAX CM2 (100/325 or 325/780kHz), CodaOctopus 460PX (100/325kHz or 325/760kHz) or Klein 3000 (130/455kHz). The Klein 3000 has the ability to acquire simultaneously at both frequencies and claims ranges of twice that of other systems of similar frequencies. All these systems are supplied with digital acquisition systems which can also be interfaced with live mosaic and navigation aftermarket software. At the high end of the market are more sophisticated pieces of equipment that have additional features. The Edgetech MPX has the ability to be towed at 14 knots, over twice as fast as conventional equipment. The Benthos SIS-1624 uses chirp technologies to gain high quality imagery at a range of frequencies simultaneously and the Klein 5500 obtains very high quality imagery by using focused beams. Geoacoustics have also pioneered a synthetic aperture sidescan sonar for very high resolution surveys (Hiller, 2005). A comprehensive and extensive round up of sidescan sonar systems is listed in the product review of the April 2004 issue of Hydro International (Hydro, 2004).

4.5. Processing and Classification of Sidescan Sonar Data

4.5.1. Processing sidescan sonar data

Although composite mosaics can be produced live whilst surveying, final imagery and classification require post processing. A number of standard formats such as XTF, QMIPS and SEG Y have become popular over the years for the recording of hydroacoustic data and most acquisition systems have the ability to produce one or all of these formats. Most post processing software similarly has the ability to read files in at least one of these formats. All the formats have the ability to store the ping by ping amplitudes of the backscatter referenced with information recorded from a number of other sensors and equipment including GPS, depth sounder, cable out counter, acoustic positioning system, motion reference unit and gyrocompass. A file produced for each track therefore contains all the information necessary to process that track into a fully georeferenced image.

The process of amalgamating all the files into a composite mosaic of the image produced is known as ‘mosaicing’ and is performed by software made available by the manufacturer or any one of a number of third party manufacturers of hydroacoustic postprocessing software. An example of a sidescan mosaic is shown in Figure 4.8a. Well known examples of these are Triton Elics, Caris, QPS, QunietiQ and Chesapeake Technologies. In the production of a mosaic, the software performs geometric and radiometric corrections to compensate for the distortions caused by the vastly differing geometry between the returns from close to the fish and from those

from the maximum extent of the range. To perform these corrections it is necessary to know the altitude of the sidescan sonar off the seabed. This is often accomplished whilst surveying by a bottom tracking routine that detects the first return for each ping and records the height off the bottom for each ping in the file. Problems with the detection of the bottom in survey can be corrected during the post processing stage. A suitable pixel size that the mosaic will be produced at is also chosen taking into consideration the resolution of the original acquisition frequency, the detail required and size of the file that will be produced.

Mosaics produced can be considered as images of the seabed and resemble in many ways a monotone aerial photograph. They are typically produced in georeferenced raster image formats such as GeoTIFF or GeoJPEG suitable for use in GIS systems.

Further information on the processing of sidescan imagery can be found in Bennell (2001).

4.5.2. Classification of the seabed using sidescan data

Classification of sidescan imagery refers to the action of aggregating areas of similar acoustic signature, and then attributing them with information relating to their biological or physical characteristics. Areas can then be described using a suite of standard descriptors known as a classification scheme. This is very rarely accomplished using only a single technique and although the sidescan imagery obtained can be of a high resolution, it generally requires ‘ground truthing’ or validation by fine scale techniques such as video and still photography or direct sampling. The data sets required to produce a classified map of the seabed are illustrated in Figure 4.8.

The process of classification of the seabed in this case can then be considered as involving two discrete tasks, although in practice there is some overlap between them. Initially, imagery of the seabed is segmented into discrete areas exhibiting a particular acoustic signature. This signature is thought of as being characterized by the amplitudes of the backscatter in the imagery and the interpixel relationships or texture within regions of the image. The segmentation can be carried out either manually by visual analysis, or automatically by specialised image classification software. It can also be carried out on either the raw waterfall images of the individual tracks or on the mosaic of all the tracks. There are a number of advantages to carrying out the analysis on the raw images as they are typically of a higher resolution than the mosaic imagery and contain information relating to the original time series recorded. This means that analysis can be carried out with reference to the original geometry with which they were acquired. Mosaiced images do not contain information on survey direction and pixels in the image cannot be referenced to their across track positions in the swath, or the beam angle for which they were acquired. It is essential therefore that all possible corrections should be applied to the sidescan data before mosaicing. The specialised nature of sonar formats means that if the raw waterfall images are to be analysed, dedicated software and some means of mosaicing the classified imagery is required.

This functionality is provided by a number of products from specialised hydroacoustic software manufacturers described in the following section. As sidescan mosaics are simply standard TIFF or JPEG images, they can be analysed by a number of image processing and GIS products such as ESRI ArcGIS, ERDAS Imagine and ER Mapper.

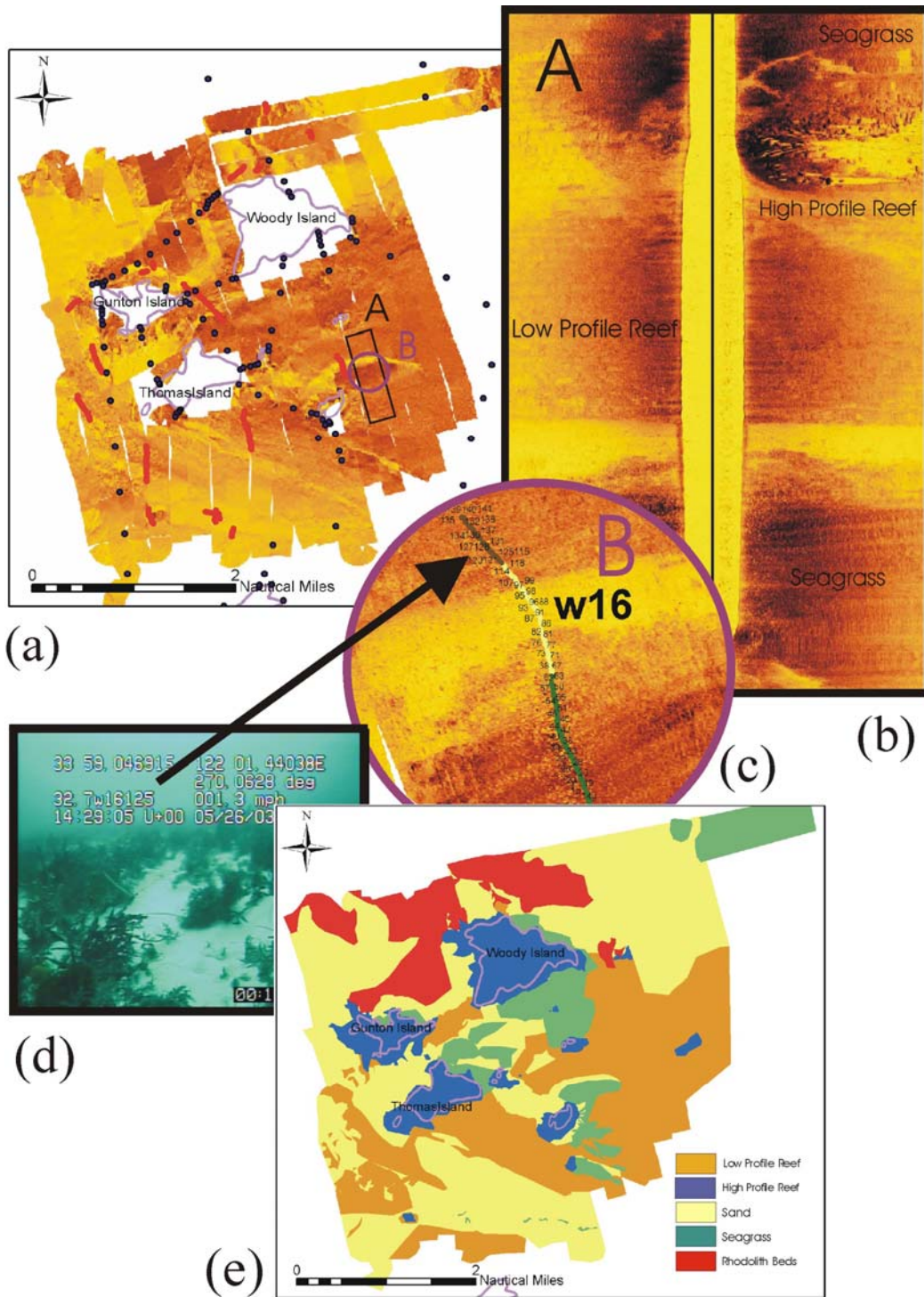


Figure 4.8. Processing of sidescan sonar and video data into a classified map of the seabed a) sidescan sonar mosaic, b) raw waterfall image c) classified video track d) timestamped and georeferenced frame of video e) classified map.

Visual segmentation of the sidescan imagery is usually accomplished in GIS software by digitizing polygons around areas of similar texture or intensity on the mosaic. This is performed with reference to all other data that is available for the area. Maintaining a continuous fixed viewing scale whilst digitizing helps maintain some uniformity in the mapping resolution.

4.5.3. Automated segmentation of sidescan imagery

Automated classification of sidescan imagery is generally carried out through analysis of the texture or amplitude within a window of a defined size. This window is then stepped across and down the image until each pixel, or group of pixels is assigned a value for each type of analysis performed. Pixels or groups of pixels with similar values are then amalgamated with reference to the required classification scheme.

As sidescan sonar obtained over large areas and varying conditions or depths typically varies in intensity, textural indices, more robust to variations in gain are often used to classify the imagery

The types of textural analysis vary, but are well documented in published literature. The most common type of textural analysis of sonar images uses Grey Level Co-occurrence Matrices (GLCM) to provide a range of second order statistics related to the texture of an area of image. The GLCM features published by Haralick *et al.* (1973) have been incorporated into a home grown package known as TexAn (Blondel and Murton, 1997; Blondel, 1998)) which has been used in a number of surveys (Blondel, 1998, Huvenne *et al.*, 2002). GLCMs were also used by Cochrane and Lafferty (2001) and have been incorporated into a number of commercial sonar processing packages such as QTC Sideview (QTC, 2002) and Triton Elics Delphmap. Brown *et al* (2002) used Delphmap to segment sidescan images in a comprehensive investigation of texture, sediment and biotope.

There are a number of other statistical methods of analysis that have also been investigated. Griffiths, *et al.* (1997) analyse real data using statistical scattering models and Reut (2000) and Finndin (1995) use power spectrum analysis of the backscatter envelope to classify images. Co-variance models are widely used in image analysis (Jain, 1989) but have been neglected in sonar classification (Finndin, 1995). Carmichael (1998) and Finndin (1995) have provided some treatment of this subject. Jiang, *et al.* (1993) and Mignotte *et al.* (2000) have employed Markov random fields to characterise the seabed texture and then employed a neural network for the classification. Neural networks have also been applied by Stewart, *et al.* (1994) in an investigation of textural features based on spectral estimates, grey-level run length, spatial grey level dependence matrices and grey level differences. Attention has been paid to derivation of features from fractal and multifractal measures by Linnett (1991) and Carmichael *et al.* (1996) and Pace and Gao (1988). Investigation into feature extraction using a spatial point model has been undertaken by Linnett, *et al.* (1995).

Sidescan sonar texture classification has also been the subject of a substantial number of Ph.D. thesis from Universities in the U.K., the research from which has inspired some of the papers cited above. From Heriot-Watt University, these include Linnett (1991), Tress (1996), Shippey (1991), Clarke (1992) and Shang (1995) and from University College, London, Dunlop (1999).

Despite the wealth of research describing textural analysis of sidescan imagery, there are only a limited number of commercially available packages dedicated to such analysis. The Seaclass extension for Delphmap from Triton Elics uses GLCMs to analyse mosaiced imagery but does not operate on the raw waterfall data. It employs a neural network to group the pixels into classifications based on the statistics. QinetiQ use fractal analysis in their mosaicing, classifying and GIS package Classiphi.

Textural analysis in Classphi can be carried out at the waterfall or mosaic level and it provides scope for training the system in the seabed types that are to be classified for supervised classification.

In their comprehensive range of sonar classification software, QTC provide for classification of sidescan imagery in their Sideview product. This takes a slightly different approach to classification of the imagery in that it uses a range of textural analysis techniques to segment the seabed. As well as using basic statistics and GLCMs, it also uses fast Fourier transforms, power spectra and fractal dimension. Using a unique clustering method it allows for both supervised and unsupervised classification based on the best features to capture seabed diversity. Sideview also offers a feature that allows sophisticated compensation of distortions and artefacts in the raw sidescan data.

GeoAcoustics (UK) offer a textural analysis package that can operate on imagery of any type, although when used with sidescan imagery it also functions as a mosaicing tool. Providing supervised classifications, GeoTexture is trained in the seabed types required in the segmentation. GeoTexture also provides sophisticated means of removing distortions and artefacts in the imagery before processing. Ocean Imaging Consultants also produce classification software for their OIC Toolkit.

The range of available publications of surveys processed is small but growing and manufacturers web sites should be monitored for recent work. Hydro (2004) highlights some surveys using automated classification software.

4.6. Seabed Surveys and Classifications using Sidescan Sonar

Although commercial hydrographic operations have been using sidescan sonar for object detection and monitoring and seabed classification for over 30 years in oil and gas and dredging work, the majority of surveys are only published in reports, much of which will not be available to the public. This review will therefore be focussed towards habitat mapping projects in continental areas and will be biased towards information that is freely available relating to relevant surveys and projects.

Sidescan records from at least as early as the 1970's appear to show evidence of seagrass beds and trawl tracks. Although many surveys have undoubtedly been carried out since this time, no published literature appears to be available relating to habitat mapping in shallow water using sidescan sonar until the late 1990s. Work carried out between these periods appears to be mainly related to deeper water and the identification of large scale geological features. Although these studies are not unrelated to seabed classification, they are beyond the remit of this review.

Barnhardt and Kelley (1998) used sidescan sonar to map and classify an area of complex seafloor in the Gulf of Maine. This survey uses visual classification of the sonar image validated with sediment samples. McRea *et al.* (1999) used sidescan sonar to characterise rockfish habitats near Kruzof Island, Alaska using sediment and video samples for validation. It is interesting to note that the sidescan used in this survey was interferometric and capable of providing bathymetry, although visually classified backscatter was predominantly used to delineate habitat type. In a

comprehensive and quantitative survey of an area in the English channel, Brown *et al.* (2002) compared sediment type, and biological sampling with sidescan sonar classifications from DelphMap software to classify benthic biotopes. GLCMs were used by Cochrane and Lafferty (2001) to distinguish areas of different texture in the Channel Islands, California.

Aside from the above review of recently published data, a number of large habitat mapping programs are underway around the world that use sidescan sonar in conjunction with other techniques. The Geological Survey of Ireland in their Irish National Seabed Survey (www.gsi.seabed.ie) are in the process of mapping an area of ocean 10 times the size of their land mass using a range of techniques including sidescan sonar. They are currently in the final phase of this project, mapping the inshore shallow areas. In Canada and the US the Gulf of Maine Mapping Initiative (GOMMI) group are in the process of mapping a 165,000 square km area (<http://www.gulfofmaine.org/gommi>). This is to name but a few of the projects that are ongoing or have been completed.

Recent habitat mapping using sidescan sonar in Australia has been carried out by the Coastal CRC in Western Australia in the Recherche Archipelago (Baxter and Bickers, 2004) and Cockburn Sound and in NSW in the Cape Byron Marine Park between 2002 and 2003 (CRC, 2004). This work was carried out using the University of Western Australia's Edgetech 272TD sidescan sonar and Chesapeake Technologies Acquisition Software and was validated by video and grab sampling. A Geoacoustics SS981/159D sidescan sonar system was used in the mapping of Pt Addis marine park in 2005 in a partnership project involving Fugro, Parks Victoria and the CRC as discussed below in Chapter 7.

The Defence Science and Technology Organisation (DSTO) have used their Klein 5500 sidescan in seabed classification of Sydney harbour as part of the data set comparing survey techniques for the Shallow Survey Conference 2003. The Klein 5500 was also used in the joint comparative study performed by Fugro and the CRC in the Marmion Marine Park off the Western Australian coast. An Edgetech sidescan system was also trialled along with a CMax sidescan and a number of multibeam systems and a GeoAcoustics GeoSwath Interferometric sidescan This work is outlined in chapter 7 below.

4.7. Use of Interferometric Sidescan

'Interferometric' type sidescan sonars have recently become popular for seabed mapping. These sonars employ multiple staves in each transducer to gain depths from interpretation of the phase angle between returning acoustic signals. Kenny *et al.* (2003) consider their genre as one of four of the main types of acoustic systems amongst single beam, sidescan and multibeam sonars. They compete with multibeam systems in the quest to provide simultaneous high quality bathymetry and backscatter from a single ping. This technique has the advantage that backscatter and bathymetry are perfectly coregistered as they are obtained simultaneously from the same acoustic transmission. Swath widths for interferometric sidescan sonars are generally quoted as being between that of conventional sidescans and multibeams. The research group active in the Gulf of Maine habitat mapping program consider that interferometric

sidecans may be more efficient for mapping in waters of less than 30m depth. This issue is addressed further in Chapters 7 and 8.

The range of interferometric sidescan equipment that is currently offered is limited in comparison with the range of standard sidescan systems. Systems are offered as being predominantly vessel mounted although towed types are available. Similar systems are offered by SEA (previously Submetrix) and GeoAcoustics in the UK. GeoSwath systems available from GeoAcoustics are vessel mounted systems available in 125, 250 or 500kHz configurations. Like multibeam systems, these systems incorporate both sophisticated motion and heading sensors for accurate positioning of the bathymetry and backscatter obtained. The range of towed systems is more limited. The Benthos C3D towed system has recently become available in 200 or 100 kHz frequencies and Klein have also completed trials with an interferometric version of their 5000 system known as a 5004. The advantage of towed interferometric systems is that using sophisticated sensors mounted inside the towed body allows surveys to be carried out at a greater range of depths with a single frequency. Towing also allows swath widths and the resolution of the data obtained to be kept constant. Positioning of the fish itself is however more difficult to estimate. Again published marine habitat mapping surveys using interferometric sidescan sonars are few, but at GeoHab 2004 a mapping project was presented using this technology (Thorsnes *et al.*, 2004). McRea *et al.* (1999) used an early interferometric sidescan to map rockfish habitats in Alaska and more recently Ojeda *et al.* (2004) used both a conventional sidescan and an SEA interferometric system on the same survey. A 250kHz GeoSwath was also used in Sydney harbour to gain information for the Shallow Survey 2003 data set and in 2004/2005 a 250kHz system was tested by Fugro and the Coastal CRC as part of the Marmion Marine Park data set discussed in chapter 7.

In Australia, as of early 2005, the availability of interferometric systems is currently limited to two GeoSwath systems. One is a 250kHz unit operated by 3D Mapping in Adelaide, and the other a 125kHz system which was recently purchased by the NSW Department of Environment and Conservation. The NSW based system will soon be used to create habitat maps of all the marine parks in NSW.

5. MULTIBEAM AND SWATH SONAR

Multibeam sonar systems (MBSS) have rapidly evolved over the last few decades, and currently are the most advanced acoustic tool for remote observations and characterisation of the seafloor. Among the existing sonar systems, MBSSs provide maximum information about the bottom properties along with a wide coverage of seafloor mapping, which is essential for rapid assessment of the benthic habitat over large areas of coastal waters. The swath width of modern MBSS is approaching the raster width of acoustic sidescan systems, while the width of individual MBSS beams can be as small as tenths of a degree. The main advantage of a modern MBSS with respect to discrimination and classification of different seafloor types is its ability to provide simultaneously a high-resolution bathymetry map and a backscatter image of the surveyed area. Most of the seafloor classification techniques developed recently are based on a mutual analysis of bathymetry or backscatter data using certain characteristics of the seafloor roughness and backscattering strength. The estimated parameters of different types are clustered to define selection criteria for individual classes of the seafloor.

The capability of multibeam systems in remote acoustic characterization of the seafloor is a subject of current research. A number of organisations and companies are currently working to provide seabed classification capability for multibeam systems. Simrad has produced the Triton system for this purpose, and an evaluation of this product has been carried out as part of the CSIRO deep water program in Australia (Kloser, private communication). The QYC and RoxAnn organisations are developing multibeam classification systems and other organisations are active in the field. The Seabeam multibeam instrument corporation has recently been advertised as offering seafloor classification capability. Several advantages of multibeam over single beam classification procedures can be noted. Firstly, multibeams provide greater area coverage, approaching that provided by sidescan systems. Secondly, the ability to infer cross track bathymetry allows for corrections to be made for seabed slope across the vessel track direction, while along track slopes may be derived from sequential depth assessments. Within the spatial limitations imposed by beam geometries and operating depths, it is thus possible to determine local angles of incidence. This relates to a third advantage, that it is in principle possible to build a model of surface roughness based on the variation of backscatter amplitude with the angle of incidence at the seabed. Multibeam systems are, however, expensive and in general require larger vessels than single beam systems. It seems likely that over time multibeam or possible interferometric sidescan systems will become the acoustic systems of choice where budget provisions allow. As is more the case than with the less effective single beam systems, however, significant research, development and proving needs to be done to realise the potential of the more complex systems for classification.

Beginning in April 2000, the project *Marine biological and resource surveys, South East Region* was begun by CSIRO Marine Research under an Agreement with the National Oceans Office. The project constitutes Australia's largest benthic survey program to date. The interim report (Kloser *et al.*, 2001a) concentrates on the comparison of high resolution swath mapping with pre-existing or known habitat types, to provide an initial evaluation of the application of rapid assessment methods based on swath mapping. Other techniques used in the field program carried out in

April-May 2000 included normal incidence echo sounding at three frequencies and a variety of conventional sampling systems. The conclusions of this report indicate that swath mapping and associated software for classification from backscatter returns, even at the present limited state of development, produces a powerful surrogate for habitat type. The report authors suggested that Australia should establish a national program of seafloor mapping using the suite of technologies used in the CSIRO project. More recently CSIRO has acquired a dedicated 30 kHz Simrad system which is mounted on the research vessel *Southern Surveyor* and further seafloor mapping using this multibeam system has begun in Australian waters.

5.1. Principles and Data Processing of MultiBeam Sonar Systems (MBSS)

General design principles of modern MBSSs are illustrated in Figure 5.1. The sonar transducer emits acoustic pulses propagated inside a wide across-track and narrow along-track angular sector. The receive array directed perpendicularly to the transmit array forms a large number of receive beams that are narrow across track and steered simultaneously at different across-track directions by a beamforming process. Thus the system performs spatial filtration of acoustic signals backscattered from different portions of the seafloor along the swath. Modern shallow-water MBSSs, such as Simrad EM 3000 and Reson SeaBat 8125, operate at hundreds of kHz, transmit short pulses of several tens of microseconds, and form hundreds of beams of about 1 degree width. Because they employ short pulse lengths, narrow-beam MBSSs are capable of resolving small features a few decimetres wide in the seafloor relief in the horizontal plane along with finer bathymetry details.

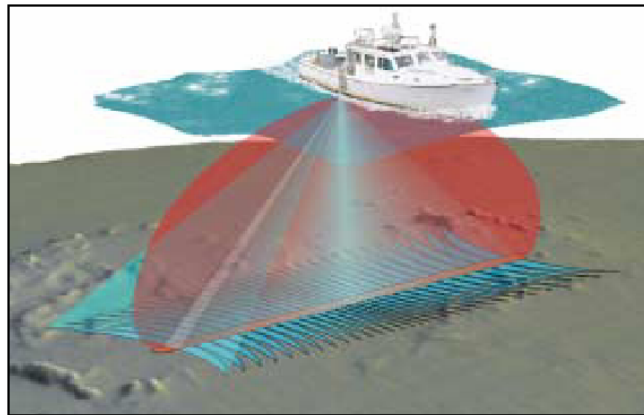


Figure 5.1. Typical geometry of the transmit and receive beams of MBSS.

The operational principles of MBSS give evident advantages for seafloor mapping. However, they result in much stricter requirements for ship's navigation than that for single-beam and sidescan systems. If ignored, ship's attitude affected by roll, pitch, and heave may distort irreparably the bathymetry and backscatter images, especially for the oblique beams of small grazing angles for which ship's motion induces a large horizontal deviation of the footprint location (see Figure 5.2, for example). Therefore swath bathymetry mapping must be accompanied with simultaneous tracking of ship's motion, including roll, pitch, heave, and yaw. The procedure for compensating for a ship's attitude for swath mapping data is well developed and described in the literature (US Army Corps of Engineers, 2002).

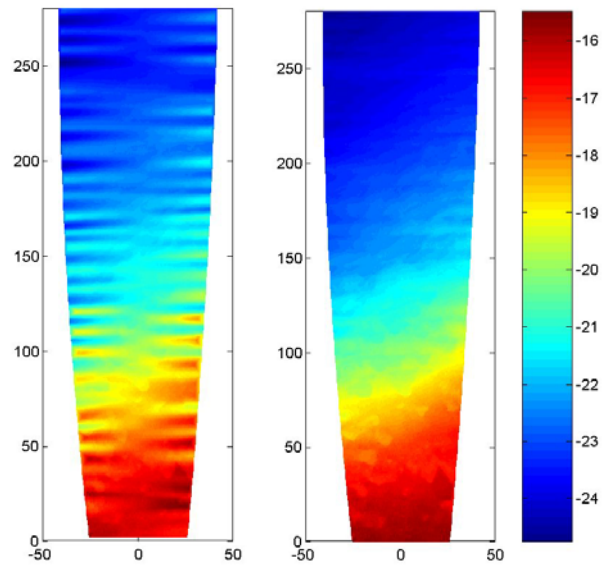


Figure 5.2. Bathymetry images before (left panel) and after (right panel) compensation for ship's motion (from the results of the Coastal Water Habitat Mapping project of the Coastal CRC).

Another serious problem specific to MBSS seafloor mapping is acoustic refraction in the water column with a depth dependent sound speed, which distorts the acoustic ray trajectories and hence the bathymetry images. Correction of swath data for the sound speed change in presence of ship's 3-D motion is a complicated problem. Possible artefacts in MBSS bathymetry imaging due to mutual effects of the sound speed variation and ship's motion are considered by Kammerer, *et al.* (2000) suggesting a new, more accurate method for removing those artefacts. The problem becomes even more complicated if the sound speed profile is time and range dependent. Hughes Clarke *et al.* (2000) propose a new operational procedure for swath mapping integrated with underway oceanographic measurements, which improves the results of acoustic mapping in a range-varying environment.

The most prevalent approaches to seafloor characterisation by using MBSSs are briefly discussed below.

5.1.1. Processing bathymetry details

Modern high frequency, narrow-beam MBSSs used for shallow-water surveys produce high-resolution bathymetry maps with a cell size of the horizontal resolution of several decimetres, which makes it possible to perform a small-scale textural analysis of seafloor relief. The purpose of the textural analysis is ideally to determine a 2-D, generally anisotropic spectrum of the bottom roughness. In practice, the capability of such an analysis is limited by the spatial resolution of MBSS, which becomes coarser with the increase of sea depth. The other problem is a large number of parameters to be estimated to define a mask for classification (spectrum width / roughness correlation length in different directions, roughness rms height, etc.). Therefore simplified criteria are commonly introduced in the mapping procedures to identify local topography features and roughness of the bottom surface. After the procedure of cleaning and gridding, the bathymetry data are represented on a regular topographic grid of which the mesh size depends on the MBSS angular resolution and typical sea depth in the surveyed region. In a gridded form, the bathymetry data are

much more suitable for raster-based processing, including 2-D filtering and a spectral analysis. The most common approach is to use a rectangular window of several grid cells width (variable in general) moving along the grid to determine local characteristics for further terrain analysis. The most prevalent characteristics are the average elevation, spatial derivatives, a topographic variability index (TVI), and a topographic amplitude index (TAI). The first-order derivatives give the slope and aspect of the bottom surface. The second-order derivatives express the curvature of the surface. The TVI and TAI indexes were introduced by Chavez *et al.* (1995) as a measure of topographic variability. Both TVI and TAI are generated from the high-pass filtered (HPF) surface elevation, which is usually obtained by subtracting the low-pass filtered (i.e. averaged within a 2-D integration window) depth values from the original bathymetry grid. The TVI is determined by sorting the pixels into two categories such that the pixel values lie either within or outside a predefined divergence from the average value. Every pixel is designated as 0 or 1 in accordance with its category, which corresponds to either negligibly small or noticeably large variations respectively. Finally, the TVI is calculated by averaging the indexes over the window. Figure 5.3 illustrates an example of terrain mapping using TVI analysis.

The TAI is defined as maximum absolute deviation of the high-pass filtered elevation of the surface relative to the average value within the integration window.

MBSS bathymetry maps are generally gridded with a variable mesh size, because the horizontal resolution of MBSS is a nearly linear function of depth. For variable grid spacing, the results of seafloor mapping by terrain attributes become somewhat indefinite, if the estimates of the terrain characteristics are markedly dependent on the mesh size of the grid. It is shown by Diaz (1999) that the TVI index is nearly invariant to changes in grid spacing. The estimates of the TAI index and spatial derivatives (surface slope and curvature) are much more dependent on the mesh size, which follows directly from the ambiguity of numerical differentiation with a variable sampling interval.

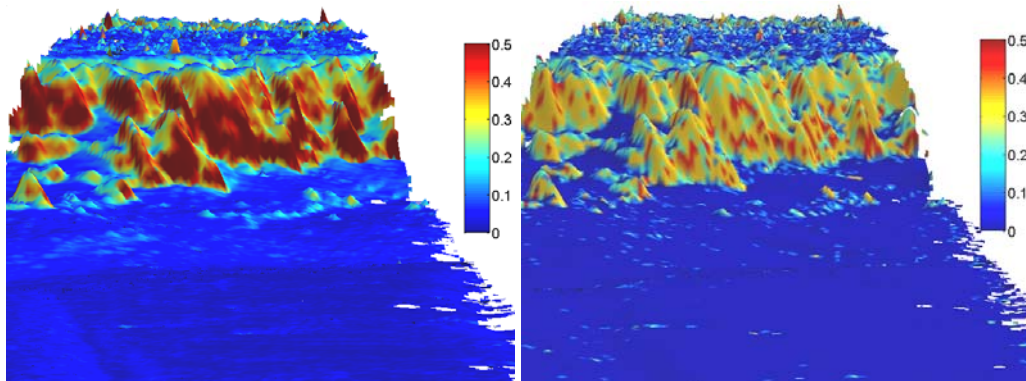


Figure 5.3. Slope (left panel) and TVI (right panel) draped over a 3-D bathymetry over the Morinda Shoal region in the Bowling Green Bay, Queensland, Australia (from the results of the Coastal CRC CWHM project).

Fractal analysis is nowadays another method that is widely used for seafloor classification using high-resolution MBSS bathymetry data. The fractal concept applied to modelling topographic relief is, in a certain sense, a modification of the 2-D spatial spectrum analysis that confines the variety of modelling spectra within a single class of fractal spectra. The shape of a fractal spectrum is defined by only two

parameters, which are a fractal dimension, and a cut-off wavenumber that determines the roughness correlation length. In the general case of an anisotropic surface, the cut-off wavenumber is different along X and Y directions. The fractal power spectrum has the following form:

$$S(u, v) = K [(u - u_c) + (v - v_c)]^{-n},$$

where u_c and v_c are the cut-off wavenumbers, K is a coefficient dependent on the rms height of roughness, and n is related to fractal dimension D by $n = 6.5 - 2D$. Figure 5.4 demonstrates a sand-ripple seafloor surface modelled by an anisotropic fractal spectrum with $D = 2.5$.

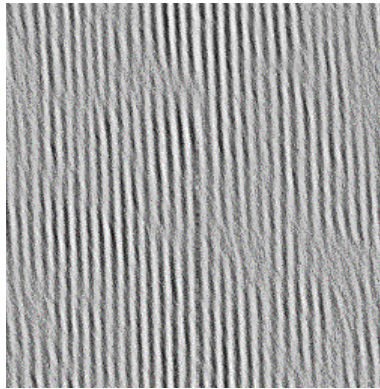


Figure 5.4. Sand-ripple roughness of seafloor surface modelled by an anisotropic fractal spectrum with a fractal dimension of 2.5.

The fractal approach to topographical classification of the seafloor has two obvious advantages:

- 1) The seafloor topography can be well modelled by a fractal structure for a broad class of seafloor relief (Hastings and Sugihara, 1994) and
- 2) The number of estimated parameters is small, which simplifies the classification procedure.

A model of acoustic backscattering from a rough seafloor surface of fractal structure is developed by Lubniewski *et al.* (2000), who also show that the parameters of fractal spectra of the seafloor surface can be derived from acoustic sonar data.

5.1.2. Processing of backscatter data

Processing of MBSS backscatter data is a more complicated procedure than the analysis of bathymetry data. There are basically two different approaches to utilisation and interpretation of backscatter data, which are commonly used in acoustic classification of the seafloor. These approaches are a textural analysis of backscatter images and an analysis of the angular dependence (AD) of backscattering strength. The textural analysis is most common, since the methods of statistical analysis of MBSS backscatter intensities are similar to those utilized for processing of side-scan sonar images. A large number of statistical characteristics are determined from backscatter data for discrimination of seafloor classes. Before performing the analysis, the backscatter intensity data are usually corrected for the angular dependence of

acoustic backscattering and for inequality of the MBSS sensitivity along different beams. An improper correction of the backscatter angular dependence may produce large errors in the estimates of the basic statistical characteristics, such as mean intensity, standard deviation, and higher-order moments, derived from backscatter images. The simplest model of well-known Lambert's law is frequently applied to backscatter data for removing angular dependence. However, this model is not accurate enough for many classes of seafloor cover, especially at near-nadir (steep incidence) angles. Hellequin *et al.* (2003) employed a simple composite model that treated the angular dependence of backscattering using the tangent plane (Kirchhoff) high-frequency approximation for near-nadir incidence angles and a Lambert-like term dominating at off-specular angles:

$$BS(\theta) = 10 \log [A \exp(-\alpha \theta^2) + B \cos^\beta \theta],$$

where BS is the backscattering strength and θ is the angle of incidence. The coefficients A , B , α , and β are estimated by least-mean-square fitting of the model function to the average angular dependence of backscatter intensity observed across representative (or training) areas. At higher frequencies of hundreds of kHz, the roughness height of the seafloor surface becomes much larger than the acoustic wavelength, so that both Kirchhoff and Lambert approximations are not accurate enough for numerical prediction of the angular dependence. For such conditions, an empirical approach to angular correction of backscatter intensity data has been developed within the CWHM project of the Coastal CRC. The developed algorithm involves calculation of an average angular response for backscatter intensity level within a spatial window of a programmed length that slides along the swath line with a 50 per cent overlap. The average angular dependence is then subtracted from the backscatter intensity level within each section of the swath line that spans the central half of the averaging window. Then the absolute level of backscatter is reconstructed by adding the average level measured within the interval of 30 ± 2 degrees. As a result, the algorithm removes artefacts of the angular dependence from backscatter images, minimizes the boundary effects due to angular correction, and, at the same time, tracks gradual variations of backscattering strength over the surveyed area and allows for preserving information on the backscatter angular dependence at a relatively high spatial resolution. The last two features of the algorithm bring certain advantages to swath backscatter mapping of the seafloor when comparing to the empirical method recently suggested by Beaudoin *et al.* (2002), in which the backscatter intensity data are corrected for the angular dependence averaged over each whole swath line. The efficiency of the newer algorithm is demonstrated in Figure 5.5.

To calculate the basic statistical characteristics, the backscatter intensity image of the entire surveyed area (backscatter mosaic) is divided into small rectangular patches for which the mean intensity, standard deviation, and higher-order moments are determined. The patch size is selected taking into consideration the spatial resolution of MBSS and data quality. In contrast to low-frequency deep-water MBSSs that have a footprint size much larger than the correlation length of seafloor roughness, modern high-frequency shallow-water swath systems operate with such narrow beams and such short pulses that the seafloor area insonified instantly is small enough to resolve individual small-scale features of seafloor relief (small rocks, sand ripples, shellfish patches, etc.). Under such conditions, the statistics of backscatter intensities is another

important measure that can be used for identification of morphological and physical characteristics of the seafloor. The statistical distribution of backscatter intensities is usually determined at lower spatial resolution over long sets of small patches (e.g. several rows of rectangles per the port and starboard sides along the swath track).

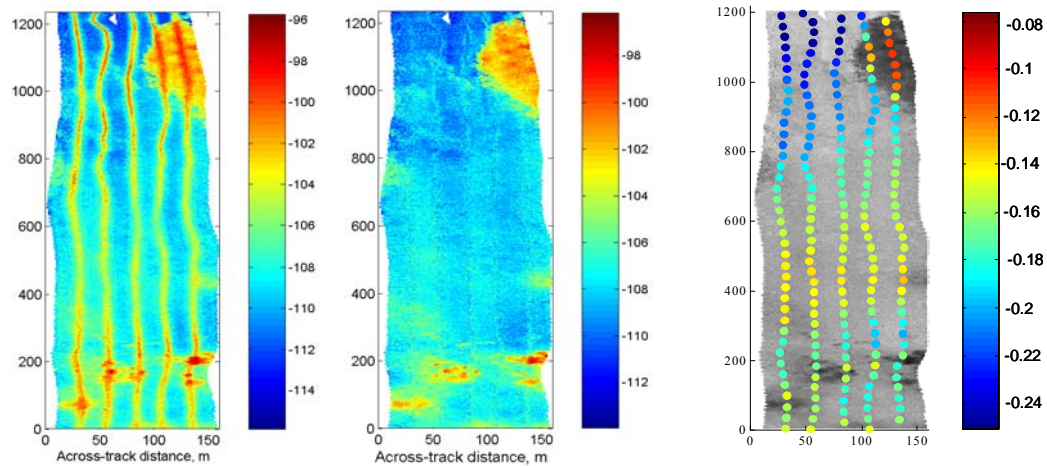


Figure 5.5. Backscatter intensity image of the seafloor build from five overlapping swath lines, before correction for the angular dependence (left panel) and after (central panel). The right panel demonstrates the mean slope of angular dependence within a $5-40^\circ$ measured at the central points of each section of swath lines, superimposed on the grey-scale backscatter image. The seafloor in the surveyed area consisted mainly of sand. Note seagrass patches of various sizes clearly visible as yellow and red coloured (dark) spots at the bottom and at the upper right corner of the area.

If the size of an instantly insonified area is much larger than the characteristic length of seafloor roughness, the number of statistically independent elementary scatterers within this area becomes large enough for the distribution of the complex amplitudes of backscattered signals to tend to a Gaussian form, which follows from the central limit theorem. Consequently, the variation of backscatter intensities tends to Rayleigh-like statistics. For high-frequency MBSSs operating with smaller footprint of individual beams and smaller areas insonified instantly, the statistics of backscatter intensities become non Rayleigh's in form. Ol'shevskii (1967) showed that broad-spectrum spatial variability of surface roughness should lead to a product model of backscatter statistics. Jakeman (1988) utilized a K -distribution as a product model for backscatter statistics that describes a Rayleigh-fluctuating process modulated by a Γ -distributed term that depends on two parameters (mean and so-called shape factor) and represents local reflectivity from the relief particularities.

Figure 5.6 demonstrates that the K -distribution fits experimental data for rougher surfaces much better than Rayleigh's one. Hellequin *et al.* (2003) show that the shape factor α_{eff} of the K -distribution estimated from backscatter intensity data can be used to distinguish different types of the seafloor cover, such as sand, rock, gravel, and rock, as shown in Figure 5.7.

Texture is one of the important characteristics that can be effectively used for identification of particular regions in an image. A texture analysis of backscatter images is widely used in processing of side-scan and MBSS data for classification of the seafloor, as noted in Chapter 4. The most common method of the texture analysis is based on determination of statistical features of the so-called grey-level co-occurrence matrices (GLCM). Statistical characteristics calculated from GLCM

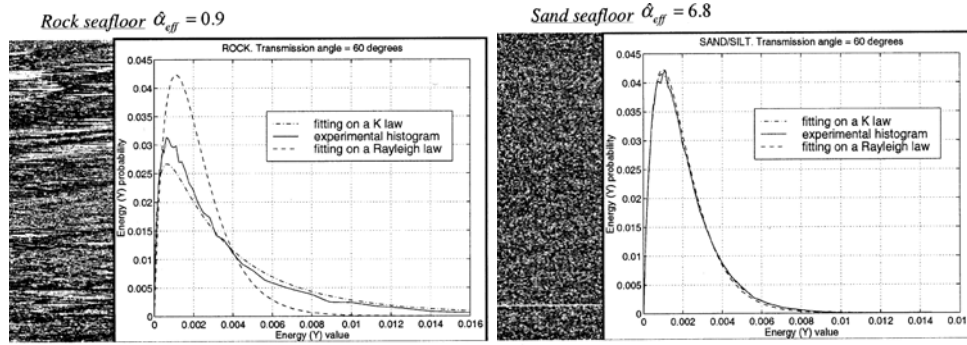


Figure 5.6. Measured histograms and statistical distribution fitting for two different types of the seafloor cover: rock – left panel; sand – right panel. Gray-scale images on the left of each graph are backscatter intensity images of the respective seafloor types (from Hellequin et al., 2003).

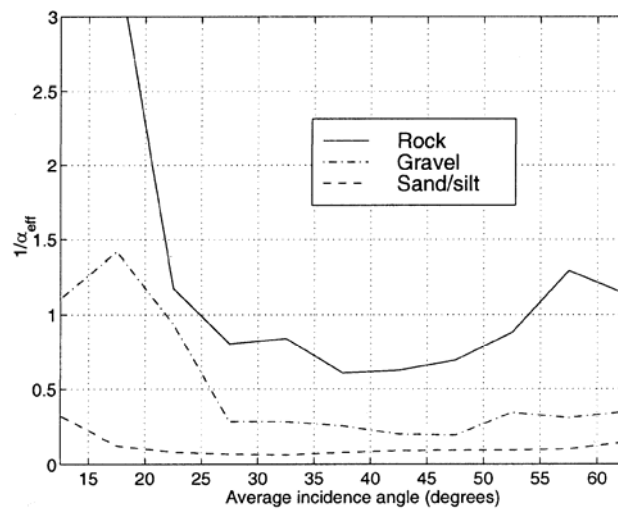


Figure 5.7. Variations of the statistical estimates of shape factor $1/\alpha_{\text{eff}}$ versus the average incidence angle (from Hellequin et al., 2003).

describe distinctive textural properties that show the relationship between a given pixel and a specific neighbour. In particular, the GLCM characteristics give a detailed description of contrast and correlation of the intensity pixels in a backscatter image. The GLCM analysis is a useful image processing technique for MBSS backscatter imagery, because its results do not depend on the absolute backscatter strength and hence on the absolute calibration of sonar systems. Moreover, it is widely believed that the angular dependence of the GLCM features is weak enough for the results of the textural analysis to be weakly dependent of the irregularity of MBSS directivity and the angle of incidence. The latter is not fully true, because statistics of backscatter intensity depends on the incidence angle (as clearly shown in Figs. 5.6 and 5.7), and hence the GLCM features also should depend on the incidence angle. The GLCM analysis is a quite sophisticated technique. Generally, GLCMs are determined for each N -by- N pixel patch of an amplitude-quantised backscatter mosaic. The elements of each GLCM are expressed as the number of times a pixel of value i neighbours a pixel of value j in direction θ , at distance d . The dimension of GLCM depends on the dynamic range of intensity variations expressed in quantising units (typically 255 for a 8-bit grey-scale image). The normal values of direction θ are 0° , 45° , 90° , and 135° , which is a unique set of directions for $N = 3$. For each GLCM derived from a

backscatter mosaic, one can calculate a large number of different textural characteristics, such as homogeneity, dissimilarity, correlation, variance, mean, entropy, contrast, angular second moment, grey-level difference vector (GLDV) contrast, GLDV mean, GLDV angular second moment, and GLDV entropy. For discrimination of different image classes in the whole backscatter image, each GLCM characteristic can be used to create a separate layer in the map of image. However, it is impractical to treat every statistical measure as a dimension in the feature vector space, because some of the GLCM characteristics are strongly correlated with each other. Moreover, most of the GLCM characteristics are nearly uninformative with respect to seafloor classification because they are not adequately correlated with the actual physical and morphological properties of the seafloor.

The angular dependence of backscattering strength is an important characteristic that distinguishes different types of the seafloor cover. Figure 5.8 demonstrates the angular dependence of backscattering strength measured for two different types of seafloor cover (seagrass and sand) using the Reson SeaBat 8125 MBSS.

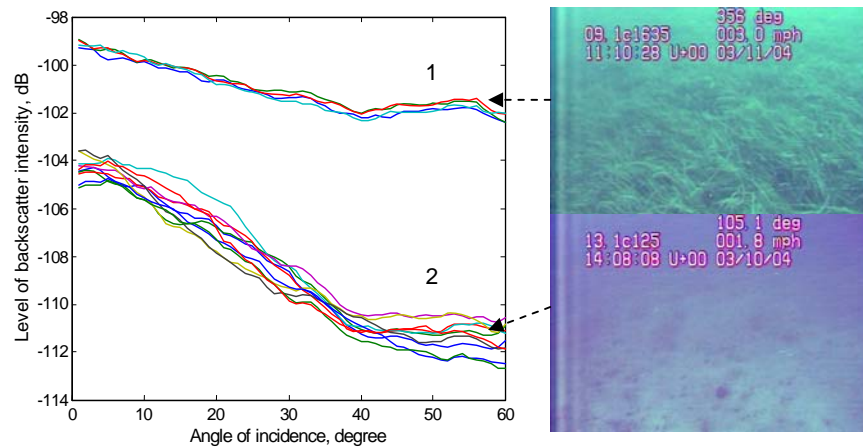
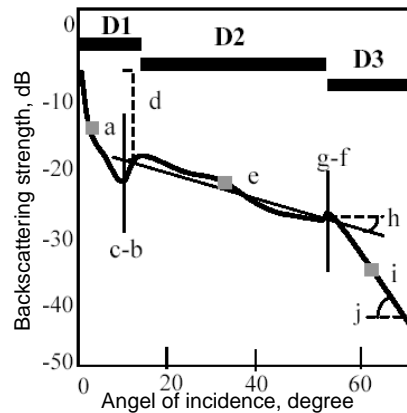


Figure 5.8. Angular dependence of backscattering strength from seagrass (1) and sand (2) measured in Cockburn Sound, Western Australia within the CWHM project [Gavrilov *et al.*, 2005].

In practice, it is difficult to define replicas of the angular dependence for every type of the seafloor and classify the bottom surface by searching for the best-fit replica for the measured backscatter data. Therefore the whole angular range is usually divided into a small number of specific domains according to the physical peculiarities of acoustic scattering at different angles. The bottom backscattering model formulated by Jackson *et al.* (1986) distinguishes three domains. At near vertical incidence, backscattering from large smooth roughness dominates the volume scattering and backscattering from small-scale roughness. The tangent plane (Kirchhoff) approximation is an appropriate approach to modelling the angular dependence within this domain. At moderate incidence angles, Bragg scattering from small-scale roughness and volume inhomogeneities is the primary mechanism that can be modelled using a composite model approach based on the small-perturbation approximation. At small grazing angles below the critical angle, the volume scattering becomes negligible, which reduces the backscatter intensity especially at lower frequencies.

The most comprehensive procedure of angular dependence (AD) classification involves determination of the domain boundaries and calculation of certain characteristic values, such as the mean backscatter intensity, AD slopes, and second derivatives, within each domain. Figure 5.9 gives an example of AD classification

with 10 selected characteristics. In practice, some of the AD parameters are not robust enough for adequate recognition of the seafloor type and therefore only a few parameters are used for seafloor classification, which usually are the mean backscatter intensities and slopes of the angular dependence measured within certain angular intervals belonging to different domains.



Parameters estimated:

- a. Mean BS intensity for **D1** (0-10°)
- b. 2-d derivative at c
- c. Location of boundary **D1-D2**
- d. dB range of **D1**
- e. Mean BS intensity for **D2** (15-50°)
- f. 2-d derivative of g
- g. Location of boundary **D2-D3**
- h. Slope **D2**
- i. Mean BS intensity for **D3** (55-70°)
- j. Slope **D3**

Figure 5.9. Three main domains (D1, D2, D3) of angular response curves and the parameters extracted to describe each domain (from Hughes Clarke et al., 1997).

5.2. Seafloor Classification Procedure

The analysis of MBSS bathymetric and backscatter data produces a large number of characteristics, as discussed in previous paragraphs. These characteristics are determined at mesh points of a grid that samples rectangular patches of the surveyed seafloor area. If the mesh size of the primary analysis is different for the parameters selected for classification, the obtained estimates are interpolated into points of a common grid. The grid spacing is usually selected such that the spatial resolution remains the maximum possible, avoiding excessive ambiguity of interpolation. As a result, N parameters selected for classification constitute N characteristic layers on the gridded map and form an N -dimensional vector space of variables. The main constituent of the classification procedure is clustering of the obtained vector space. It is impractical to apply clustering for a vector space of dimensions as high as several tens or even hundred of variables. Therefore the number of variables is usually reduced by searching for the parameters which, in combination, contribute most to the total variance over the gridded area, so that the rest of the parameters and their combinations could be disregarded. A principal component analysis (PCA) is the most common method for selecting appropriate combinations of the classification parameters (Reed and Hussong, 1989). Usually the top two or three combinations are enough to model variations over the mapped seafloor area.

There are, in general, two different approaches to clustering MBSS data for seafloor classification. The first, realized in Quester Tangent's QTC Multiview system (Preston et al., 2001) is the most comprehensive and ambitious. It involves a simultaneous analysis of all characteristics that can be obtained from both bathymetric and backscatter data of MBSS. Specifically, the QTC Multiview system treats initially over 130 different features extracted from MBSS data. Then the PCA procedure is applied to reduce the number of features to three combinations of parameters, which are used for classification of the seafloor. The second approach is to perform separate

clustering for the parameters extracted from different categories of MBSS data, such as bathymetry, backscatter mosaic, and the angular dependence of backscattering. Then the clustered combinations of the most informative features defined by PCA in each category are used for building a number of different characterisation maps of the seafloor. The obtained characterisation maps are compared to each other in order to determine the correlation between the seafloor classes defined from the data of different categories.

For building the final classification model, both approaches need ground-truthing by comparing the seafloor classes defined from the MBSS data to the results of sediment core sampling and underwater video recording made within a number of training patches representing the most characteristic types of the seafloor. The efficiency and adequacy of seafloor classification by using either one or another approach to interpretation of MBSS data is still a subject of serious discussion. Although the multi-parameter method realized in some MBSS processing systems, such as QTC Multiview, attempts to automatically interpret the maximum information that can be extracted from MBSS data, a separate analysis of specific bathymetric and backscatter features obtained with MBSS sometimes gives better results with respect to the correctness of seafloor discrimination. Figure 5.10 demonstrates that the seafloor classes defined from the textural analysis of backscatter mosaic do not always distinguish the actual grain size of the sediment. Only two of five classes (1 and 2) represented in this plot by large numbers of core samples have noticeable peaks distinguishing certain domains in the grain size scale. However these domains are too broad for classification of the sediment. The example in Figure 5.11 shows the correlation between the grain size of sediments and the seafloor classes defined from the AD analysis of MBSS backscatter data. The correlation is better, but the AD classes distinguish the sediments by their grain size only as a very broad trend, even if AD classes 3 and 4 are merged. These results are not promising for these particular techniques, however, median grain size is only one of the sediment or habitat properties that influence acoustic backscatter.

An example of seafloor mapping using the data of a MBSS survey in the Morinda Shoals area off the Queensland coast is given in Figure 5.12. This example clearly demonstrates that the backscatter intensity data from MBSS (right-bottom panel) amplify the bathymetry data with additional information that can be used for better discrimination of the seafloor habitats.

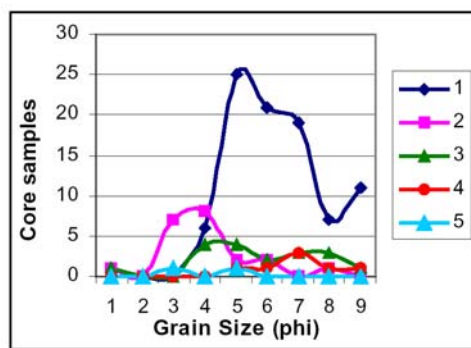


Figure 5.10. Frequency of textural classes plotted against grain size determined from core samples (from Diaz, 1999).

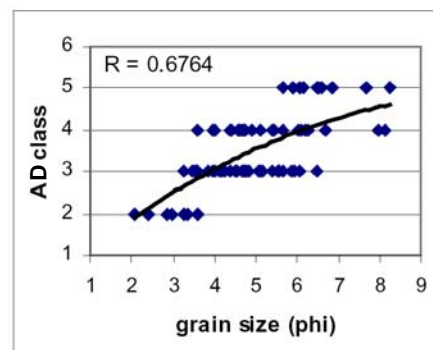


Figure 5.11. AD classes plotted against grain size from core samples (from Diaz, 1999).

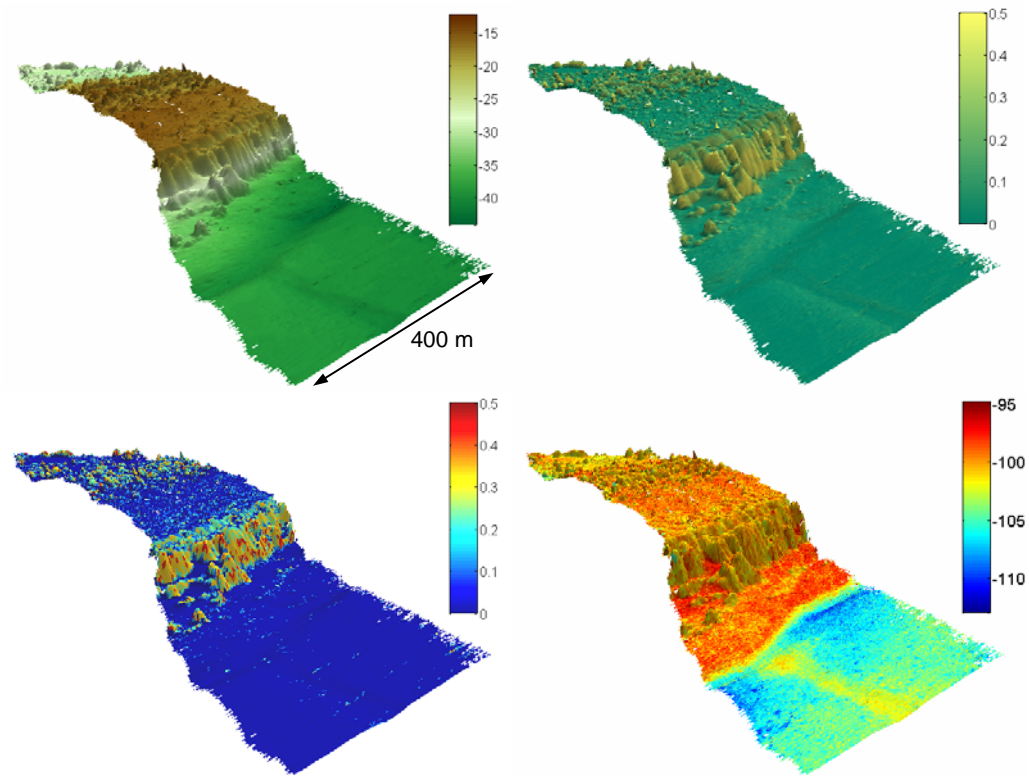


Figure 5.12. 3-D views of the seafloor across a coral reef in Morinda Shoal, Bowling Green Bay, Queensland.. The images show four colour-coded attributes extracted from the MBSS data: bathymetry (upper-left), slope (upper-right), TVI (bottom-left), and backscatter intensity (bottom-right). All of them are draped over the 3-D bathymetric map. Colour spots indicate the location of sampling stations for assessing fish abundance.

6. SUBSURFACE SENSING TECHNIQUES

6.1. Introduction

The geology of the seafloor and underlying strata represents key physical features of benthic habitats. Underwater acoustics have for many years been a fundamental tool for oceanography and marine geology because of the ability of these methods to determine physical properties of the seafloor, and to identify geological acoustic reflectors below the seafloor (McQuillin *et al.*, 1984). In recent years, acoustic methods have also been used to measure small scale sedimentary structures and processes, with high temporal and spatial resolution, and they have been widely adopted by marine researchers because of their ability to rapidly and non-intrusively collect data (Davis *et al.*, 2002, Walter *et al.*, 2002, Kim *et al.*, 2002). Although most acoustic sub-bottom profiling systems have been designed to acquire information about geological boundaries well below the seafloor, information relating to surficial and near-surficial sedimentary environments is also inherent in many of the commercially available systems (Davis *et al.*, 2002). These data are valuable because seabed geomorphology can provide a good first approximation of different types of benthic environments and habitats (Kloser *et al.*, 2001b).

6.2. Principles of Sub-bottom Profiling

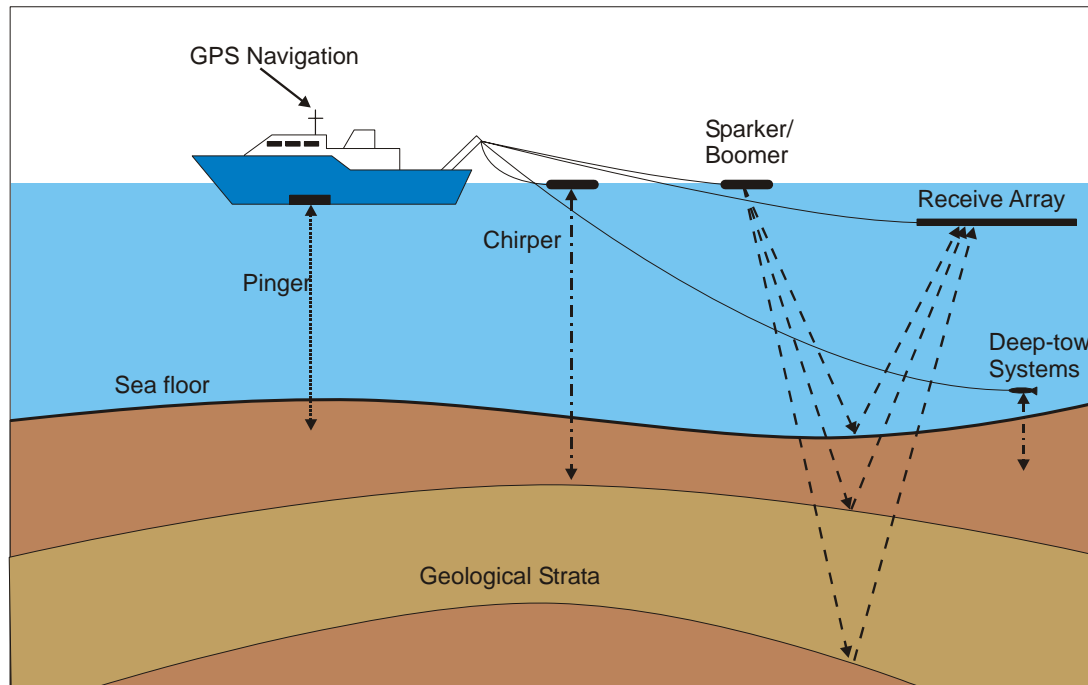


Figure 6.1. Deployment of various shallow-water sub-bottom profiling systems. After Stoker *et al.* (1997).

Sub-bottom profiling systems comprise a sound source, either towed behind a vessel or firmly mounted to the hull, that produces an acoustic pulse of set frequency, power, and time duration. The acoustic pulses generated may be described as a ‘single-beam’ (see Chapter 3). The acoustic pulse travels through the water column (at a rate

determined by water temperature, salinity and suspended material concentration), and penetrates the seafloor (Figure 6.1).

Some of the acoustic signal is reflected from the seafloor, whereas the remainder penetrates the seafloor and is reflected when it encounters boundaries between layers that have different acoustic impedance. The acoustic impedance of a material, Z , is dependant on the wet bulk density (of the sediment), ρ , and the compressional wave velocity, c , where:

$$Z = \rho c \quad (1)$$

The Rayleigh coefficient of reflection, R , is defined as the ratio of the reflected amplitude to the incident wave amplitude. For a normal incident acoustic wave this reflection coefficient is related to acoustic impedance by the relationship:

$$R = (Z_2 - Z_1)/(Z_2 + Z_1) \quad (2)$$

Subscripts 1 and 2 respectively refer to the impedance of the mediums above, and below, the reflecting interface. For reflection at the seabed, R will be positive when the acoustic impedance of the sediment is greater than that of the overlaying water (Davis *et al.*, 2002, Walter *et al.*, 2002).

The reflection of acoustic energy takes place at boundaries of differing acoustic impedance, and the reflection strength depends on the degree of impedance contrast. Typically, a portion of the incident energy is reflected from the sediment-water interface, whereas the remainder is transmitted deeper into the substrate (McQuillan *et al.*, 1984, Stoker *et al.*, 1997). The returning sound waves are recorded by an array of hydrophones (also usually towed further behind the vessel), or by a transducer/transceiver, depending on the type of system (Verbeek and McGee, 1995, McGee, 1995). The acoustic receiver resolves the various pulses of energy, with backscatter from shallower reflectors arriving first, forming a profile of information. The result is a continuous real-time displayed record of bathymetry (the first significant reflecting surface) and the boundaries between sub-bottom strata.

Several physical parameters of the acoustic signal emitted, such as output power, signal frequency, and pulse length affect the performance of the instrument and influence its usefulness in various marine environments. Increased output power allows greater penetration into the substrate, however, in the case of harder seabeds (for example gravels or highly compacted sands), or very shallow water, will result in multiple reflections and more noise in the data (McQuillan *et al.*, 1984). The resolution of acoustic systems is defined as their ability to differentiate closely spaced objects, or resolve discrete echoes returning from closely spaced reflectors. In general, higher frequency broadband signals are more discriminating, although higher frequencies are preferentially filtered out in the environment. Higher frequency systems (2 to 20 kHz) produce high definition data of sediment layers immediately below the seafloor. These higher frequency signals have shorter wavelengths, and they are able to discriminate between layers that are close together (e.g. 10's of cms). Lower frequency systems give greater substrate penetration, but at a lower resolution. Longer pulse length transmissions (or 'pings') yield more energy, and result in greater substrate penetration. On the other hand, longer pulse lengths decrease the receivers ability to discriminate between adjacent reflectors, thus decreasing the system

resolution. However, the penetration depth depends on the hardness of the overlying layers and the presence of gas deposits, such as methane (Davis *et al.*, 2002). The presence of sub-surface gas deposits can significantly degrade an acoustic signal because it may result in a negative R impedance value (see Equation 2 above). In addition to the frequency and bandwidth, other factors affecting system resolution are beam width (or area of seabed insonified), depth of water below the transmit/receive array, signal to noise ratio, and electronic signal processing.

The resolution obtained in a sub-bottom profile is related to the frequency of the acoustic source, higher frequencies providing greater detail. However the attenuation of sound and therefore bottom penetration is inversely related to frequency, necessitating a variety of sub-bottom profiling tools specific to different marine environments (Stoker *et al.*, 1997). Single-beam acoustic reflection systems operating within the low kHz range are useful for high resolution assessment of the top 100 m of sedimentary material below the sea floor, with penetration depth inversely related to transmit frequency. The correlation between signal frequency and penetration is not linear – at frequencies below approximately 800 Hz the penetration increases dramatically (Figure 6.2).

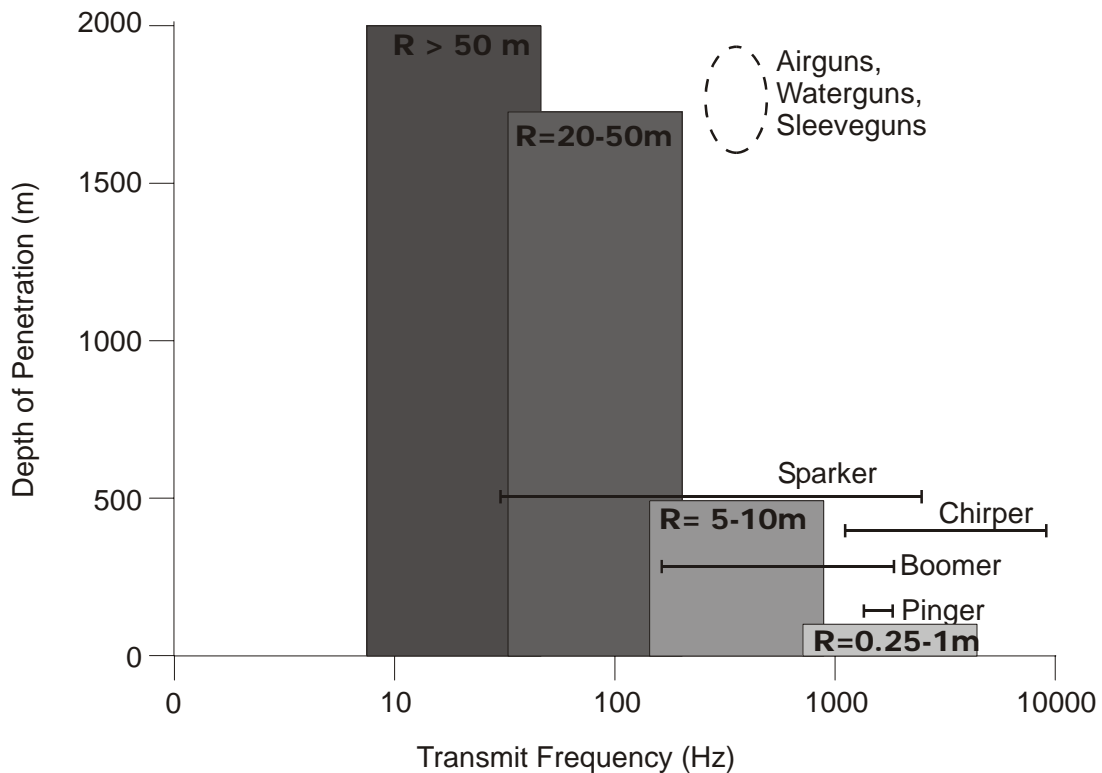


Figure 6.2. Frequency, depth of penetration, and approximate system vertical resolution (R), with typical sonar system ranges (depicted by horizontal bars). After Stoker *et al.* (1997).

Sub-bottom profiling systems are limited by a narrow swath width (or small area of seabed insonified), so comprehensive coverage of the seafloor is time-consuming and expensive to obtain. As with other single-beam acoustic methods, the footprint is relatively small and dependent on depth. Acquisition lines are often spaced closely together or in transects across the area of interest (depending on the purpose and constraints of the survey), allowing sub-surface reflectors to be traced in three dimensions from line to line. Shallow water surveys allow faster shot rates and vessel

speed, although speeds greater than 10 knots may result in interference due to high degrees of ship noise and water turbulence (Stoker *et al.*, 1997).

6.3. Types of Sub-Bottom Profilers

In the years since the first crude sub-bottom profiling systems were developed (Knott and Hersey, 1956), a multitude of processes and techniques have been utilised to produce acoustic pulses, detect their returning echos, and subsequently process this information into a meaningful representation of acoustically reflective surfaces. As discussed above, limitations related to frequency, resolution and depth of penetration have led to a diversification in system design (Lean and Pratt, 1991). Many types of sub-bottom profilers are currently available, and there is a great range of variation between types of systems and also between various equipment manufacturers.

High frequency (> 2-3 kHz) boomer, pinger and chirper systems are tailored to give very detailed information about near surface features, with bottom penetration in the order of 100 m. Medium frequency (~1 kHz) profilers such as the sparker system can penetrate to a depth of approximately 500 m, and maintain relatively good resolution. Very low frequency and high energy systems (<1 kHz), such as airgun systems may penetrate a number of kilometres into the seabed, with a corresponding reduction in resolution (Stoker *et al.*, 1997).

Table 6.1. System characteristics of various classes of sub-bottom profilers.

System	Operating Frequency	Acoustic Source	Receive Array	Typical Resolution	Depth of Penetration	Source Mounting Style
Sparker	50Hz - 4 kHz	Electrical spark in water	Towed streamer	> 2 m	500 m	Towed
Chirper	Swept 1-10kHz	Swept frequency transducer (1-10kHz)	Transducer	~0.05 m	< 100 m	Hull mounted or towed
Boomer	300 Hz to 3 kHz	Boomer plate	Towed streamer	0.5 to 2 m	< 200 m	Towed sled
Pinger	Tuned between 2-12 kHz (eg 3.5kHz)	Combined piezo-transducer/transceiver	Combined piezo-transducer/transceiver	0.2 m	10 - 50 m	Hull mounted

This review will focus on the high to medium frequency systems as these are most relevant for the study of modern and recent seabed geomorphology in shallow marine environments. Table 6.1 summarises some of the basic details about various classes of sub-bottom profiling systems.

6.3.1. High frequency systems

High resolution, tuned-frequency profilers typically operate at frequencies that range between 1 to 30 kHz. This achieves relatively high depth resolution, however the bottom penetration is significantly less than that obtained by lower frequency systems.

Signal penetration is further limited in coarse sediment or highly compacted sands, due to scattering (Damuth, 1975, Whitmore and Belton, 1997). Tuned-frequency profilers typically use the same transducer for both transmitting and receiving the signal. The source signal frequency is also highly consistent between pulses in order to provide better resolution and tracking of thin subsurface layers.

Chirper Systems

Chirper systems are so named due to their emission of a chirp sound (rather than a ping) for a single frequency unit. A chirp sonar is a wide-band, frequency modulated (FM) sub-bottom profiler that is capable of producing very high resolution profiles in soft sediments. The system generates an FM pulse from a resonant source that is phase and amplitude compensated, which helps to suppress noise (Schock *et al.*, 1989, McGee 1995). These units obtain very good subsurface images due to their ability to sweep through a range of frequencies (by varying the amplitude and frequency of the emitted pulse in a predetermined pattern), usually between 1.5 to 11.5 kHz for shallow water applications, or as low as 0.4 to 8 kHz for deep seismic reflection (McGee 1995). A complex signal processing algorithm correlates returns, and estimates the attenuation of sub-bottom reflections by waveform matching with a theoretically attenuated waveform. Chirp sonars are typically able to achieve vertical resolutions down to ~ 5 cm, and can provide relatively artefact free sub-bottom profiles attenuating to 100 m depth (Schock *et al.*, 1989). Longer chirp pulses can be used for deeper penetration. Noise is suppressed, and resolution is improved in chirp systems due to lower peak input power to the transducer, and transducer voltage is controlled to prevent source 'ringing' (decaying oscillations in the transmitted acoustic pulse). The chirp system transducer may be towed or hull mounted, and can operate in water as shallow as 30 cm (Schock *et al.*, 1989), or can be used in the deep ocean if mounted within a towed vehicle (Parent and O'Brien 1993).

Pinger Systems

Single-beam acoustic sub-bottom profilers and bottom-detection units are often referred to as 'pingers'. These systems are similar to the depth-sounding units used for navigation on most vessels, however are tuned to a lower frequency for penetration into the seabed (Luskin *et al.*, 1954). Single-beam systems are described more fully in Section 3.2. Pinger systems comprise a piezoelectrically resonated ceramic element within the transducer/transceiver, to produce (and receive) a controlled pulse length, narrow-frequency acoustic signal (McGee, 1995). Pinger-type profilers are specifically tuned to a particular frequency. For simple bottom detection in shallow waters this frequency may be as high as 200 kHz, however for significant water depth and substrate penetration frequencies of 12 or most commonly 3.5 kHz are employed (Damuth, 1980). Operation of pinger sub-bottom profilers at 3.5 kHz typically results in 10 - 50 metres of substrate penetration, at a resolution down to 0.2 metres, depending upon sediment type.

6.3.2. Low and medium frequency systems

Many low frequency systems are regarded as low-resolution profilers – for example water and air guns, sparkers, sleeve exploders, bubble pursers, and boomers. In these systems, the energy source transmits a signal of broad spectral content, and requires separately towed hydrophone arrays for receiving the return signal.

Sparker Systems

The sparker is a relatively higher powered sound source, dependant on an electrical arc which momentarily vaporizes water between positive and negative electrodes (Trabant 1984). The collapsing bubbles produce a broad band (50 Hz - 4 kHz) omnidirectional acoustic pulse. Sparkers typically yield better penetration, but poorer resolution than boomer systems, with depth of penetration up to 500 metres (Stoker *et al.*, 1997), and vertical resolution usually greater than 2 metres (depending on energy settings). Sparker sources are commonly used in regions where compacted sands and other coarse semiconsolidated sediments are found. Some sparker seismic systems have been developed in which the electrical discharges take place at the focus of a paraboloidal reflecting surface, in order to obtain a downward-oriented, approximately plane acoustic wavefront. This system enables a greater substrate penetration (Gasperini *et al.*, 1993).

Boomer Systems

Boomer sub-bottom profilers comprise an insulated metal plate adjacent to an electrical coil, typically mounted on a towed catamaran. This electro-mechanical transducer is known as a 'boomer plate'. A powerful electrical pulse, generated by a shipboard power supply and capacitor banks discharges to the electrical coil, causing a magnetic field to explosively repel the metal plate. This energetic motion generates a broad band, high amplitude impulsive acoustic signal in the water column (Trabant 1984, McGee 1995). The frequency of the acoustic pulse is in the range 300 Hz to 3 kHz (or more) with the majority of the energy being directed vertically downward (Verbeek and McGee, 1995). Most boomer systems rely on a (potentially dangerous) high voltage power supply and capacitor banks for the generation of the high voltage electrical pulses required. More recent developments in efficient, low voltage boomer systems have circumvented some of the problems inherent with the high voltage systems (Davis *et al.*, 2002). Resolution of boomer systems ranges from 0.5 to 2 m, and penetration typically ranges from 50 to 200 metres, depending on sediment type. A limitation of these systems is that the transmitted acoustic pulses do not have the repeatability necessary to provide high accuracy measurements of seafloor properties.

Other Sub-Bottom Profiling Systems

A large number of lower frequency sub-bottom profiling systems are currently in use, including low frequency sparkers, parametric echo-sounders, airgun/sleevegun systems (of various volumes), watergun systems, and multi-channel receive techniques. These systems are not treated here as they are more relevant for deeper water geological investigations (Stoker *et al.*, 1997, Lean and Pratt, 1991, Verbeek and McGee, 1995). Some shallow-water work has been undertaken using single, small-volume airgun systems coupled with multi-channel receive arrays, achieving resolution approaching that of standard 3.5 kHz (pinger) sub-bottom profiles, although obtaining much greater substrate penetration (Lee *et al.*, 2004).

6.4. Interpretation of Surficial Seabed Properties from Sub-Bottom Profilers

The physical properties of the seabed (eg sediment bulk density, grainsize) can be approximated from analysis of the acoustic reflection response, with sediment depth dependant on the resolution of the profiling system. Much information can be gained about benthic habitats through the analysis of sub-surface reflectors, and the thickness of surficial sedimentary units. Analysis of both newly acquired (and the large volumes of previously archived) sub-bottom profiling information is a relatively under-utilised source of information about seafloor sedimentary environments. A number of studies have attempted to quantitatively determine or discriminate sedimentary features of the seafloor from profiling data (de Moustier and Matsumoto, 1993). These have involved the direct measurement of a pressure coefficient of the seafloor (Kim *et al.*, 2002), statistical approaches utilising the entire acoustic echo signal, such as the Karhunen-Loeve transform (Milligan *et al.*, 1978), and highly quantitative approaches such as the inversion of boomer acoustic impedance values (Davis *et al.*, 2002), and use of swept-frequency chirp system impedance and attenuation coefficients (LeBlanc *et al.*, 1992a, Kim *et al.*, 2002).

6.4.1. Shallow sub-bottom reflectors – links to benthic habitats

Depositional and post-depositional processes play a major role in determining the nature and spatial distribution of seafloor sediments, integrating factors such as geological setting, sediment supply, oceanographic conditions, and sea-level change (Davis *et al.*, 2002). Acoustic reflection systems can provide important insights into the physical character of the seabed and sub-surface that help in the interpretation of other remotely sensed benthic data (such as sidescan, single and multibeam echosounder data, video, satellite and airborne scanner imagery) and indicate the physical processes responsible for present-day form and distribution of benthic habitats. Sub-bottom reflectors provide information relevant to an assessment of present day benthic habitats at a range of scales. A basic measure provided is the depth to the bedrock reflector that underlies any seabed sediment, which indicates whether an area is a site of sediment accumulation or erosion. Also, former reefs now buried by sediment can be identified in sub-bottom profiles, providing a useful record of major environmental changes that have occurred (Figure 6.3).

Similar insights can be provided into the spatial distribution of benthic habitats, for example bedrock reflectors may extend to the surfaces and provide habitats that may significantly contrast with the surrounding seabed (Figure 6.3). These types of acoustic data can also allow the discrimination of relatively hard sedimentary bottoms from bedrock reefs, which may have similar echosounder characteristics or may not be visually discernible when covered by marine organisms. The dynamics of benthic environments can also be indicated by surface and preserved subsurface bedforms. For example, dune and sand-wave structures in sandy deposits indicate they are highly mobile, while planar bedforms in certain areas reflect significant sediment accumulation (Figure 6.3).

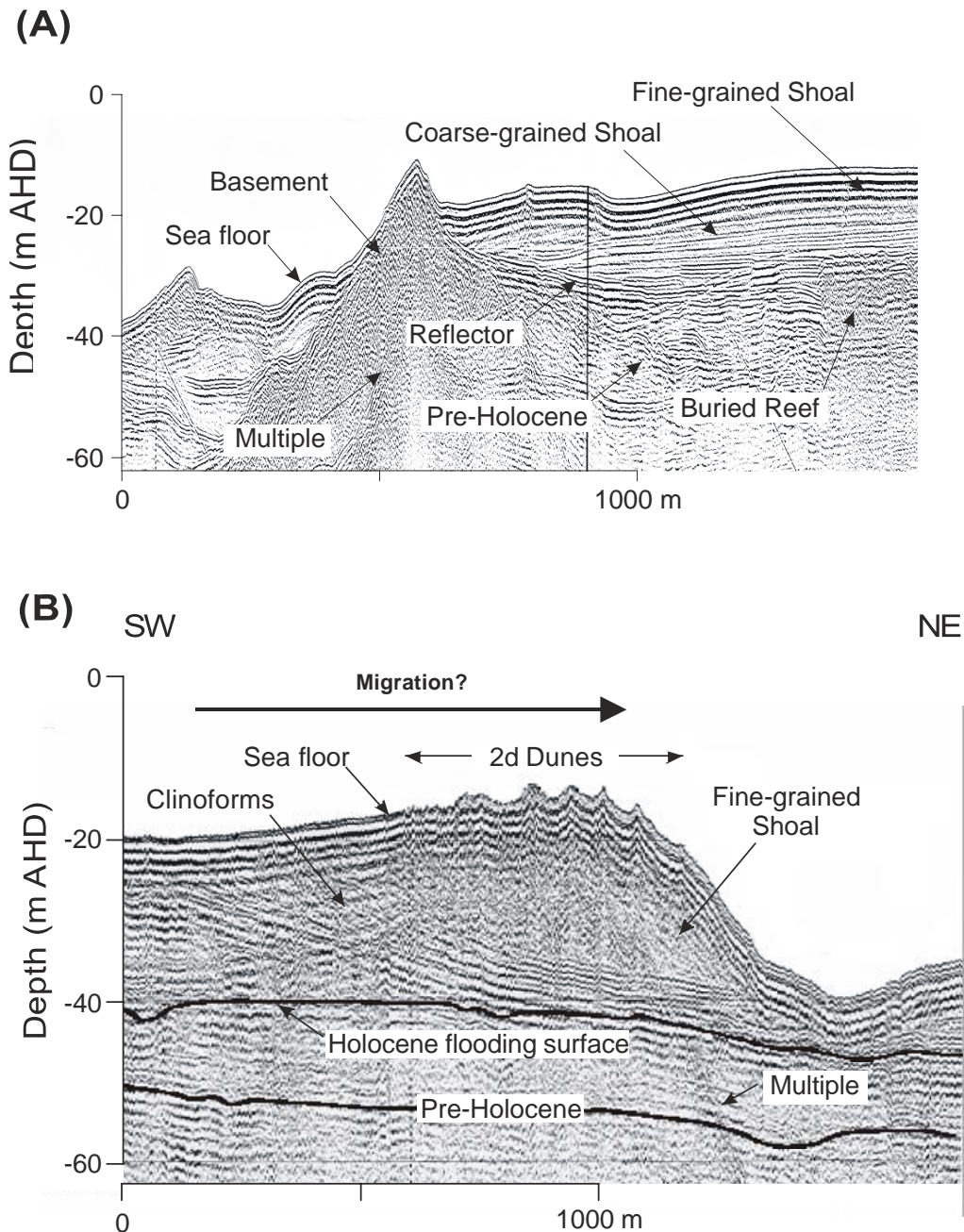


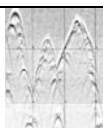
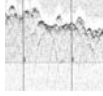
Figure 6.3. Boomer sub-bottom profiles of the seafloor around the Whitsunday Islands, Great Barrier Reef platform, Australia (after Heap, 2000). The system used was an EG & GTM Uniboom sounder, triggered every 0.5 s at 200 J, and towed 0.3 m below the surface 11 m behind an 8 element hydrophone array. (A) The reflectors reveal a range of recent, Holocene, and pre-Holocene features, showing an exposure of bedrock surrounded by recent sand accumulations. (B) Steeply NE dipping bedding structures (clinoforms) and surficial dune bedforms record the accumulation and present-day movement of sand into a depocentre.

6.4.2. The Damuth classification scheme

Since the 1960's, 3.5 kHz systems have been used to gain seafloor penetration of 100 m or greater, and Damuth (1975) developed a surface sediment classification system for 3.5 kHz echograms based on an earlier, lower penetration 12 kHz system data (Hollister 1967). The simple echo characteristics of the seafloor may be classified into

three main categories, based on parameters that include the clarity and continuity of echoes, which show a qualitative relationship with seafloor morphology. These include distinct echoes, prolonged indistinct echoes, and hyperbolic indistinct echoes (Table 6.2).

Table 6.2. Description and examples of echo character types (after Damuth, 1980, Whitmore and Belton, 1997, Rollet et al., 2001).

Class	Sub-Class	Type	Example	Description
Distinct		IA		Sharp continuous with no sub-bottom reflectors
		IB		Sharp continuous with numerous parallel sub-bottom reflectors
		IC		Sharp continuous with non-conformable sub-bottom reflectors
Indistinct	Prolonged	IIA		Semi-prolonged with intermittent parallel sub-bottom reflectors
		IIB		Prolonged with no sub-bottom reflectors
	Hyperbolae	IIIA		Large, irregular hyperbolae with varying vertex elevation (>100m)
		IIIB		Regular Single hyperbolae with varying vertices and conformable sub-bottom reflectors
		IIIC		Regular overlapping hyperbolae with varying vertex elevation (<100 m)
		IIID		Regular overlapping hyperbolae with vertices tangential to the seafloor
		IIIE		Type IIID hyperbolae with intermittent zones of distinct (IB) echoes.
		IIIF		Irregular Single hyperbolae with non-conformable sub-bottoms

These parameters were further sub-divided based on presence or absence of a sub-bottom reflectors, and the hyperbolae characteristics which relate to the morphology of the seafloor. Different types of echoes form through the interaction between the seabed and the echo-pulse, and sediments affect the echo return depending on their density, layering structure, and topography (Flood, 1980).

To construct an echo-character map based on 3.5 kHz data, the bottom returns of all available survey lines across a region need to be examined to develop a classification system that is suitable and specific to that area. Importantly, the number and spacing of survey lines and the variability of echo types will determine whether it is reasonable to extrapolate between them, and thereby produce meaningful maps of the seabed (Damuth, 1980).

However, comprehensive ground-truthing information is required to validate these interpretations. These should include a large number of bottom samples, such as sediment grabs, cores, or dredges, from varied geographic and bathymetric locations as well as from each distinct facies type encountered (Whitmore and Belton, 1997). Although relatively qualitative, this method has been effectively used to classify both deep and shallow water sediments in numerous studies (Hollister 1967, Damuth, 1975, Damuth, 1980, Blum and Okamura, 1992, Whitmore and Belton, 1997, Rollet *et al.*, 2001).

6.4.3. Quantitative sonar classification

The remote classification of shallow marine sediments can also be carried out in a more quantitative manner with a high resolution chirp sonar. LeBlanc *et al.* (1992a) first used this equipment to characterise depositional environments using acoustically derived density, sediment compressibility, rigidity, and acoustic impedance parameters (based upon a function of the Rayleigh reflection coefficient, given in equation 2 above). From these measured values, models allow the prediction of sediment sound velocity, porosity, and wet bulk density (Figure 6.4).

This method relies on the construction of a database of quantitative reflection parameters for each depositional environment, necessitating significant ground truthing (e.g. sediment cores). Further work by LeBlanc *et al.* (1992b) focussed on the determination of mean sediment grain size based upon modelling of acoustic attenuation in sediments. Based upon a large compilation of historical attenuation data, an empirical equation was developed to predict sediment type in real time from chirp sonar data. More specifically, a relationship between sediment type and ‘relaxation time’ is discussed, which equates to a measure of the time needed to change the density by application of a sudden pressure (Figure 6.5).

Further work into classification techniques for chirp sonar data has resulted in the development of techniques that utilise the entire acoustic echo signature, rather than just the reflection coefficient (Kim *et al.*, 2002). These have involved cluster analyses of whole datasets (Milligan *et al.*, 1978), and statistical properties of the bottom type based on time-frequency analysis (Andrieux *et al.*, 1995). More recently, application of a similarity index to the uncorrelated principal components of the echo signature (which are derived from the Karhunen-Loeve transform) have been used to classify the seafloor (Kim *et al.*, 2002). This index is based upon the first principal component of the reflected echo (see Kim *et al.*, 2002), and has been shown to correlate with sediment facies based upon grain size, particle sorting, hardness, and homogeneity of the substrate.

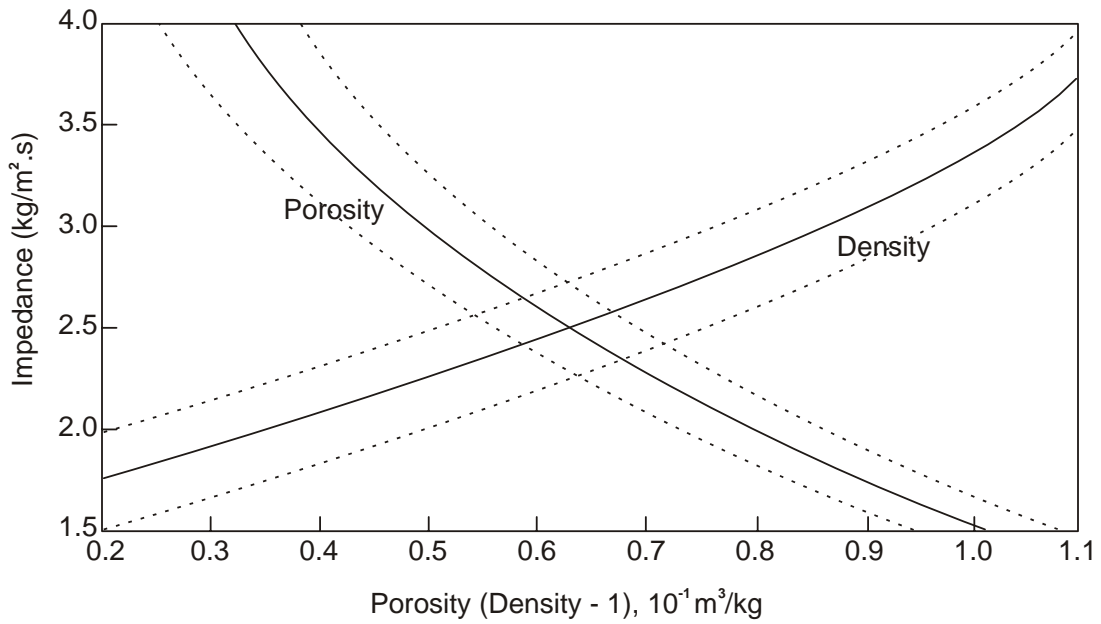


Figure 6.4. Acoustic impedance as a function of both sediment porosity and wet bulk density (after LeBlanc et al., 1992a).

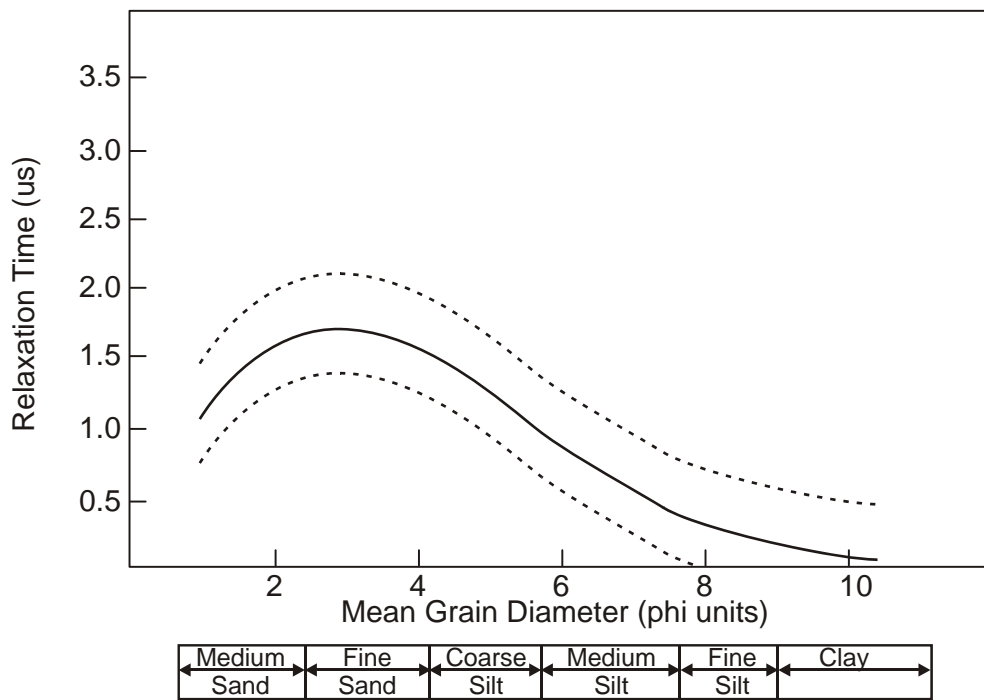


Figure 6.5. Sediment acoustic attenuation measurements, or relaxation time values plotted as a function of mean grain size in phi units (after LeBlanc et al., 1992b).

7. A COMPARISON AND APPLICATION OF ACOUSTIC SYSTEMS

7.1. Introduction/Background

This chapter describes a systematic comparison of the GeoAcoustics GeoSwath against the Reson 8125 and Reson 8101 Multibeam systems. It has been drawn from a technical report prepared by Fugro Survey in preparation for a major benthic mapping project off the Victorian coast in Australia. The prospect of broad scale habitat mapping on a commercial scale off the Victorian coastline triggered the creation of a decision making process to identify the most appropriate hydro acoustic and video survey hardware for that project. Carried out in Marmion Marine Park, this selection process came to be known as the “Marmion trials”.

Acquisition, Processing and analysis of acoustic data is discussed. A key issue addressed in this Chapter was to determine which of several possible full coverage acoustic systems would be preferable for the Victorian task; notably whether an interferometric sidescan or a multibeam system would be preferred. The GeoSwath interferometric system showed considerable potential, but the comparison work undertaken led to the selection of a Reson 8101 system for the survey. Subject to a few outstanding issues, none of which are insurmountable, the interferometric system will provide a good alternative to the established Multibeam technologies. Multibeam backscatter data from the systems is also discussed, and the prospect of this replacing traditional Sidescan sonar is suggested. Data deliverables for habitat mapping projects are described.

7.1.1. State of Victoria Habitat Mapping Project

A series of marine parks under the management of Parks Victoria and the Australian National Heritage Trust were targeted for broad scale habitat mapping. These parks totalling more than 70,000 hectares were generally in remote exposed locations, far from port or shelter (see Figure 7.1). Water depths ranged from 10 to 90m. 100% mapping coverage was required for each park, such that a full understanding of the existing habitats within those parks could be established.

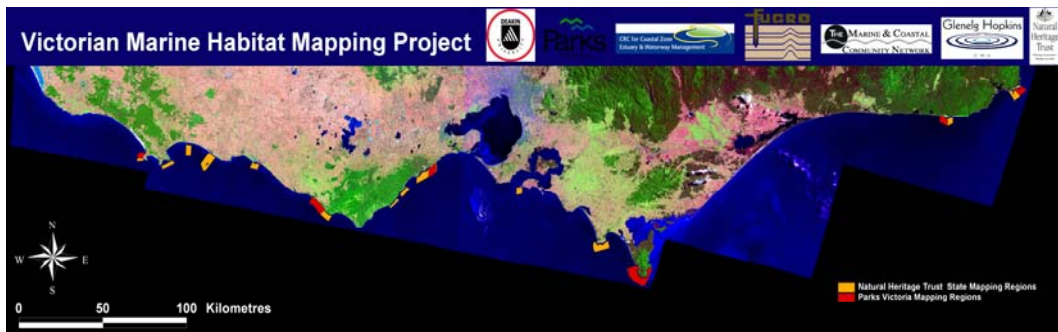


Figure 7.1. Polygons representing the marine parks to be mapped. The remote locations and long transit times between sites imposed some constraints on the project.

7.1.2. Marmion Marine Park: Area A

Marmion Marine Park is located off the metropolitan region of Perth, Western Australia (Figure 7.2). A few minutes steam from Hillary's boat harbour, near Perth in Western Australia, this area is both easily accessible, and has a high variability of habitats.



Figure 7.2. Primary area for habitat mapping trials. A 2km by 0.5km detailed site survey over ecologically sensitive seabed of coastal habitat mapping significance within the Marmion Marine Park. Surveyed with Reson 8101, Reson 8125 and GeoAcoustics GeoSwath Multibeam systems, and EG&G 272, C-Max and Klein 5500 Sidescan sonar systems, this data provides an excellent proving ground.

7.1.3. West End, Rottnest Island: Area B

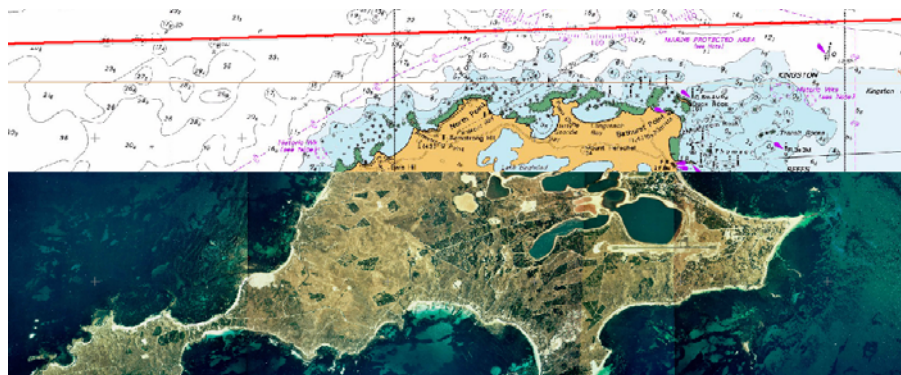


Figure 7.3. A single line of data was acquired for deep water trials west of Rottnest Island with a GeoAcoustics GeoSwath interferometric sonar.

In order to establish a realistic and reliable operational maximum depth for the GeoSwath, a transit from shallow to deep water was selected off the north-western end of Rottnest Island, Western Australia (Figure 7.3). Depths ranged from 30-200 metres.

7.2. Objectives

Objectives of the trials were grouped into specific commercial requirements for the Fugro Group, and generic habitat mapping requirements as follows:

Fugro Survey Requirements

- Validate the Starfix interface to the GeoSwath system in both an online driver capacity and an import wizard for the data logged by GeoSwath Plus software
- Field test a wireless radio link for construction applications
- Validate the GeoSwath XTF data format
- Field test the F180 motion sensor to attempt to replicate time jumps that have been reported in some field operations
- Train new Fugro Survey Pty Ltd field personnel on Multibeam operations, calibrations and systems
- Produce Fugro marketing material that may benefit the company and be incorporated into brochures
- Validate the Starfix interface to the Klein 5500 system in both an online driver capacity and an ability to log XTF data
- Increase our knowledge of the GeoSwath

Habitat Mapping Requirements

- Determine the true usable swath width of the GeoSwath systems in varying water depths over varying seabed types
- Determine the maximum useful operating water depth of the GeoSwath
- Validate the quality of the bathymetry acquired by the GeoSwath interferometric system in comparison with the known quality of the Reson 8101 and Reson 8125 systems
- Conduct a comparison of GeoSwath, Seabat, EG&G analogue Sidescan and Klein 5500 digital backscatter
- Determine the angular and spatial extent of the known data ‘holiday’ under the nadir of the GeoSwath system
- Exchange technical information with the Coastal CRC to determine the required deliverables for habitat mapping and further Fugro’s knowledge base in this field
- Derive recommendations for the Victorian habitat mapping project
- Conduct a side-by-side system comparison of the GeoSwath, 8101 and 8125 for the purpose of habitat mapping

Personnel

Eleven personnel from Fugro and the University of Western Australia were involved in the comparison exercise.

7.3. Equipment

To provide a unbiased comparison of the various hydro acoustic systems, the operating environment for each of the surveys had to be identical. The following constraints were set for all data collection during the trials;

- The same vessel

- The same bow mounting
- The same vessel driver
- The same navigation equipment
- The same motion sensor
- The same survey lines in the same direction
- The same survey operators

Vessel

The vessel used for the trials was the 12.5m long F/V Mirage (Figures 7.4 and 7.5), an ex-fishing vessel owned by Hillary's Yacht Club.



Figure 7.4. The M/V Mirage – A photo of the Mirage showing the GPS antennas and the bow installation to mount the acoustic sensors.

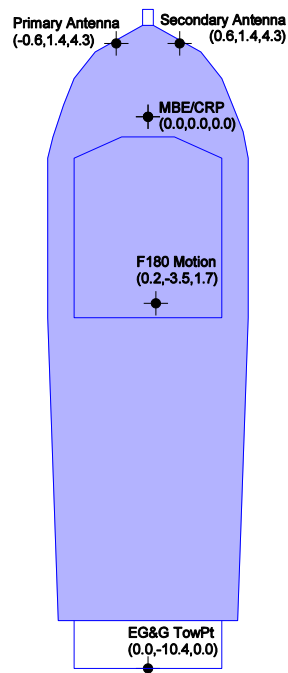


Figure 7.5. Offset diagram of the M/V Mirage – showing the three dimensional offsets of the equipment installed on the vessel.

Surface Navigation Sensors

The surface navigation sensors (Figure 7.6) used for the trials were the same for the entire trials; this largely eliminated external error sources.

- Starfix.Seis online navigation system
- Starfix online logging and display system
- F180 inertial position, heading and motion sensor
- Fugro OmniSTAR 3000L differential corrections receiver
- Honda 2.2kV generator
- 2 Uninterruptible power supplies

Backup/spare systems

- Fugro OmniSTAR 3000L differential corrections receiver
- Applanix POS M/V inertial position, heading and motion sensor

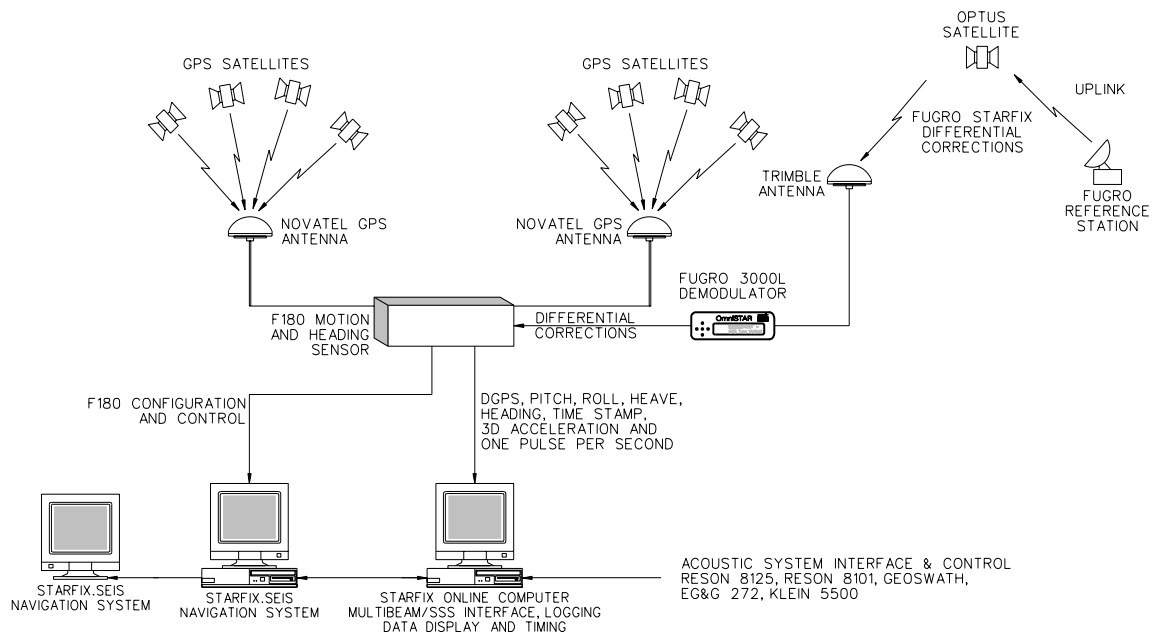


Figure 7.6. Surface navigation equipment.

Transducer Mounting

Traditional single beam operations using a vessel of opportunity, are typically conducted using an over the side pole arrangement. Unfortunately, this installation approach is often adopted for Multibeam operations resulting in pole wobble, which introduces motion artefacts into the bathymetry data. Rectifying these artefacts during data processing is extremely time-consuming. At best it is a workaround. More commonly, and at worst they cannot be fixed, thus compromising the quality of the bathymetric surface.

Best practice methodologies for transducer installation are direct hull mounted flanges. This requires the boat to be slipped, a flange and cable gland to be installed through the vessel hull. Divers are then used to install the transducer, and wet mate the deck cable to the transducer. Second tier practice is to bow mount the transducer with a flush mounted pole running parallel to the vessel bow (see Figure 7.7). This

ensures the pole does not have sufficient unrestrained length to introduce wobble. As the boat travels faster, the mount becomes more stable.

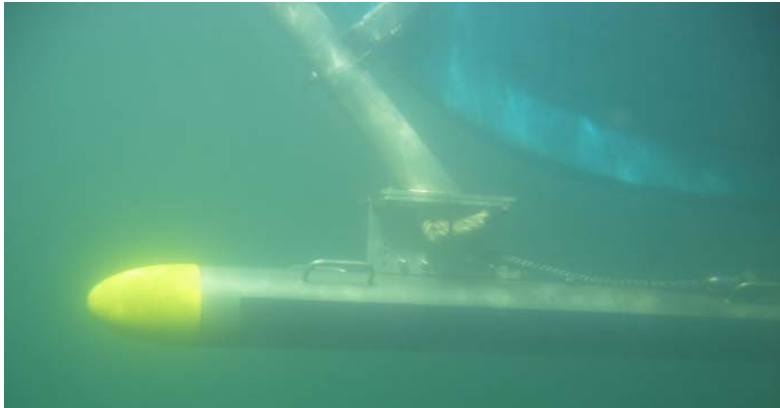


Figure 7.7. Bow pole arrangement for fixing the hydro acoustic transducers. All systems were mounted to this common flange. This ensured no additional error sources were introduced in the systematic comparison. In this case, the freestanding section is less than 300mm in length.

In the case of MV Mirage, the hull is wooden, precluding the installation of a hull flange. Instead, an aluminium bow pole was employed. The pole was purpose designed for the shape of Mirage's bow, to minimise the freestanding section (Figure 7.7).

Hydro Acoustic Sensors

The following hydro acoustic devices were mobilized for the trials:

- GeoAcoustics GeoSwath MBES
- Reson Seabat 8101 MBES
- Reson Seabat 8125 MBES
- EG&G 272 Analogue Sidescan sonar
- Klein 5500 multiple beam digital Sidescan sonar
- C-Max Sidescan sonar

GeoAcoustics GeoSwath

The GeoSwath (Figure 7.8) is an interferometric swath system that can be configured either with 125 kHz or 250 kHz transducers. The unit used for these trials was fitted with 250 kHz transducers. As this system is interferometric the number of beams across a swath is defined by a user defined sample rate. Essentially this sample rate is configured in software rather than by the physical design of the transducers.

GeoAcoustics published (GeoSwath 2004) specifications for the GeoSwath state that the system is capable of a swath width twelve times the water depth or 161 degrees with a maximum operating depth of 100m. The GeoSwath produces a travel time and vertical angle for each beam across the swath and two channels of Sidescan intensity data. Data is logged to proprietary Raw Data Files (RDF).

Due to its claims of high resolution, very wide swath, and excellent backscatter, the GeoSwath was considered a likely candidate for the Victorian habitat mapping project.



Figure 7.8. The GeoSwath transducer mounted on MV Mirage bow mount.

It should be noted that the GeoSwath trials were not without problems. Field trials were initially carried out on October 2004 and repeated in April 2005.

Unfortunately, the results from the first survey were unacceptable. Bathymetry quality was poor, backscatter was unusable, and there was a clear time stamping issue that could not be resolved. Most of these problems were identified as software problems, or user documentation related.

In order to give the system a further opportunity, GeoAcoustics were invited to attend a second trial. With the addition of Tom Hiller of GeoAcoustics, and new software, data quality was significantly improved. Once again, this trial revealed a problem in the synchronisation of the GeoSwath time stamping algorithm to GPS 1 pulse per second (PPS). This jitter in acquisition time stamps resulted in motion artefacts visible in the resulting bathymetric surface. GeoAcoustics made attempts to post-process this error out of the data, but it was still apparent in the resulting data. Data from the second trial is presented in this document. The first trial has largely been discarded.

Reson Seabat 8101

The Reson 8101 (Figure 7.9) is a traditional beam forming Multibeam system that operates on a frequency of 240 kHz. This system measures 101 ranges at 1.5 degree spacing resulting in a 150 degree (or 7.4XWD) swath to a maximum depth of 200m. Whilst not at the cutting edge of technology, due to its reliability, accuracy and flexibility, the 8101 is considered one of the workhorses of the commercial Multibeam survey industry.

The 8101 produces a travel time for each beam, two channels of Multibeam Sidescan and two channels of snippets backscatter data derived from the individual beams. All these are logged to XTF files in real time.

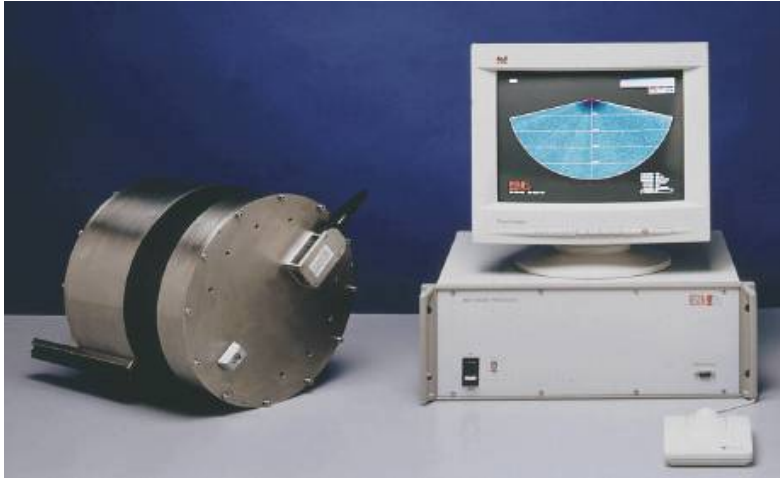


Figure 7.9. The 8101 transducer and the topside 81P processor.

Unfortunately due to operational time constraints the only operational time window available for trials with the 8101 was during unfavourable weather. Notwithstanding this, the results from the 8101 are excellent.

Prior to the trials, the 8101 was considered to be the second best option for the Victorian habitat mapping project. Its 150 degree swath width was considered a limitation to cost-efficient, broad scale mapping. The system was operated on a 75m range using standard Fugro operation settings.

Reson Seabat 8125

The 8125 (Figure 7.10) operates at a frequency of 455 kHz to produce 240 individual beams at 0.5 degree spacing from the transducer. This system has been designed for shallow water channel and clearance surveys and as such has a relatively narrow swath width of 120 degrees and a shallow maximum operating depth between 45m and 60m depending on seabed type.



Figure 7.10. The Reson 8125 transducer on the bow mount of the MV Mirage. Note the requirement for the SVP probe alongside the head. The flat acoustic transducer face requires an instant and accurate value for the velocity of sound at the head. This is used for determination of direction of acoustic reception.

In a similar manner to the 8101, the 8125 produces a travel time for each beam, two channels of Multibeam Sidescan and two channels of snippets backscatter data derived from the individual beams. All these are logged to XTF files in real time.

Due to the relatively narrow scanning sector combined with the maximum depth limitation, the 8125 was not a considered a viable option for the Victorian habitat mapping project, but it is widely considered the benchmark in Multibeam echosounder systems, by which all other systems are compared.

The system was operated on a 75m range using standard Fugro operation settings.

EG&G 272 analogue Sidescan sonar

The EGG 272 analogue Sidescan sonar (Figure 7.11) is a conventional single frequency sonar operating at 100 kHz. For the trials, the 272 was run on a range scale of 75m per channel. Chesapeake SonarWiz was used to perform the A/D conversion, and data was logged to XTF files via a post process format conversion routine.

Traditional survey techniques for the gathering and assessment of geological and benthic presence on the seafloor commonly use Sidescan technology. As such, the Sidescan sonar was considered as a basic requirement.



Figure 7.11. The tow fish and its descendant, the GeoAcoustics 159D, are the real workhorses of the shallow geophysical industry. Simple to operate and maintain, they are well understood, robust and reliable.

Klein 5500 multiple beam digital Sidescan sonar

Kindly provided by the DSTO the Klein 5500 digital Sidescan sonar (Figure 7.12) consists a five beam Sidescan sonar (Figure 7.13) designed for Hydrographic applications requiring high resolution images of the sea floor and bottom obstructions while operating at tow speeds of up to 10 knots.

The system achieves this by creating five acoustic pings simultaneously at different frequencies along the length of the 2m tow fish, thereby ensonifying 2m of seabed along track with each ping and enabling the fish to move 2m before the next ping without creating data gaps/holidays. With a 100m per channel range scale the fish can ping seven times per second and therefore move at 14 knots.

The Klein 5500 is widely considered the ‘Rolls Royce’ of Sidescan sonar’s. Whilst the equipment was not available or considered for the Victoria habitat mapping project, it was included in the trials as it an ideal benchmark.

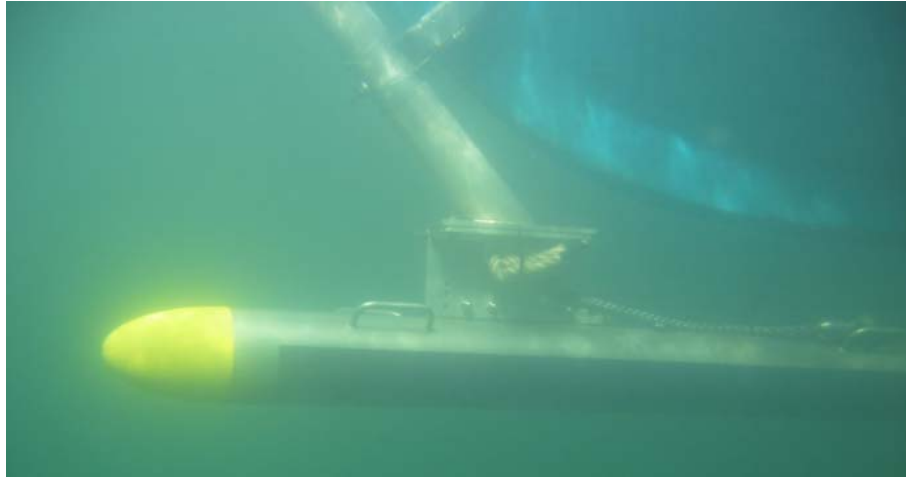


Figure 7.12. The Klein 5500 installed on the bow of MV Mirage. Although this is not a standard operating mode, it provided excellent geo-referencing of the data, and was the safest option in such shallow water.

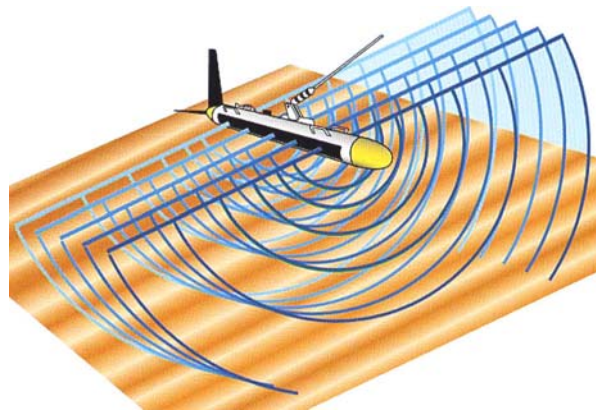


Figure 7.13. Klein 5500 beam pattern. With the five simultaneous beams, 100% coverage at a high survey speed is possible.

C-Max CM2 digital Sidescan sonar

The C-Max CM2 digital Sidescan sonar (Figure 7.14) is modern, dual frequency sonar operating at either 325 or 780 kHz. A second unit operating on 100/325 is also under manufacture but was not available for trials.

For the trials the CM2 was run on a range scale of 75m per channel.



Figure 7.14. The CM2 digital tow fish off the stern of MV Mirage. As the fish has no fixed mounting point, it had to be towed behind the vessel. Also shown is the “CM2 C-Case” all in one acquisition and logging unit.

Towed video camera

The University of Western Australia provided a towed video camera system for the purposes of visual inspection (ground truthing) of the surveyed area (Figure 7.15). The system comprised a high resolution CCD colour camera in an underwater housing. A composite video signal to a topside digital video logging (DV) combined with a digital video overlay of time and position was used to geo-reference the video data. No USBL and no artificial lighting were employed for these trials.



Figure 7.15. The UWA towed video system. The underwater lights in this photo were not used in these trials.

7.4. Survey Design and Parameters

All coordinates are referenced to the World Geodetic System 1984 (WGS84) datum. Fugro's Differential GPS Reference Stations are currently defined in the International Terrestrial Reference Frame 2000 (ITRF2000 Epoch 2004.75) datum. Due to the continual refinement of the WGS84 reference frame, for all cases, the transformation parameters indicate that the WGS84 and ITRF2000 reference frames are essentially identical.

Datum

Reference Spheroid : World Geodetic System 1984
Semi Major Axis : 6378137.000m
Inverse flattening : 298.257223563

The provided survey locations are grid coordinates in the Universal Transverse Mercator grid projection.

Grid projection

Projection : Universal Transverse Mercator
Latitude of Origin : 0°
Central Meridian : 117° E (UTM Zone 50)
Central Scale Factor : 0.9996
False Easting : 500000m
False Northing : 10000000m
Units : Metres

A primary factor in the survey line design was the purpose of the survey. Commercial surveys typically utilise a line pattern with optimally spaced parallel and an agreed line overlap. For the Marmion area depth range of 5m to 16m (average 10m), and the specific project requirements, a line spacing of 20m was used (see Figure 7.16). This provided a heavy degree of overlapped data, which could be utilised in the analysis of the outer beams with respect to both inner and nadir beams of adjacent lines.

For a commercial operation, 40m line spacing would be more appropriate.

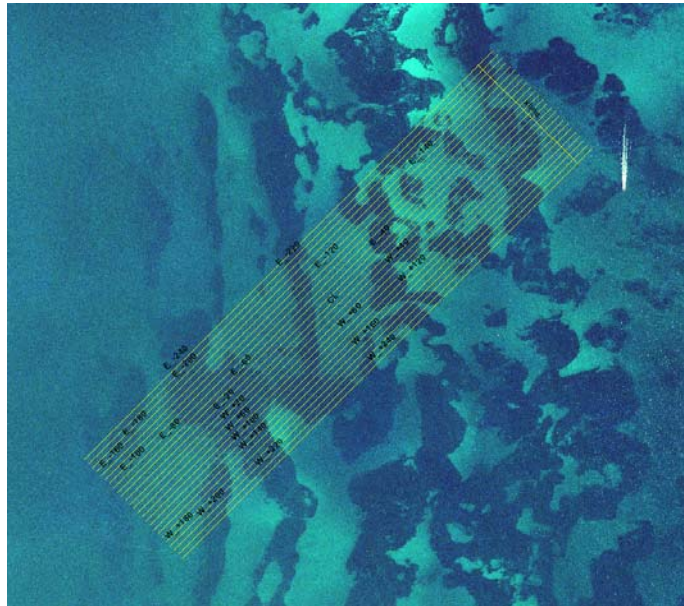


Figure 7.16. Survey line plan in Marmion Marine Park. Double density line spacing was used to provide excellent overlapped Multibeam bathymetry. This assisted in the analysis and comparison of the various systems.

7.5. Data Processing Methods

A primary aim of the trials was to process the data from the various systems as fairly as possible, such that sensible comparisons could be made.

In all cases, data was processed using industry standard ‘best practice’ as much as possible. In many instances, the Fugro Starfix suite was utilised. This provided a single platform to process the various datasets. This ensured common processing procedures and algorithms were followed. In some instances, such as the GeoSwath system, a comprehensive processing suite from the equipment vendor was used.

In all instances care was taken to perform similar de-spiking and smoothing processes. This provided a realistic product from the systems under trial. All Multibeam bathymetry was reduced to LAT Hillary’s boat harbour using observed tides for Hillary’s from the Department of Land Information (DLI). All Multibeam bathymetry was gridded to a 0.5m pixel size using the same gridding engine. This ensured the gridding algorithm was not a factor in the final data comparisons. All Sidescan sonar backscatter data was gridded (mosaiced) to a 0.5m resolution. This permitted perfect overlap and alignment with the Multibeam bathymetry. In each case, the Sidescan was mosaiced using the same software. On completion of processing, all data was

imported into the Marine Survey Data Model (MSDM). This is a relational data model residing within the ESRI ArcGIS 9.0 environment.

7.5.1. Reson Seabat 8101 and 8125

Both Reson systems were processed using Starfix.Proc. Proc provides both an automated batch processing engine and interactive manual editing framework to marine survey data sets. Heavy emphasis is placed on the batch processing of data, as this ensures consistency, efficiency and repeatability. Manual interaction is largely reduced to quality control of the automation process.

The basic processing flow is as follows (Figure 7.17):

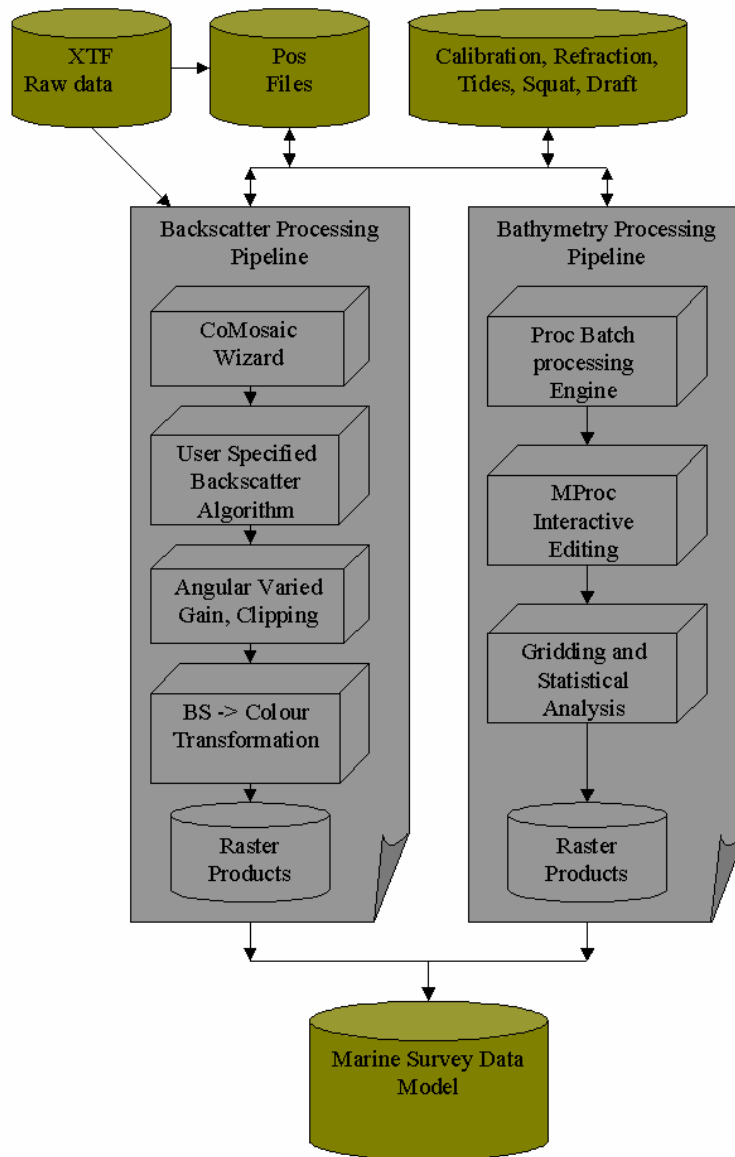


Figure 7.17. Data processing pipeline for the Reson Seabat systems. Both Reson data sets were processed without any difficulties. Processing rates exceeding real time capture rates were easily achieved.

7.5.2. GeoAcoustics GeoSwath

The GeoSwath was processed using the GS+ software version 3.08. This is a manual interactive application which permits the user to replay the acquired data, apply filters, tides, calibration corrections and reduce the data to both random XYZ swath (bathymetry) files, and XYI swath (backscatter) files in a single integrated environment.

The basic processing flow is as follows (Figure 7.18):

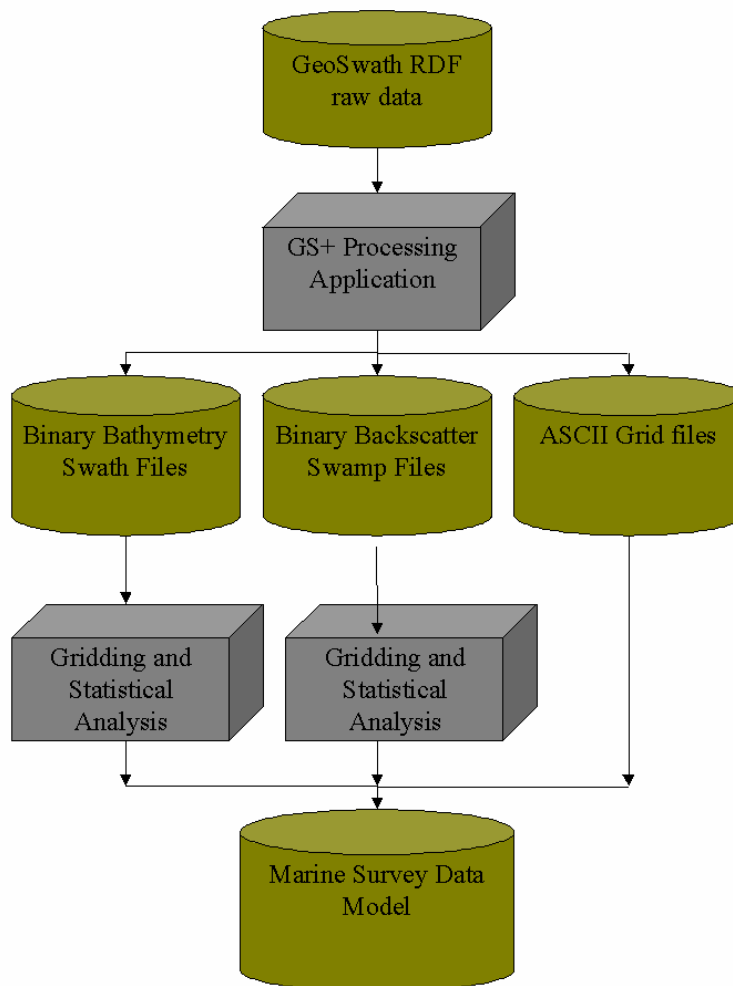


Figure 7.18. Data processing pipeline for the GeoAcoustics GeoSwath system.

It should be noted that the significant problems in the October 2004 trials data resulted in it being discarded. These problems are discussed below. Processing rates for the GeoSwath data did not exceed data capture rates. This was largely due to replay approach to data processing, in which the user is required interact with the processing filters during processing. On a flat seafloor, unattended GeoSwath processing may be possible, but in the reef zone of Marmion Marine Park, this was not feasible.

7.5.3. EG&G 272 analogue sidescan sonar

The EG&G system was logged and processed using the Chesapeake SonarWiz software by Andy Bickers at UWA. The results of the mosaicing engine are geo-referenced tiff files, which are imported into the MSDM (see Figure 7.19).

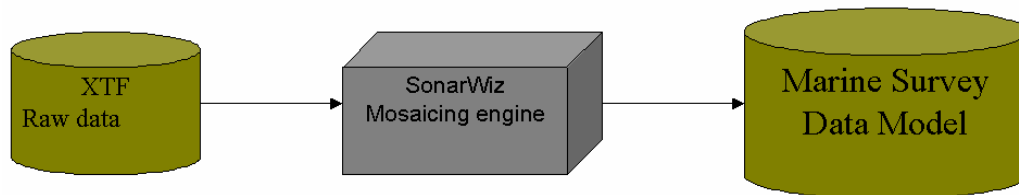


Figure 7.19. Data processing pipeline for the EG&G 272 Sidescan sonar.

7.5.4. Klein 5500 multiple beam digital sidescan sonar

The Klein 5500 system was logged with the Klein SonarPro acquisition system into .SDF files. These were converted into XTF files using a utility from Klein. The XTF files were then mosaiced using both CODA and Starfix.SonarMap. The results of the mosaicing engine are geo-referenced tiff files, which are imported into the MSDM (see Figure 7.20).

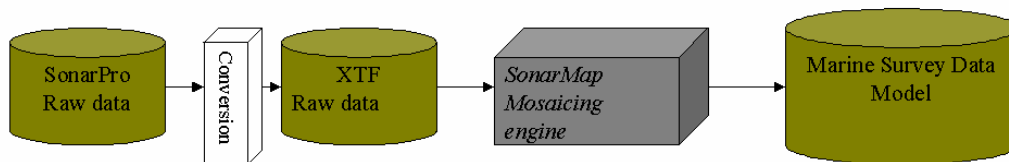


Figure 7.20. Data processing pipeline for the Klein 5500 Sidescan sonar.

7.5.5. C-Max CM2 digital sidescan sonar

The CM2 digital logging system was used to acquire data, and Chesapeake SonarWiz was used to convert into regular XTF format. The XTF files were then mosaiced using SonarWiz, CODA and Starfix.SonarMap. The results of the mosaicing engine are geo-referenced tiff files, which are imported into the MSDM (see Figure 7.21).

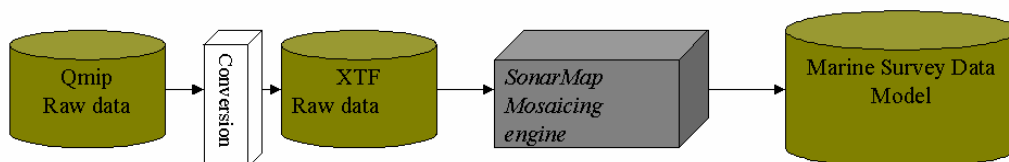


Figure 7.21. Data processing pipeline for the C-Max Sidescan sonar.

7.6. Results

Due to the objectives covering many areas each goal is addressed in turn for clarity.

7.6.1. Validate the Starfix interface to the GeoSwath system

The GeoSwath system is an interferometric system using phase measurements to calculate the angle of the incoming seabed return. As such, the number of individual depth measurements taken across the swath is purely dependant on how frequently the angle measurement is taken. Given that there is no physical limitation to the number of soundings that can be sub-sampled for each acoustic ping the manufacturer calculate as many angles as they deem necessary.

GeoAcoustics have decided to take advantage of this ability and have designed the system to take an enormous number of angle measurements per ping. As the system is taking an angle measurement at each epoch the number of measurements increases with the user selected swath width.

Due to the large quantity of data the system produces with each ping, several modifications to the Starfix suite were required to interface and log the raw data from the GeoSwath.

Interfacing to the GeoSwath

A driver was written to decode the ethernet packets from the system and publish them from IOWin. This allowed the raw data to be logged in Starfix time stamp format within IOWin.

As the system has separate transducers for port and starboard, which each have there own set of pitch, roll and yaw/alignment corrections, the data is published as two separate Multibeam devices from the one IOWin DLL.

The message manager system is designed to deal with data packets of a maximum 32 kilobyte size. If the GeoSwath system is set to operate on a swath greater than 25m per channel, the output data packets exceed this maximum message size. MMDDataLib.DLL was modified to publish a header for each ping and then follow this header with as many separate packets that are required to handle the ping. This modification allowed other applications to subscribe to the messages.

Displaying the GeoSwath data in real time

When configuring the system to display in real time for waterfall and coverage displays both port and starboard transducers must be configured in Multibeam. The corrections for the roll angle of each head must be entered into the Multibeam setup, the port transducer roll correction being approximately -30° +/- patch test result and starboard being $+30^{\circ}$ +/- patch test result.

RTGraph was modified to allow the intensity window above the waterfall display to show up to 2,500 beams per Multibeam swath. Both Multibeam messages can be displayed in real time waterfall and one shot displays. These real time displays have been modified to display only one depth per pixel, which is the mean depth within that across track distance. GeoSwath intensity data can be displayed by selecting the palette and intensity options in RTGraph; these will also be decimated in real time display to one intensity value per pixel.

As the displays in the real time coverage package decimate the displayed data by binning it to a grid size this application required no modification.

Logging the GeoSwath data

The data is currently logged in STS format in IOWin. No facility has been made to log Fugro Binary Format files (FBF) as this package is designed to use fixed packet files and does not use MMDDataLib. There is also no ability to log the data in XTF format as there are no packages Fugro presently operate that could read GeoSwath XTF files. This could be incorporated if there was a use for this format.

Processing the GeoSwath data

The GeoSwath logs Raw Data Files (RDF) in real time that contains all data in a range and angle pseudo raw format. An import wizard to bring this data into Proc in POS format has been written. As the system is capable of collecting data to twelve times water depth even though it only receives a seabed return from eight times at best, the import wizard has been configured to allow the user to import a requested swath angle rather than all the data.

The GeoSwath Plus software will process the data to produce SWATH files containing bathymetry data and SWAMP files containing intensity data. SfxXYZ has been modified to read these files allowing them to be displayed in DataView, converted to other standard file formats and gridded using DTM to produce bathymetry grid or intensity mosaics. As DTM has no de-spiking or TVG controls the data must be processed via the GeoSwath Plus playback software prior to gridding.

7.6.2. Determine the true usable swath width of the GeoSwath systems in varying water depths over varying seabed types

As with all swath bathymetry systems the usable swath width of the system is dependant on the seabed sediment type, seabed topography, water depth and prevailing weather conditions. An example for the GeoSwath system is shown in Figure 7.22.

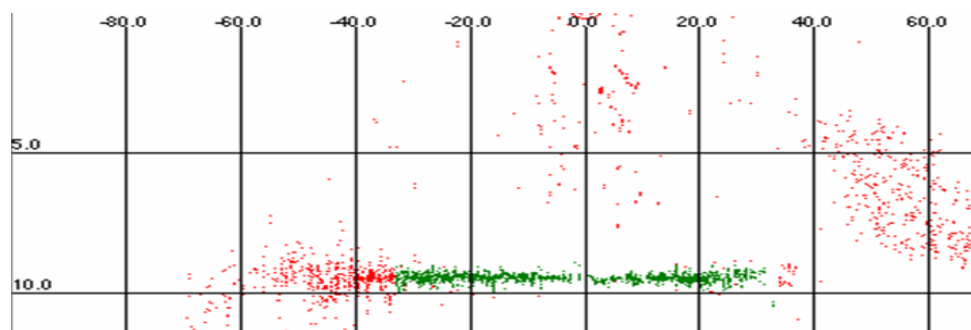


Figure 7.22. GeoSwath swath width examples. The green soundings above indicate the soundings that fall within eight times the water depth. The red soundings are those that fall between the eight and twelve time's water depth.

Data was logged in very calm weather offshore of Hillary's marina over a flat seabed consisting of coarsely grained sand in approximately 9m depths. This ensured almost

no motion, minimal seabed artefacts or slopes with a strong seabed return well within the operating depths of the system.

Given optimum system operating conditions the maximum usable swath width achievable with the 250 kHz supplied was eight times the water depth. It is envisaged that less than ideal weather conditions will see the useable swath width reduce.

7.6.3. Determine the maximum operating water depth of the GeoSwath

To determine the maximum operating water depth of the 250 kHz system data were logged over a sandy seabed to a water depth of 100m, west of Rottneest Island. The system was configured with maximum power setting and pulse length.

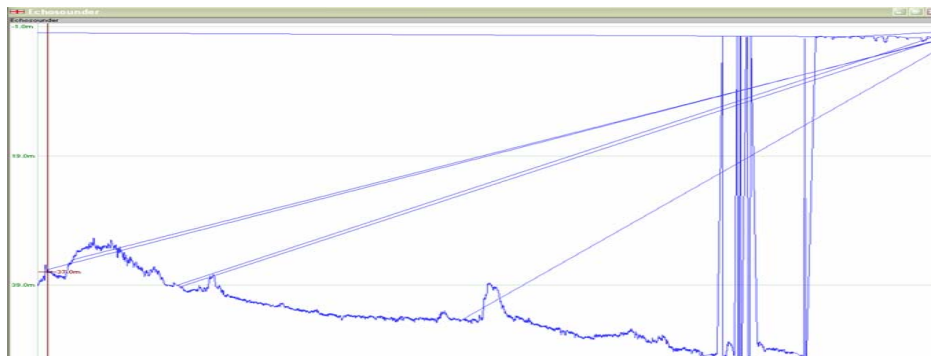


Figure 7.23. GeoSwath single beam maximum operational depth was not as good as expected.

The GeoSwath uses a narrow single beam echosounder mounted between the two transducers to assist in depth determination at nadir. This echosounder lost track of the seabed at approximately 50m depths and did not record any usable depths beyond this depth (Figure 7.23). The sounder did return to normal operation at almost exactly the same depth upon return to shallow water.

The interferometric swath data continued to track the seabed with a continual narrowing in usable swath width. At approximately 75m depths the usable swath width reduced to approximately two times the water depth and the ambiguity between soundings had increased to approximately 2m in height making the true location of the seabed questionable (Figure 7.24).

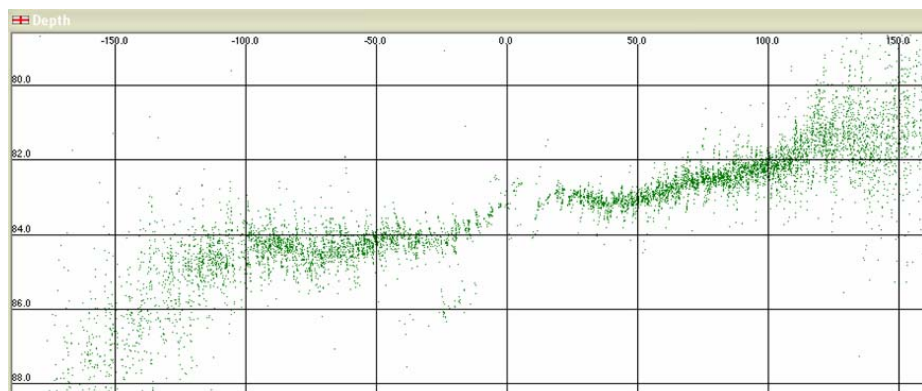


Figure 7.24. GeoSwath cross profile in 82m water depths. This cross profile is indicative of the data collected off Rottneest.

7.6.4. Validate the quality of the bathymetry acquired by the GeoSwath interferometric system in comparison with the known quality of the Reson 8101 and Reson 8125 systems

To provide a valid comparison, the operating environment of close each system was as to identical as possible. Each system was operated using the same vessel, mount, positioning system and motion sensor over the same patch of seabed. This makes the Marmion dataset somewhat unique.



Figure 7.25. Reson 8101 survey weather conditions were less than ideal. Credit should be given to the F180 GPS system which performed admirably underwater!

Unfortunately the only variable beyond operator control was the weather. The 8101 data was collected in less than ideal weather conditions and the data suffered as a result (see Figure 7.25).

Quality of individual soundings across the swath

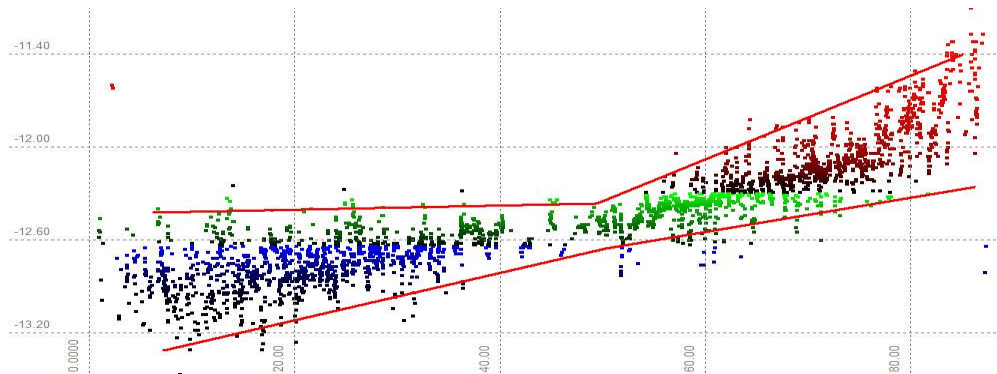


Figure 7.26. A cross profile of a single swath of filtered GeoSwath data. The soundings here are all considered good.

Several operators have noted the “bow tie” effect across the swath of the GeoSwath data (see Figure 7.26). This artefact is common to all data logged during these trials. As seen in a single swath of GeoSwath data below (clipped to the eight times water depth as mentioned in Section 5.2), the uncertainty in depth at nadir spans approximately 0.2m from 12.4m to 12.6m depths (Figure 7.26). The uncertainty in depth increases with the distance from nadir, at a distance two times water depth from

nadir (four times water depth total swath width) the spread of uncertainty increases to 0.8m from 11.8m to 12.6m on the starboard channel and 12.5 to 13.3m on the port channel. Note that this data has already been de-spiked for gross outliers.

This profile was measured over a hard, relatively flat seabed (slight side slope) with minimal motion in shallow water and is representative of the dataset.

Does the system fit within International Hydrographic Organization guidelines?

Computation of a Multibeam error budget to IHO specifications requires an integration of error budgets for all the devices used in the survey, including the motion system, the positioning system, the tide gauge etc. Every system put in place for these trials was to industry best practice, and each system exceeds the IHO special order specifications.

The cross profile display presented above indicates a significant variability in depth, increasing with across track distance. Taking each beam on an individual basis these trials initially suggest the achieved accuracy was sufficient to meet IHO Special Order guidelines for the data collected in less than 20m depths for a swath width of approximately one times water depth. Any data collected beyond the one times water depth swath width or in water deeper than 20m met IHO first order specifications to a maximum swath width of approximately six times water depth at which point the data quality drops to IHO Order 2.

Indeed, as often noted by GeoAcoustics, beams should not be taken on an individual basis. The true depth will not be represented from any individual observation. The true depth is represented by a statistical model of the observations, typically generated by a gridding process. This is based on sound principals and is a valid approach.

Real-time/Online data de-spiking and filtering

There are no operator configurable filters that can be used to smooth the data but there are several configurable gate and de-spiking settings that greatly improve the data. The figure below shows the same swath of data shown in Figure 7.27 illustrating the online de-spiking, where the individual red data points have been rejected and the green accepted. The large red and green blocks are the extents of the gating values.

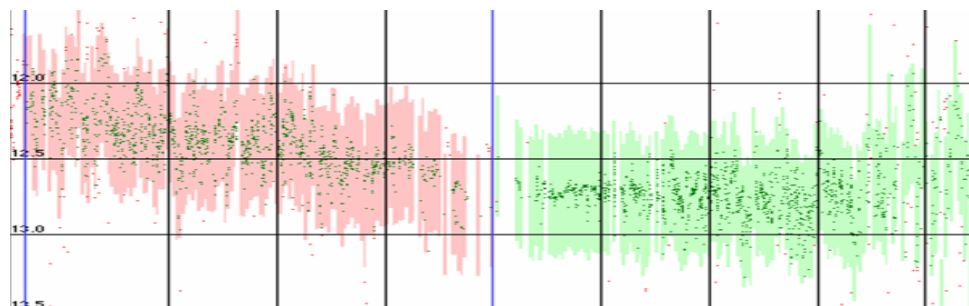


Figure 7.27. A single swath of de-spiked GeoSwath data.

Given the large volume of data in each swath and the large vertical spread between individual soundings across the swath the filters do a very good job of de-spiking, thereby limiting the volume of data written to the processed Swath files.

Given the GeoSwath interferometric approach, can it handle slopes?

The GeoSwath does suffer on slopes where there is ambiguity in the grazing angle for a given epoch. As with all interferometric systems when the slope on the seabed reaches a stage such that the seafloor is perpendicular to the acoustic transmission, the phase calculation begins to fail.

Use of the de-spiking and gating in the GeoSwath Plus software can aid in the tracking of the seabed over steep terrain, but require constant attention over an undulating seabed. In the case of the Marmion data, this proved a successful technique, and resulted in a good clean dataset. The cost impact of this approach is discussed in the conclusions below.

How does a GeoSwath compare to conventional Multibeam bathymetry?

For purposes of Multibeam bathymetry comparison, we gridded the three datasets using the same parameters (Figures 7.28 to 7.30). Gridding was carried out to a 0.5 metre pixel resolution, which is appropriate in the 5-16m water depth range. Following gridding, interpolation across empty pixels using a search radius of 5 * 5 pixels (2.5m) was employed to provide a seamless surface. Finally, the surface was smoothed using a median 3 * 3 filter. This largely removed any remaining noise in the surface, whilst retaining the seafloor features.

By clipping the outer beams to between six and eight times water depth, the GeoSwath gridded bathymetry compared well with the Reson systems. The slight drop in sharpness of seafloor features is to be expected, and does not significantly impact the final result.

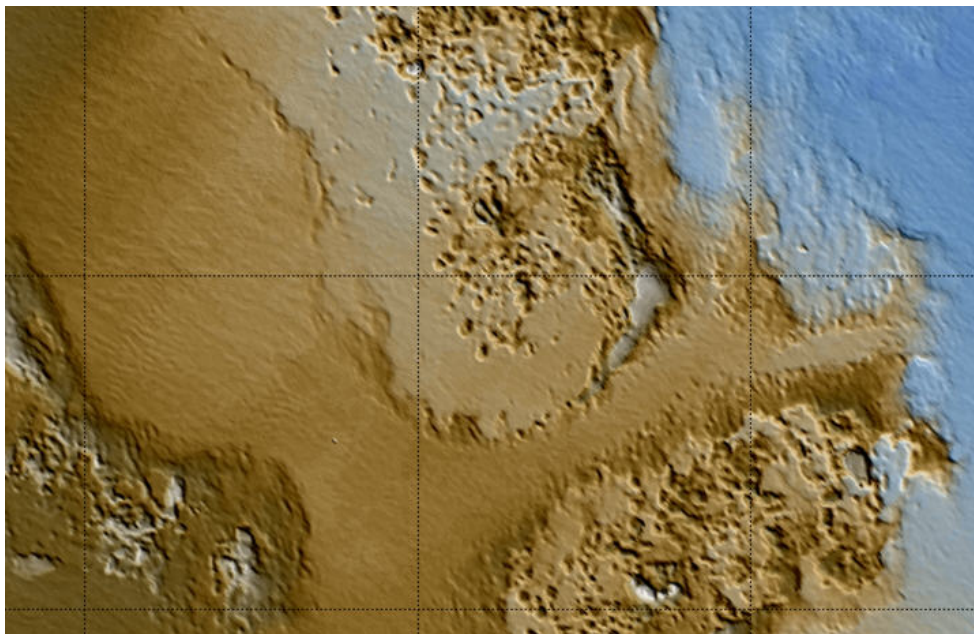


Figure 7.28. Gridded Reson 8125 bathymetry over a shallow reef. Note how clearly the features are defined. Grid axes spacing is 50m.

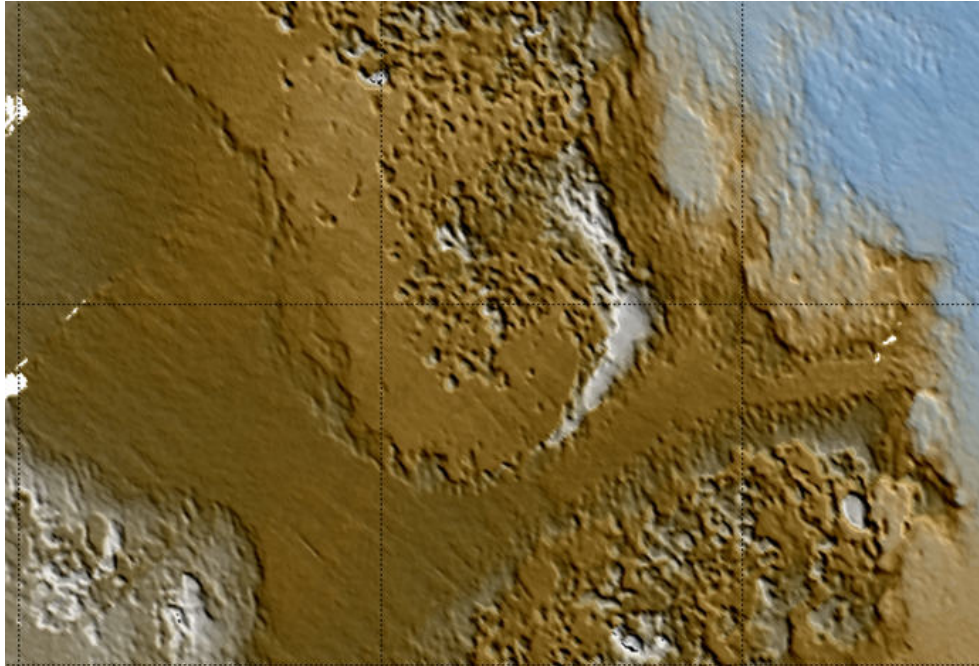


Figure 7.29. Gridded 8101 bathymetry over the same shallow reef. Note the small artefacts in the data due to adverse weather conditions.

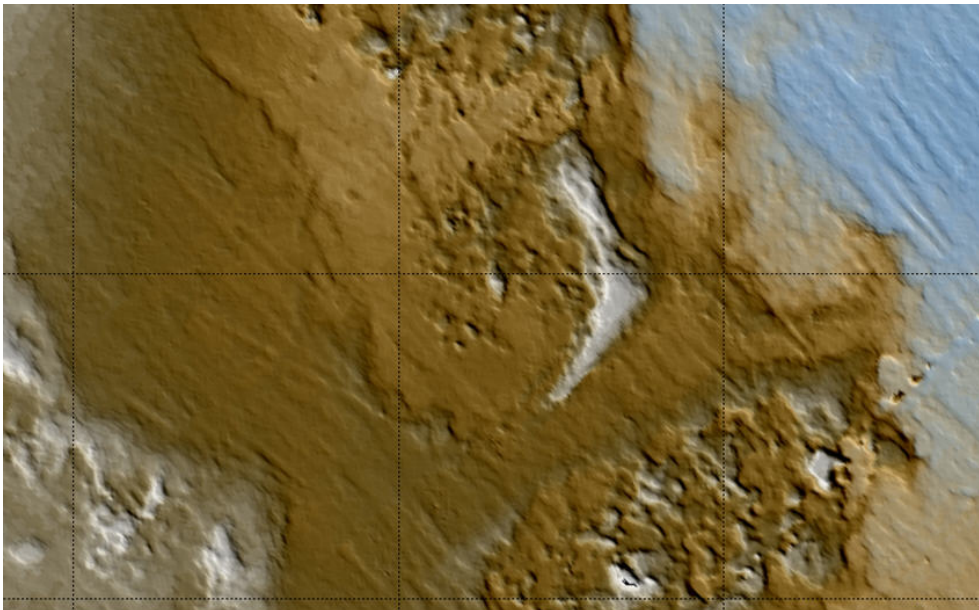


Figure 7.30. Gridded GeoSwath bathymetry data over the same shallow reef. Whilst all the features are still in place, and have similar depths, there is smearing of the features. This is caused by the higher variance in the point cloud. Note the artefacts due to the time stamping issue.

7.6.5. Determine the angular and spatial extent of the data ‘holiday’ under the nadir of the GeoSwath system

Prior to these trials it had been reported that the GeoSwath system suffered from a data gap under nadir and determining the extent of this gap was one of the objectives of the field trials.

This gap no longer exists. Even if the Sidescan data is logged without any slant range correction the bathymetry still applies a slant range correction. Initially it was assumed this bathymetry slant range correction was supplied by the echosounder but during the deep water phase of the trials after the echosounder failed at 50m depths the bathymetry was still slant range corrected.

7.6.6. Determine the required hydro acoustic deliverables for habitat mapping through exchange of technical information with the Coastal CRC, extend the Fugro knowledge base, and derive recommendations for the Victorian Habitat Mapping Project

The primary goal for habitat mapping is to accurately identify the spatial location, extent and characteristics of differing habitats on the seafloor. Traditional approaches of diving, still camera or towed video surveys provide the most direct mechanism to observe the characteristics of habitats. Unfortunately, these fall short on the spatial location and extents of the habitat in question. When costed on a coverage basis, these traditional techniques prove to be prohibitively expensive, prone to omissions and relatively unsafe survey techniques. A more cost effective and rigorous approach is required to identify all habitats at a broad scale as efficiently as possible. This would then be followed up with targeted towed video camera and stills photography in identified areas of interest. Data from this follow up survey is used for the actual habitat classification of the areas identified in the hydro acoustic survey.

It should be noted that Hydro acoustic survey techniques do not directly observe marine habitats, but the data they collect can be used as a surrogate to identify differing habitats.

For the purposes of seafloor mapping, broad scale hydro acoustic survey acquisition generally fall into the realm of Multibeam bathymetry and Sidescan sonar. Whilst it is also possible to include single beam echo sounding in this category, it is not considered to be a cost effective solution where full coverage of the seafloor is expected, so is not included in this discussion.

7.6.7. Multibeam bathymetric data deliverables

A typical deliverable from a Multibeam survey is a bathymetric surface. This surface is the result of a complex series of processes, including calibration, filtering, reduction, gridding and smoothing. Once a seamless bathymetric surface achieved, it is possible to derive other surfaces such as slope, aspect, and rugosity.

Presented below are examples of surfaces generated from Multibeam bathymetry (Figures 7.31 to 7.34).

Whilst not a direct classification mechanism, surface of shaded relief are intuitive mapping techniques. The use of slope often highlights subtle changes in relief as low as 5cm. These can often easily be identified as sand waves, outcropping rock, reef, and even biota such as seagrass.

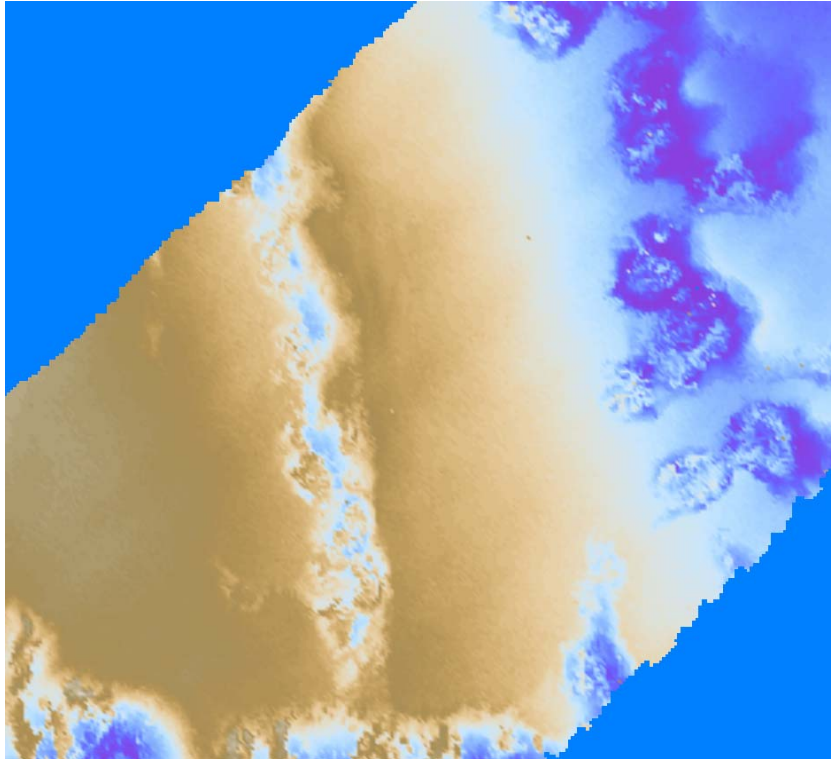


Figure 7.31. Surface of seafloor depth from the Reson 8101. A simple transform of depth to colour provides useful of information. It is widely understood that habitats change with depth. As such, seafloor depth is a significant factor in automated classification algorithms.

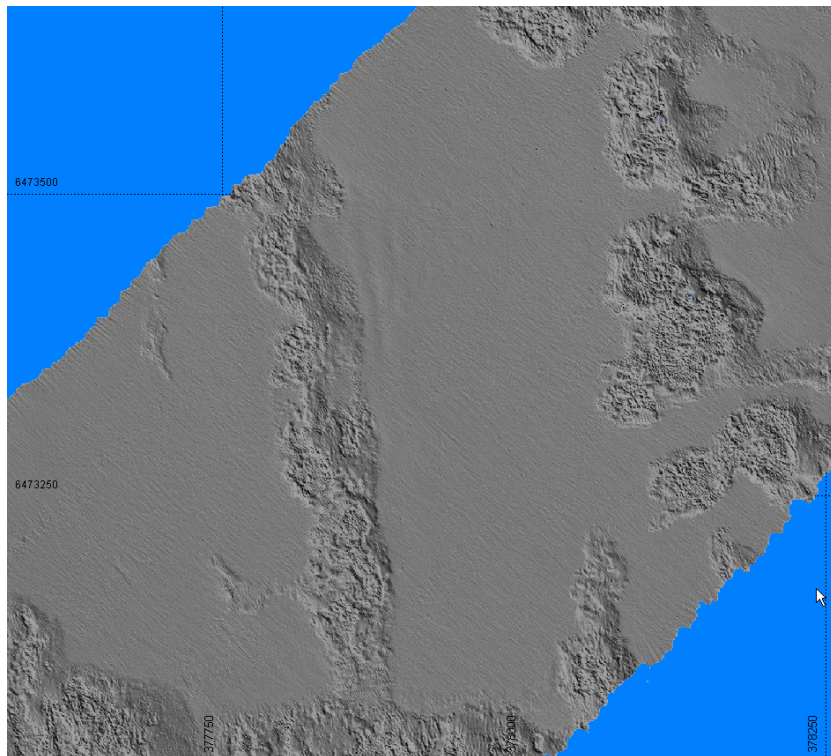


Figure 7.32. Surface of seafloor slope from the Reson 8101. Depiction of relief via the use of shaded relief maps provides immediate visual cues to the location and spatial extents of potential habitats.

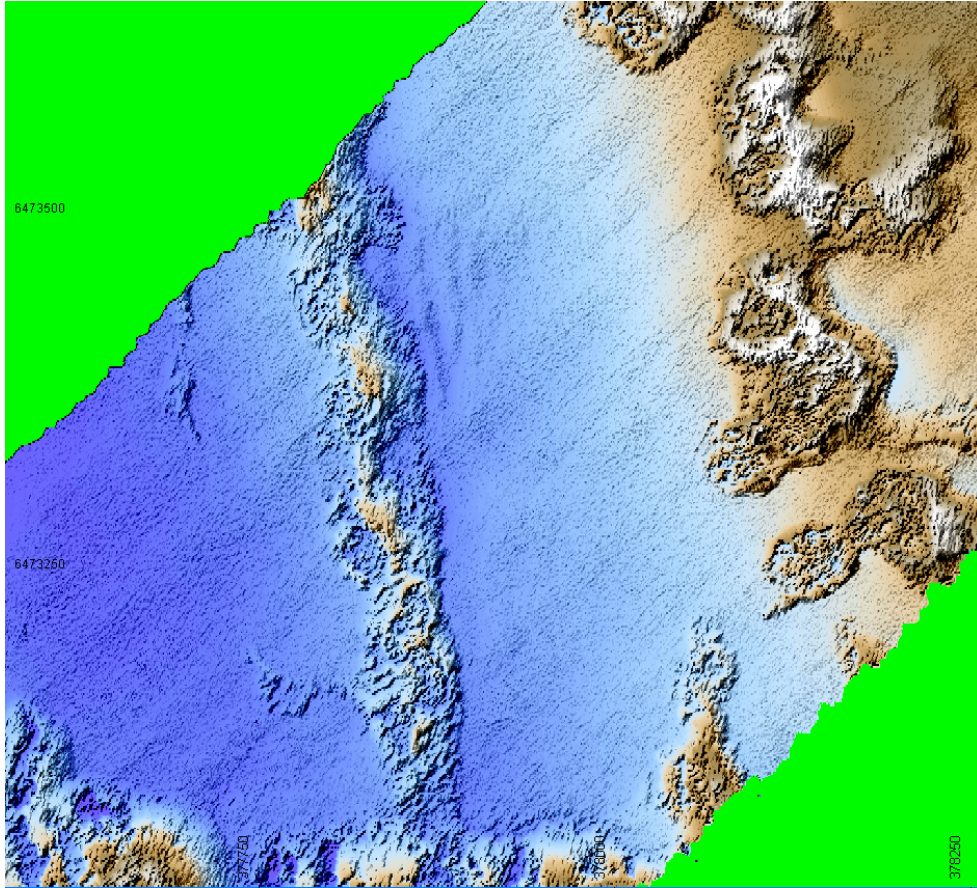


Figure 7.33. The combination of shaded relief and colour depth surfaces provides a primary presentation mechanism for the bathymetric data component of any Multibeam survey. It is easily understood by a casual observer and skilled technician alike.

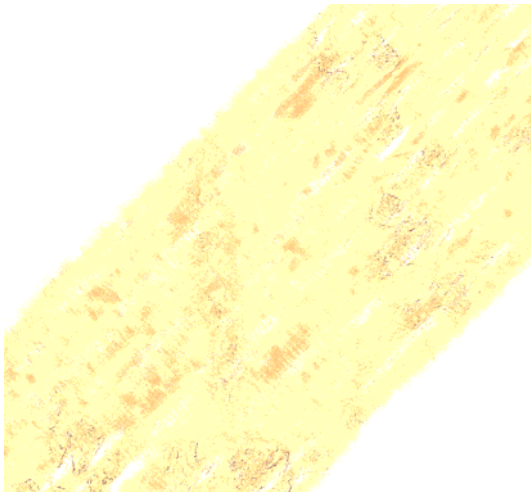


Figure 7.34a. Bathymetry quality surface provides a useful metadata layer. This can be used as a masking layer to omit noisy or unreliable data from classification systems.

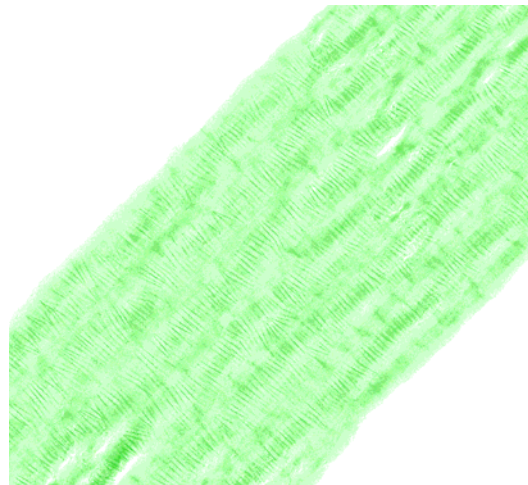


Figure 7.34b. NSamples surface provides a metadata surface indicating how many bathymetric observations were utilised in order to determine the depth for each pixel. This surface is very useful when analysing the survey to determine how efficiently it was undertaken.

7.6.8. Multibeam backscatter data – snippets

As discussed in Chapter 5, an emerging by-product of Multibeam bathymetric systems is backscatter acoustic intensity from the seafloor. This data can be used as a surrogate to infer impedance and roughness of the seafloor (Beaudoin *et al.*, 2002). This data is logged simultaneously with the Multibeam bathymetry. For each ping, each sample of backscatter is associated to the relevant beam number. This permits correct co-registration of the backscatter with respect to the seafloor (Fugro 2005).

Configuration of the Multibeam hardware to simultaneously acquire high quality bathymetry and backscatter is still the subject of review. There is a trade off between the two datasets. A perfect configuration for bathymetry can have a detrimental impact on the backscatter and vice versa. From field trials, we have established optimum operational parameters. Additional options within the Multibeam system to configure the type of backscatter logged (eg flat bottom or uniform) have significant impact on the quality of backscatter data. This can be noted in the difference in the 8101 and 8125 data presented below (see Figures 7.35 to 7.39).

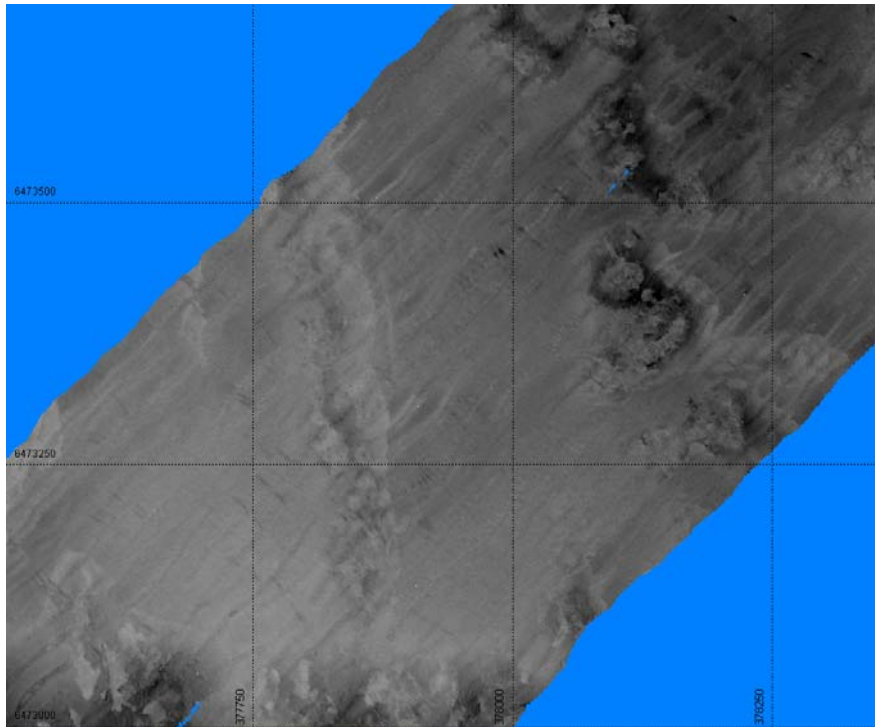


Figure 7.35. Snippet backscatter data from the 8101 using the UNBI processing algorithm. All major features are identified within the backscatter data, and co-location of adjacent swaths is correct. It should be noted that the “uniform snippet” backscatter was used in this trial (Reson 2000). Subsequent to these trials it is suggested that “FlatBottom snippets” is more appropriate (Gavrilov¹, personal communication).

¹Dr. A.N. Gavrilov is a Professor in Underwater Acoustics at the Centre for Marine Science and Technology in the Curtin University of Technology, Perth, Western Australia.

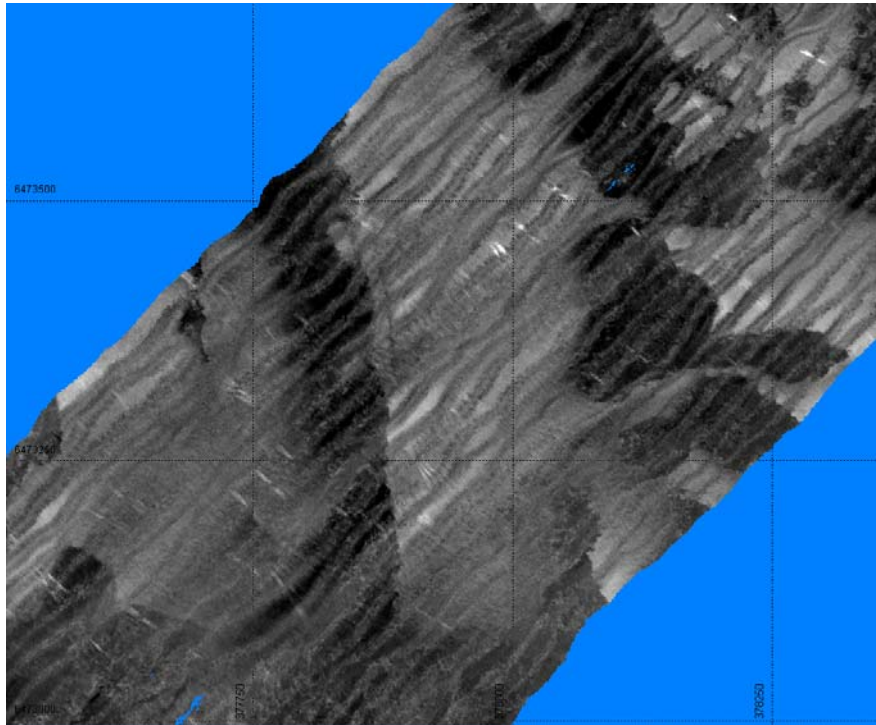


Figure 7.36. Snippet backscatter data from the 8101 using a Per Beam Variance processing algorithm. All major features are identified within the backscatter data, and co-location of adjacent swaths is correct. It should be noted that the “uniform snippet” backscatter was used in this trial. Subsequent to these trials it is suggested that “FlatBottom snippets” is more appropriate (Gavrilov, personal communication).

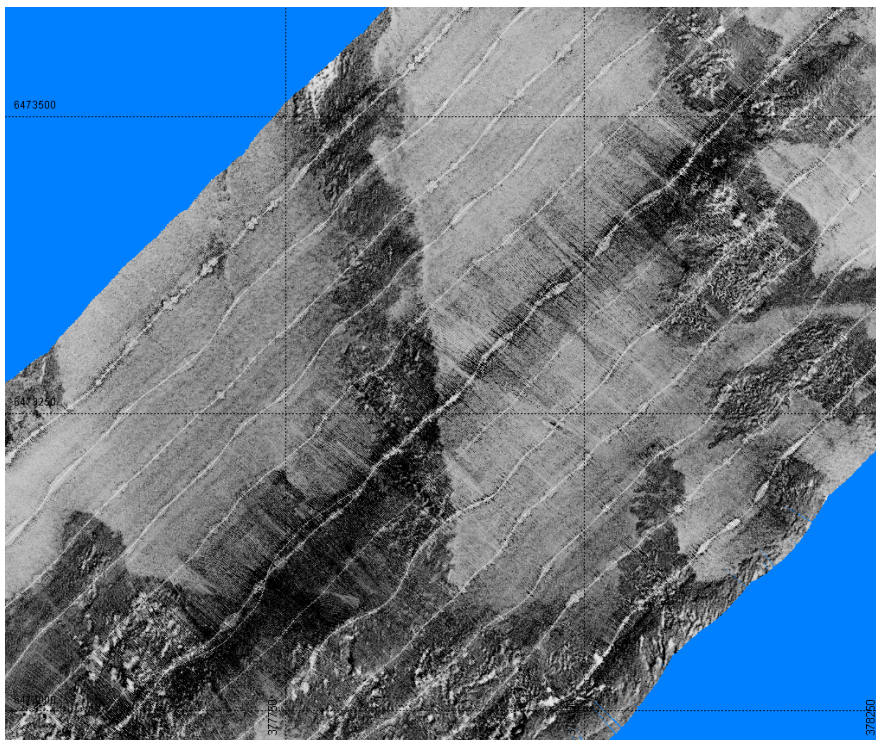


Figure 7.37. Backscatter data from the GeoSwath. All major features are identified within the backscatter data, and co-location of adjacent swaths is correct. Nadir effects in the data possibly caused by interferometric bottom tracking problems can clearly be seen. Overall, the GeoSwath provided the highest resolution backscatter of all the Multibeam systems used.

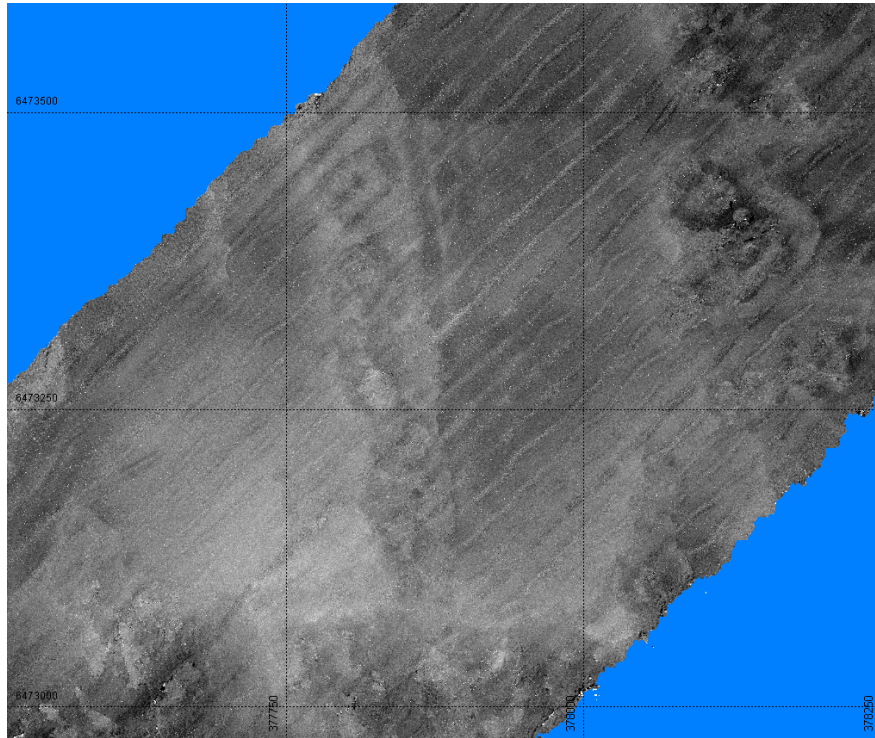


Figure 7.38. Snippet backscatter data from the 8125 using the UNBI processing algorithm. All major features are identified within the backscatter data, and co-location of adjacent swaths is correct. Minor features were not as clearly identifiable as the GeoSwath. Reef structure was not as clearly defined in the 8125 backscatter. Nadir effects are not as pronounced as the GeoSwath data.

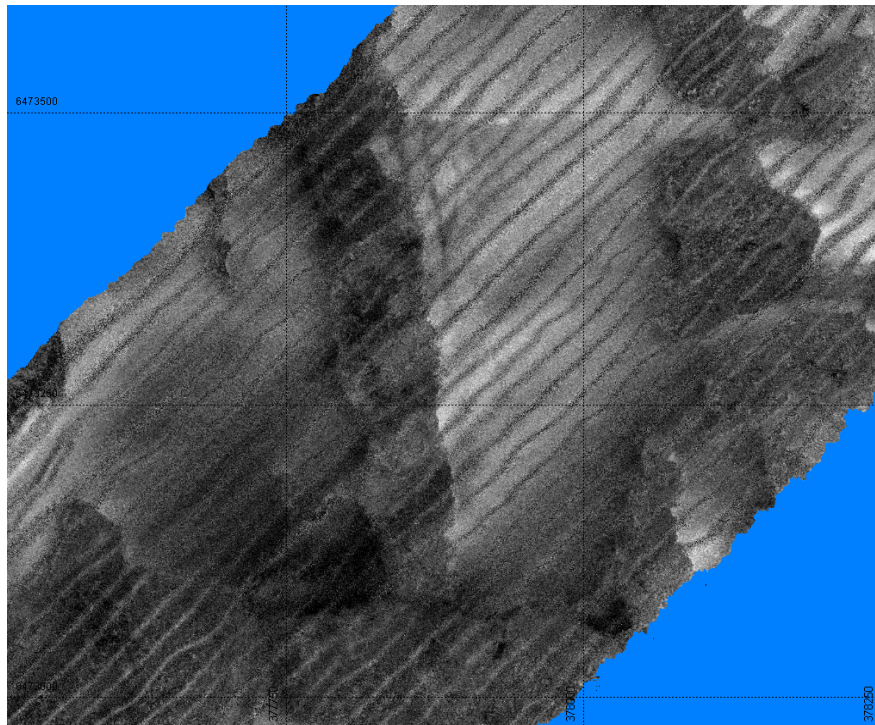


Figure 7.39. Snippet backscatter data from the 8125 using the Per Beam Variance processing algorithm. All major features are identified within the backscatter data, and co-location of adjacent swaths is correct. Minor features were as clearly identifiable as the GeoSwath. Reef structure was well defined in the 8125 backscatter. Nadir effects are not as pronounced as the GeoSwath data, but still a serious impediment to automated classification.

7.6.9. Sidescan sonar

Mosaics for each of the Sidescan sonar's are presented here (see Figures 7.40 to 7.42). It should be noted that the EG&G and C-Max were towed behind the vessel rather than bow mounted. This resulted in improved data quality, but degradation in the co-registration of data with respect to adjacent survey lines. This poor geo-referencing causes significant processing delays, and has implications on the consistency of automated classification systems.

7.6.10. Classification maps

The ultimate goal of a habitat mapping project is to generate a classified map of the various habitats in the survey area. A long standing goal is to create a rigorous automated classification system. The success of such a system requires good quality data inputs. At present the bathymetric surfaces consistently provide such quality surfaces (see Figure 7.43).

Research using the backscatter surface for the purposes of classification is underway. Nadir artefacts in the backscatter data are the subject of much scrutiny. These must to be resolved in the classification algorithms are to prove robust.

7.7. Conduct of a System Comparison for Habitat Mapping Purposes of the GeoSwath, 8101 and 8125

The best hydro acoustic system for habitat mapping is a system that can comprehensively map the seafloor to identify all significant features with minimal vessel time and equipment cost. In the first respect, all Multibeam systems tested identified all significant bathymetric and textural features in the trial area. Similarly, all the Sidescan sonar systems identified all significant textural features. Validation of these features was carried out using the towed video system. This confirmed the existence and correct identification of the features.

Although the Reson 8125 system has the highest resolution bathymetry, and very good backscatter, depth range limitations preclude the system from being an option for the Victorian habitat mapping project. Had the depth range not been an issue, the 8125 would still have been rejected on the basis of the relatively narrow (120-degree) swath width. This relatively narrow sector would increase the survey duration beyond economic limitations.

Given the depth range provided by the Marmion site, both bathymetry and backscatter from the GeoSwath was more than adequate for the purpose of habitat mapping. The hull mounted transducers make this a good option over the combination of 8101 and towed Sidescan, as this ensures excellent backscatter registration with respect to the bathymetry. As discussed earlier the GeoSwath trial was conducted on two occasions. Data from the second trial was much improved, but the significant time stamping problems identified in the first trial were still unresolved. Following the 2005 trials, GeoAcoustics have advised us a hardware modification to the GeoSwath system has resolved these time stamping issue. A third trial has been proposed, to confirm the system is fully operational. The second unresolved problem was of maximum

operational depth. The useable cross profile in 75m water depths was reduced to a relatively narrow swath. It is considered that this was due to software problems in the first trial and should no longer be an issue, but field trials need to confirm this.

The Reson 8101 produced excellent bathymetry and good backscatter. Questionable backscatter at nadir, together with immature backscatter processing algorithms and associated applications at one stage made the proposition of only using the 8101 (i.e. without a towed Sidescan) a high risk venture. Further developments during 2005 have led however to a revision of this conclusion and at the time of writing, only the Reson 8101 will be deployed, with processing to yield both bathymetry and backscatter data.

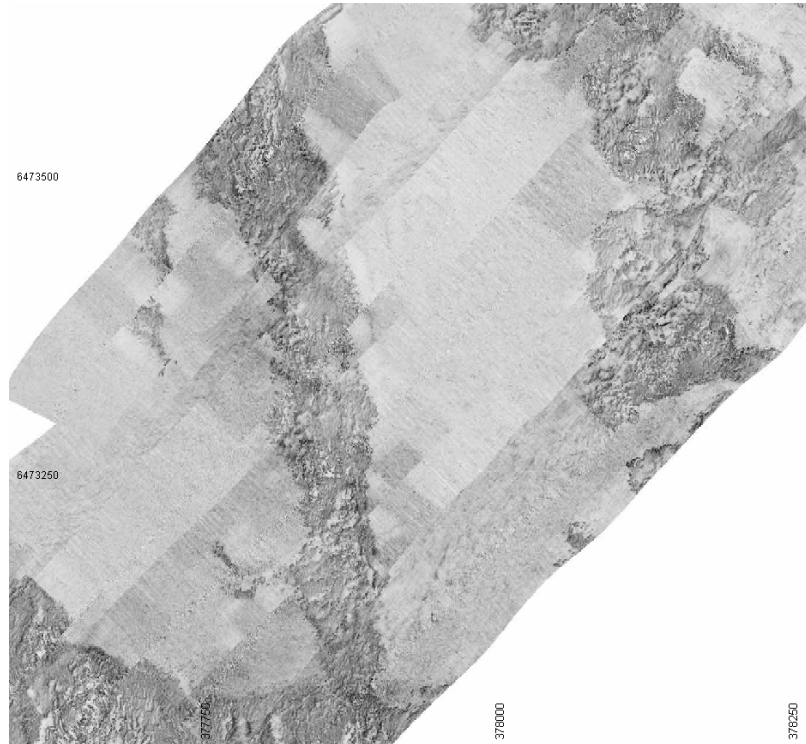


Figure 7.40. EG&G 272 Sidescan sonar. Good across track resolution and a high degree of discrimination make this an invaluable tool. Poor geo-referencing of the towed fish caused by lack of accurate navigation, pitch, roll and heading reduce the absolute accuracy of the resulting mosaic, but relative positions of features are maintained.

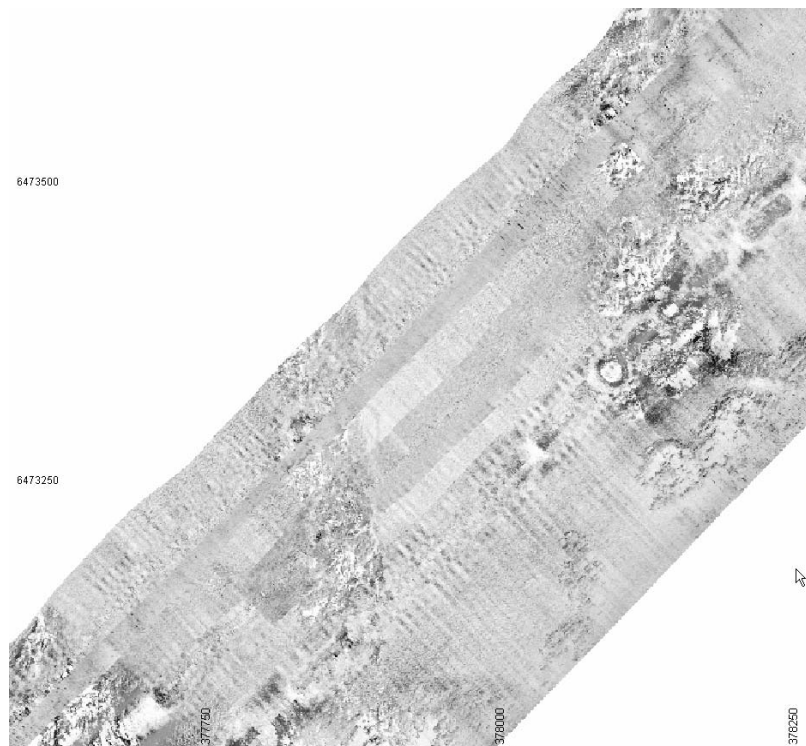


Figure 7.41. C-Max Sidescan sonar suffered from bottom tracking problems. This caused significant AVG artefacts in the across track direction. The bottom tracking algorithm built into the C-Max is still under development.

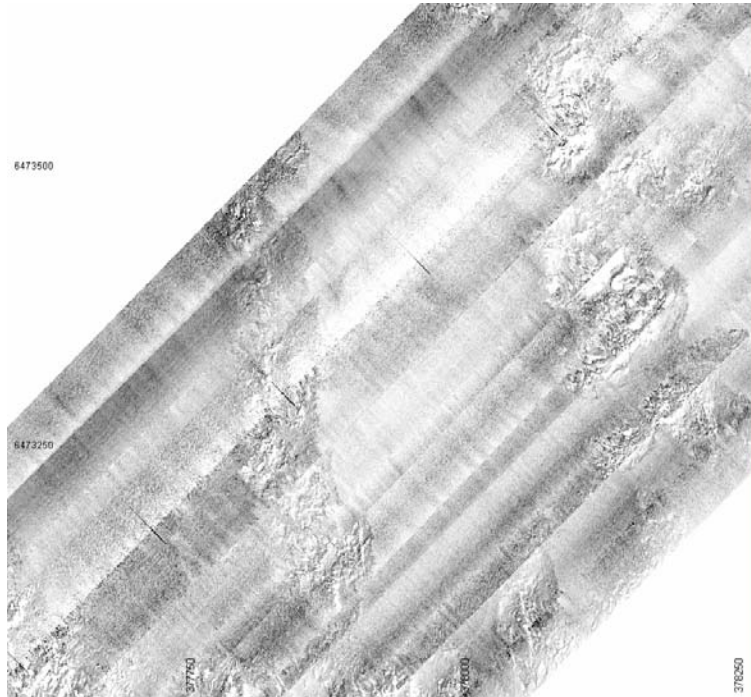


Figure 7.42. The Klein 5500 has the best along track and across track resolution. Together with the accurate co-registration via the bow mount, this provided the highest backscatter from the Sidescan sonar's in the trial.

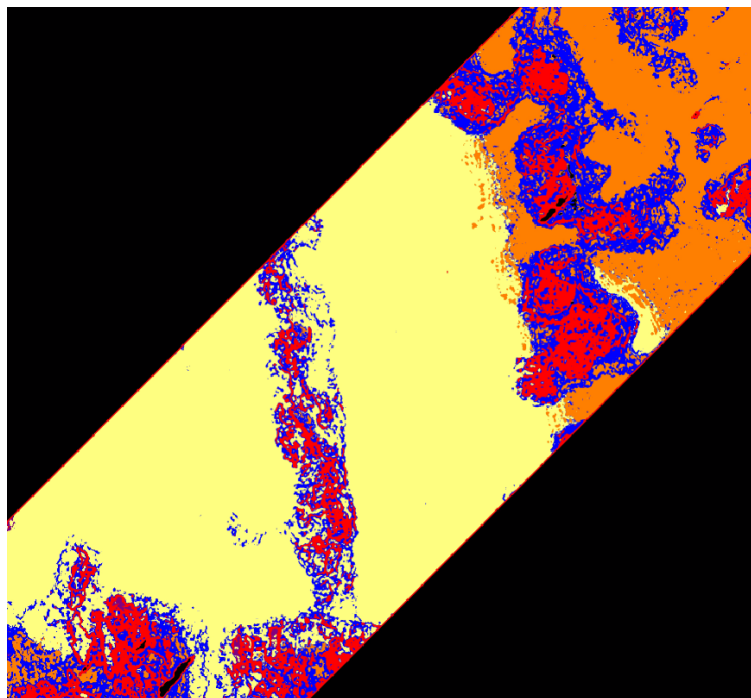


Figure 7.43. An ISO unsupervised classification based on the bathymetric surface and its derivatives (Holmes¹, personal communication). The region has been classified into areas of low reef, high reef, deep sand and sand inundated. Correlation to the bathymetry and backscatter surfaces can clearly be seen.

¹Dr. K. Holmes is a Postdoctoral Research Fellow at the School of Earth and Geographical Sciences in the University of Western Australia, Perth, Australia.

8. ACOUSTIC SYSTEM SELECTION

Benthic habitat maps derived from acoustically sensed data are, in general, not biologically or geologically definitive but represent distributions of habitat surrogates. Therefore, there will always be a degree of uncertainty associated with these types of habitat maps, which will depend on systems used, coverage, ground-truthing and the type of habitats being mapped. Furthermore, marine environments are dynamic regions, thus, the distributions of the different habitats will change over time. A sonar signal does not directly identify a seabed type, usually a type must be identified by a ground-truth sample then correlated with the sonar signal. The ability of acoustic systems to identify different habitats/biotopes can only be realised where the seabed or its contents modifies the sonar signal to provide contrast with the background. For instance, an area of seabed that would be considered a biologically different region from another might not be acoustically or topographically different, but needs to be if it is to be distinguished. Notwithstanding these limitations, the capacity of acoustic systems, and the value of the surrogate measures provided from them, are well established so that for many survey requirements the need is to select the appropriate acoustic system, rather than decide if acoustic technology should or should not be adopted.

Brown *et al.* (2001) provided a comprehensive set of relevant conclusions at that time, which, in summary were:

- A combination of photography, direct sampling and acoustic techniques should be used in seabed assessment
- Acoustic techniques should always be used in conjunction with direct sampling methods
- Swath acoustic systems out-perform single beam acoustic systems
- Acoustic and other techniques are evolving rapidly
- As many components of the benthic community as possible should be sampled during benthic assessment
- Sediment type and seabed morphology appeared to be the major variables influencing community composition in the areas studied

More recently Kenny *et al* (2003) have emphasized that selecting the most appropriate acoustic system or systems to utilise for seabed mapping is an important issue in coastal zone management. They proposed that the most important factors to consider when deciding the appropriate acoustic mapping technique are:

- (i) Size of area to be mapped
- (ii) Depth range in the survey area
- (iii) Object detectability

In addition, it is often the level of resources available that will dictate what acoustic and other mapping techniques are employed. Many potential users in e.g., developing countries and under-funded government departments of developed nations, have limited resources available to them. Hence, a compromise is often made concerning coverage, resolution and the amount of ground truth information obtained. There is thus scope to consider a range of acoustic techniques for benthic habitat assessment, allowing for optimal and sub-optimal methodologies, according to survey purposes and available resources. Ultimately cost is a major factor in the decision of what

technique is used, but it is also important when making decisions on the details of surveys to be clear about what type of information is required. The techniques used and the outcomes of mapping projects are typically driven by the types of management decisions that are required although the mapping usually only is a small input into the decision making process.

Comparisons between survey techniques are required to facilitate decisions on the types of technologies that should be employed in a survey. A history of Shallow Survey conferences traces surveys undertaken to compare techniques and equipment for mapping the seabed. The Marmion Marine Park trials discussed in Chapter 7 compare multibeam systems and traditional and interferometric sidescans. Uniquely this survey used the same tracks for each technique, allowing detailed and accurate high resolution comparisons between data sets.

Assuming the use of aerial and satellite imagery is inappropriate (e.g. the water is too turbid or too deep for optics) and there is no requirement for sub-bottom information, there are six particular acoustic remote sensing strategies that could be employed, in increasing order of cost and, as outlined below, largely in benefit to habitat mapping:

1. Single-beam sonar – see Chapter 3
2. Sidescan sonar – see Chapter 4
3. Sidescan and single-beam sonar
4. Interferometric sidescan sonar – see Chapters 4 and 7
5. Multibeam sonar – see Chapters 5 and 7
6. Multibeam and sidescan sonar – see Chapter 7

The cheapest and simplest acoustic system to operate is a single beam echo-sounder using one or other form of ground discriminating system (e.g. RoxAnn, QTC View or ECHOplus) or if the raw wave form is recorded a similar type of analysis can be performed independently (see Siwabessy, 2001). Single beam systems are however limited by two issues concerning spatial coverage. One concerns the size of the insonified footprint associated with most single beam sounders (a function of beam width and depth). This may well be sufficiently large to provide inadequate spatial resolution in habitats of interest; thus limiting the object detectability factor listed by Kenny *et al.* (2003). The second, and often critical spatial limitation factor concerns coverage. Unlike more complex systems, where full area coverage is often a realistic option, single beam surveys commonly do not employ sufficiently close line spacing to approach full coverage, due to issues of vessel time, and thus, costs.

By contrast, sidescan and swath systems offer workable 100% coverage for many applications, and can provide textural information, which is useful in identifying morphological features such as sand ripples and bedforms. If quantitative bathymetry is not required, then sidescan sonar offers a practical way to map benthic habitat boundaries and geological features. At the time of preparation of this review, it appears that a combination of fine spatial scale bathymetry, perhaps better termed bottom topography, and textural information are of great value in habitat mapping. Thus, for low end users or exploratory surveys, a good strategy is to use a single-beam sounder with ground discrimination processing capability and sidescan sonar. Sidescan sonar now finds itself sandwiched in cost between the choice of using single beam echosounder or multibeam systems. Brown *et al.* (2005) report on a recent comparison between single beam and sidescan mapping. Although traditional

sidescans provide little information about bathymetry the high resolution, almost photo realistic images that can be obtained reveal much about seabed types. The wide swath and ease of mobilisation and deployment also maintains the position of sidescan in the market.

At the other end of the user spectrum, where more money is available, a multibeam sonar linked with either a sidescan system or acoustic backscatter processing of the swath signals themselves represents the optimum approach. Although multibeam systems are more expensive to purchase and run, faster speeds of operation (up to 9 kts), precise positioning and improvements in the quality of backscatter processing, not to mention the confident production of high resolution bathymetric maps are now ensuring that multibeam systems are competing financially for mapping projects. This is especially true where the vessel, crew and logistical costs form a high proportion of the survey cost. Cost efficient mapping of habitats on a broad scale is essential to any successful project. In many cases, the most expensive line item in a project is the vessel and its day rate. Therefore making the most efficient use of ship time is essential in any project. Line turn time, online survey speed and swath width (coverage) are major factors affecting survey efficiency. Traditional survey speeds of 4 knots are required to maintain a sidescan sonar fish altitude close to the seafloor, especially in deep water. Deeper water requires more tow cable behind the vessel, which in turn increases line turn time. Accurate positioning of the tow fish requires the use of an Ultra Short Baseline System (USBL), increasing the survey cost even further. With the approaching maturity of Multibeam backscatter acquisition and processing, the prospect of habitat mapping without the use of Sidescan sonar is becoming a reality. This removes the requirement for a USBL, winch, topside acquisition system, systems engineer and post processing of tow fish navigation, whilst simultaneously improving safety aspects associated with fish deployment and winch operations. Additional trials should be carried out at high survey speeds of 12 knots or more. This has a significant impact on the efficiency of survey operations. In the Victorian Marine Parks project discussed in Chapter 7, the initial survey was carried out using a combination of multibeam to yield bathymetry/topography and sidescan to provide backscatter maps. Later surveys in this series are to use multibeam alone, with backscatter maps derived from processing of the swath returns.

Another option is to use one of the interferometric sidescan systems, which offer a cheaper alternative to multibeam, but as discussed in the example Chapter 7, appear to offer reduced performance compared to an optimum swath system. Interferometric sidescans have attempted to fill a gap in the market, promising sidescan resolution backscatter, with high quality bathymetry over wide swath widths for less cost than multibeam systems. For surveys from relatively small vessels in less than 30 m (and lower cost) in sheltered waters, this equation is likely to be true. In surveys where logistical costs are higher however and more expensive and competent motion sensors are required to cope with worse conditions, savings in costs by using an interferometric sidescan over a multibeam system may be negligible in comparison with total project cost.

Figure 8.1 represents one aspect of the comparison between the acoustic systems discussed, noting that all systems represented apart from the single beam example will often lend themselves to full coverage operation.

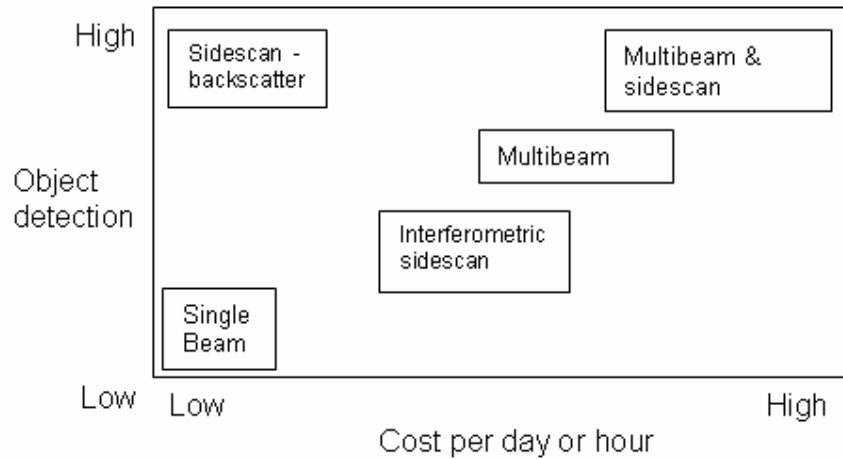


Figure 8.1 Outline of object detection ability vs cost of operation for several acoustic systems

The relationship between the immediate sub-surface constitution of the seabed, including in-benthos organisms, and the visually observed surface and epibenthos is of continuing interest. In this regard, the acoustic systems described in Chapter 6 are of importance. The information that sub-bottom sensing can provide on near surface geological structures is often significantly related to the recent history of the seabed. The emergence of instrumentation providing high levels of depth resolution may also facilitate routine investigation of structure within the top metre or less of sedimentary seabeds.

In conclusion, developments in sonar technology coupled with improved accuracy and precision of ancillary systems, such as GPS and motion sensors, have enabled acoustic techniques to become useful tools in contemporary marine resource management. Acoustic techniques rely on the connectivity of biological communities with physical parameters to enable the generation of broad scale maps of biological resources. Hence, as for any remote sensing technology, it is important to obtain adequate ground truth information, in order to optimize the interpretation of the sonar images. There are various acoustic systems and combinations of systems that could be employed to facilitate the production of benthic habitat maps, each with varying costs and benefits. Acoustic system selection has to take into consideration the depth of water operating in and the objectives of the project. However, it is usually a compromise between the size area to be mapped and the time and resources available for the project. Overall, an integrated approach in mapping is best to identify all features.

REFERENCES

- Anderson, J.T., Gregory, R.S. and Collins, W.T. (2002). "Acoustic classification of marine habitats in coastal Newfoundland." *ICES Journal of Marine Science* 59(1): 156-167.
- Andrieux, N., Delachartre, P., Vray, D., and Gimenez, G. (1995). "Lake-bottom recognition using a wideband sonar system and time-frequency analysis." *Journal of the Acoustical Society of America* 98(1): 552-559.
- Anonymous. (2001a). "ECHOplus aids in seabed archaeology; one of the first seatronics products." *Sea Technology* 42(10): 69.
- Anonymous. (2001b). "ECHOplus sale to national Coral Reef Institute." *Sea Technology* 43(7): 59.
- Barnhardt, W.A., Kelley, J. T., Dickson, S.M. and Belknap, D.F. (1998). "Mapping the Gulf of Maine with Side-Scan Sonar: A New Bottom-Type Classification for Complex Seafloors." *Journal of Coastal Research* 14(2): 646-659.
- Bates, C.R. and Whitehead, E.J. (2001a). "ECHOplus measurements in Hopavågen bay, Norway." *Sea Technology* 42(6): 34.
- Bates, C.R. and Whitehead, E.J. (2001b). "ECHOplus measurements in Hopavågen Bay, Norway." *The Oceanography Society, Biennial Scientific Meeting*, April 2001.
- Bax, N.J., Kloser, R.J., Williams, A., Gowlett-Holmes, K. and Ryan, T. (1999). "Seafloor habitat definition for spatial management in fisheries: a case study on the continental shelf of south east Australia using acoustic and biotic assemblages." *Oceanologica Acta* 22(6): 705-719.
- Baxter, K. and Bickers, A.N. (2004). "Characterising the Fish Habitats of the Recherche Archipelago." *Final draft report: FRDC 2001/060 - Habitat Mapping*. G. Kendrick, University of Western Australia.
- Beaudoin, J., Hughes Clarke, J., van den Ameerle, E. and Gardner, J. (2002). "Geometric and radiometric correction of multibeam backscatter derived from Reson 8101 systems." *Proceedings of the Canadian Hydrographic Conference 2002*, Canadian Hydrographic Association, Ottawa, Ontario, Summer, CD-ROM, pp. 8.
- Bennell, J.D. (2001). "Procedural Guideline No. 1-5 Mosaicing of sidescan sonar images to map seabed features." *Marine Monitoring Handbook*. J. Davies.
- Blondel, P. and Murton, B.J. (1997). *Handbook of Seafloor Sonar Imagery*. Chichester. John Wiley and Sons.
- Blondel, P., Parson, L.M. Robigou, V. (1998). "TexAn: Textural Analysis of Sidescan Sonar Imagery and Generic Seafloor Characterisation." *Proceedings of Oceans '98* vol. 2: 419-423.

- Blum, P., and Okamura, Y. (1992). "Pre-Holocene sediment dispersal systems and effects of structural controls and Holocene sea level rise from acoustic facies analysis: SW Japan Forearc." *Marine Geology* 108: 295-322.
- Bornhold, B.D., Collins, W. and Yamanaka, L. (1999). "Comparison of seabed characterization using sidescan sonar and acoustic classification technique." *Proceedings of the Canadian Coastal Conference 1999*, 15pp.
- Brekhovskikh, L. and Lysanov, Y. (1982). *Fundamentals of ocean acoustics*. Ed. L. Felsen. Springer Series in Electrophysics Volume 8. Springer-Verlag, Berlin.
- Brown, C.J., Mitchell, A., Limpenny, D.S., Robertson, M.R., Service, M. and Golding, N. (2005). "Mapping seabed habitats in the Firth of Lorn off the west coast of Scotland: evaluation and comparison of habitat maps produced using the acoustic ground discrimination system, RoxAnn, and sidescan sonar." *ICES Journal of Marine Science* 62(4): 790-802.
- Brown, C.J., Cooper, K.M., Meadows W.J., Limpenny D.S. and Rees H.L. (2002). "Small-scale Mapping of Sea-bed Assemblages in the Eastern English Channel Using Sidescan Sonar and Remote Sampling Techniques." *Estuarine, Coastal and Shelf Science* 54(2): 263-278.
- Brown, C.J, Hewer, A.J., Meadows, W.J., Limpenny, D.S., Cooper, K.M., Rees, H.L. and Vivian, C.M.G. (2001). "Mapping of gravel biotopes and an examination of the factors controlling the distribution, type and diversity of their biological communities. *Sci. Ser. Tech. Rep.*, CEFAS Lowestoft.
- Burczynski, J. (1999). *Bottom classification*. BioSonics Inc., 4027 Leary Way NW, Seattle WA 98107, USA. [See http://www.biosonicsinc.com/product_pages/vbt_classifier.html].
- Burns, D.R., Queen, C.B., Sisk, H., Mullarkey, W. and Chivers, R.C. (1989). "Rapid and convenient acoustic seabed discrimination", *Proceedings of the Institute of Acoustics* 11: 169-178.
- Carmichael, D. (1998). "Image processing techniques for the analysis of sidescan sonar survey data." *IEE Colloquium on Underwater Applications of Image Processing* (Ref. No. 1998/217).
- Carmichael, D.R., Linnett, L.M., Clarke, S.J. and Calder, B.R. (1996). "Seabed Classification Through Multifractal Analysis of Sidescan Sonar Imagery." *Radar, Sonar and Navigation, IEE Proceedings* 143(3): 140-160.
- Caughey, D.A. and Kirlin, R.L. (1996). "Blind Deconvolution of Echo Sounder Envelopes." Presented *ICASS 96*. 1996 International Conference on Acoustics, Speech and Signal Processing, page 3150. May 7-10. 1996. Marriott Marquis Hotel, Atlanta, Georgia. Institute of Electrical and Electronics Engineers Signal Processing Society.
- Caughey, D., Prager B., and Klymak J. (1994). "Sea Bottom Classification from Echo Sounding Data." Contractor's Report 94-56 prepared for Defence Research Establishment Pacific, Canada. Document number SC93-019-FR-001,

Quester Tangent Corporation, Marine Technology Centre, 99-9865 West Saanich Road, Sidney, British Columbia, V8L 3S1, Canada. 35pp

- Chavez Jr., P.S and Karl, H.A. (1995). "Detection of barrels and waste disposal sites on the seafloor using spatial variability analysis on sidescan sonar and bathymetry images", *Marine Geodesy* 18: 197-211.
- Chivers, R.C., Emerson, N. and Burns, D.R. (1990). "New acoustic processing for underway surveying." *Hydrology Journal* 56: 9-17.
- Clarke, S.J. (1992). "The analysis and synthesis of texture in sidescan sonar data." PHD Thesis, Heriot-Watt University, UK.
- Clarke, P.A. and Hamilton L.J. (1999). "Analysis of Echo Sounder Returns for Acoustic Bottom Classification." *DSTO General Document DSTO-GD-0215*. 42pp. [<http://www.dsto.defence.gov.au/corporate/reports/DSTO-GD-0215.pdf>].
- Cochrane, G.R. and Lafferty, K.D. (2001). "Use of acoustic classification of sidescan sonar data for mapping benthic habitat in the Northern Channel Islands, California." *Continental Shelf Research* 22(5): 683-690.
- Collins, W.T. and McConnaughey, R.A. (1998). "Acoustic classification of the sea floor to address essential fish habitat and marine protected area requirements." *Proceedings of the Canadian Hydrographic Conference*, March 1998, Victoria, Canada.
- Collins, W.T. and Lacroix, P. (1997). "Operational philosophy of acoustic waveform data processing for seabed classification." *Proceedings of the Oceanology International 1997 - COSU '97*, 8pp.
- Collins, W., Gregory, R. and Anderson, J. (1996). "A digital approach to seabed classification." *Sea Technology* 37(8): 83-87.
- Collins, W.T. and Rhynas, K.P. (1998). "Acoustic seabed classification using echo sounders: operational consideration and strategies." *Proceedings of the Canadian Hydrographic Conference*, March 1998, Victoria, Canada, 8pp.
- Connor, D.W., Dalkin, M.J., Hill, T.O., Holt, R.H.F., and Sanderson, W.G. (1997). *Marine Nature Conservation Review: marine biotope classification for Britain and Ireland. Vol. 2. Sublittoral biotopes. Version 97.06*. Joint Nature Conservation Committee Report, No. 230.
- CRC, C. (2004). *Cape Byron Marine Park - Habitat Mapping*. Brisbane, QLD.
- Damuth, J.E. (1975). "Echo character of the western equatorial Atlantic floor and its relationship to dispersal and distribution of terrigenous sediment." *Marine Geology* 18: 17-45
- Damuth, J.E. (1980). "Use of high frequency (3.5 - 12 kHz) echograms in the study of near bottom sedimentation processes in the deep sea." *Marine Geology* 38: 51-75.

- Davis, A., Haynes, R., Bennell, J., Huws, D. (2002). "Surficial seabed sediment properties derived from seismic profiler responses." *Marine Geology* 182: 209-223
- Davies, J., Foster-Smith, R. and Sotheran, I.S. (1997). "Marine biological mapping for environment management using acoustic ground discrimination systems and geographical information systems." *Journal of the Society for Underwater Technology* 22: 167-172.
- de Moustier, C., and Matsumoto, H. (1993). "Seafloor acoustic remote sensing with multibeam echo-sounders and bathymetric sidescan sonar systems." *Marine Geophysical Research* 15:27-42.
- Diaz, J.V.M. (1999). "Analysis of multibeam sonar data for the characterization of seafloor habitats", MoE Thesis, University of New Brunswick, Canada.
- Dugelay, S., Pace, N.G., Heald, G.J. and Brothers, R.J. (2000). "Statistical analysis of high frequency acoustic scatter: what makes a statistical distribution?" *Proceedings of the 5th European Conference on Underwater Acoustics*, 10-13 July 2000 vol. I: 269-274.
- Dunlop, J. (1999). "Texture analysis in sonar images." PhD Thesis, University of London, UK.
- Finndin, R. (1995). "Seabed Visualization and Characterization: Processing of Underwater Video and Side-Scan Sonar Imagery." Department of Naval Architecture and Ocean Engineering, Goteborg, Chalmers University of Technology.
- Fish, J.P. and Carr, H.A. (1991). *Sound Underwater Images: A guide to the generation and interpretations of sidescan sonar images*. Cataumet, American Underwater Search and Survey Ltd.
- Flood, R. (1980). "Deep Sea sedimentary Morphology: Modelling and interpretation of echo-sounding profiles." *Marine Geology* 38: 77-92.
- Foster-Smith, R.L., Davies, J. and Sotheran, I. (1999). *Broad scale remote survey and mapping of sublittoral habitats and biota*. European Commission on Life Programme, Newcastle University, UK.
- Foster-Smith, B., Brown, C., Meadows, B., White, W. and Limpenny, D. (2001). "Ensuring continuity in the development of broad-scale mapping methodology – direct comparison of RoxAnn and QTC View technologies". QTC technologies. *SeaMap/CEFAS Report*, 113pp.
- Fox, D., Amend, M., Merems, A., Miller, B. and Golden, J. (1998). *Nearshore Rocky Reef Assessment*. Newport, Oregon: Oregon Department of Fish and Wildlife, Marine Program. 54pp.
- Fugro. (2005) *Backscatter Bible.Doc*. Internal technical note.
- Galloway, J.L. and Collins, W.T. (1998). "Dual frequency acoustic classification of seafloor habitat using the QTC View." *Proceedings of Oceans '98* vol. 2: 1296-1743.

- Gasperini, M., Ferretti, P., Ligi, M., and Zucchini, P. (1993). "A Paraboloidal sparker seismic source." *Bollettino Di Geofisica* 35(139): 327-338.
- Gavrilov, A.N, Duncan, A.J., McCauley, R.D., Parnum, I. M., Penrose, J. D., Siwabessy, P. J. W., Woods, A. J. and Tseng, Y-T. (2005). "Characterization of the seafloor in Australia's coastal zone using acoustic techniques." *Proceedings of Underwater Acoustic Measurements Conference*, Heraklion, Crete, Greece, June 2005.
- Greenstreet, S.P.R., Tuck, I.D., Grewar, G.N., Armstrong, E., Reid, D.G. and Wright, P.J. (1997). "An assessment of the acoustic survey technique, RoxAnn, as a means of mapping seabed habitat." *ICES Journal of Marine Science* 54(5): 939-959.
- GeoSwath. (2004). *Swath-6199_BJ (Operation Manual)*. Gt Yarmouth, UK
- Griffiths, H.D., Dunlop, J. and Voles, R. (1997). "Texture Analysis of Sidescan Sonar Imagery Using Statistical Scattering Models." *High Frequency Acoustics in Shallow Water, NATO SAACLANTCEN*, Lerici, Italy.
- Hamilton, L.J. (2005). "A bibliography of acoustic seabed classification." *CRC for Coastal Zone and Waterway Management Technical Report*.
- Hamilton, L.J. (2001). "Acoustic seabed classification systems." *DSTO Technical Note* *DSTO-TN-0401*. 66pp.
<http://www.dsto.defence.gov.au/corporate/reports/DSTO-TN-0401.pdf>].
- Hamilton, L.J. (1999). "RoxAnn™ Acoustic Seabed Classification of Sydney Harbour." *Shallow Survey 99 Proceedings - International Conference On High Resolution Surveys In Shallow Water*, Sydney, Australia. 18-20 October 1999.
- Hamilton, L.J., Mulhearn, P.J. and Poeckert, R. (1999). "Comparison of RoxAnn and QTC View acoustic bottom classification system performance for the Cairns area, Great Barrier Reef, Australia." *Continental Shelf Research* 19: 1577-1597.
- Haralick, R. M., Shanmugam, K. and Dinstein, I. (1973). "Textural features for image classifications." *IEEE Transactions Systems, Man and Cybernetics SMC3*: 610-621.
- Harden-Jones, F.R. (1994). *Fisheries ecologically sustainable development: terms and concepts*. Institute of Antarctic and Southern Ocean Studies, Hobart, Tasmania.
- Harvey, E. and Cappo, M. (2000). "Video Sensing of the Size and Abundance of Target and Non-target Fauna in Australian Fisheries." *Proceedings of the National Workshop*, 4 – 7 September 2000, Rottneest, Western Australia.
- Hastings, H.M. and Sugihara G. (1994). *Fractals. A user's guide for the natural science*, Oxford University Press, 1994, pp.7-77.

- Heald, G.J. and Pace, N.G. (1996). "An analysis of the 1st and 2nd backscatter for seabed classification." *Proceedings of the 3rd European Conference on Underwater Acoustics*, 24-28 June 1996 vol. II: 649-654.
- Heap, A.D. (2000). "Composition and dynamics of Holocene sediment next to the Whitsunday Islands on the middle shelf of the Great Barrier Reef platform, Australia." PhD Thesis, James Cook University, Townsville, Queensland. 116pp.
- Held, A.H., Dekker, A., Anstee, J. and S. Ranson. (2000). "Ball AIMS Data Collection and Processing Report. Sydney Harbour Hyperspectral Trial for DSTO Maritime Operations Division." Ball Advanced Imaging and Management Solutions Pty Ltd (Ball AIMS), Canberra.
- Hellequin, L., Boucher, J.M., and Lurton, X. (2003). "Processing of high-frequency multibeam echo sounder data for seafloor characterization", *IEEE Journal of Ocean Engineering* 28(1): 78-89.
- Hiller, T. and Minto, C. (2005). "What can SAS do for me?" *Hydro International*.
- Hollister, C.D. (1967). "Sediment distribution and deep circulation in the Western North Atlantic." PhD Thesis, Columbia University, Palisades, NY, USA.
- Hughes Clarke, J.E., Danforth, B.W., and Valentine, P. (1997). "Areal seabed classification using backscatter angular response at 95 kHz", *Proceedings of SACLANT Conference - High Frequency Acoustics in Shallow Water*, June 1997, Lerici, Italy, *SACLANT CP-45*, 5 pp.
- Hughes Clarke, J.E., Lamplugh, M., and Kammerer, E. (2000). "Integration of near-continuous sound speed profile information", *Proceedings of the Canadian Hydrographic Conference*, 16-18 May 2000, Montréal, Canada.
- Hundley, A.J., Zaboudil and Norall, T. (undated). *A review of the applications of acoustics for marine resource estimation and monitoring*. Offshore Scientific Services, Sydney.
- Huvenne, V.A.I., Blondel, Ph. and Henriot, J.-P. (2002). "Textural analyses of sidescan sinar imagery from two mound provinces in the Porcupine Seabight." *Marine Geology* 189(3-4): 323-341.
- Hydro, I. (2004). "Product survey - sidescan sonars." *Hydro international* 8: 36-39.
- Jackson, D.R., Winebrenner, D.P., and Ishimaru, A. (1986). "Application of the composite roughness model to high-frequency bottom backscattering." *Journal of the Acoustical Society of America* 79(5): 1410-1422.
- Jagodzinski, Z. (1960). "Multiple echoes in echosounders and the probability of detection of small targets." *International Hydrographic Review* 37(1): 63-68.
- Jain, A. (1989). *Fundamentals of Digital Image Processing*. Prentice-Hall.
- Jakeman, E. (1988). "Non-Gaussian models for the statistics of the scattered waves", *Advances in Physics* 37(5): 471-529.

- Jiang, M., Stewart, W.K. and Marra, M. (1993). "Segmentation of seafloor sidescan imagery using Markov random field and neural networks." *Proceedings of Oceans '93*: 456-461.
- Kammerer, E. and Hughes Clarke, J.E. (2000). "New Method for the Removal of Refraction Artifacts in Multibeam Echosounders Systems." *Proceedings of the Canadian Hydrographic Conference*, 16-18 May 2000, Montréal, Canada.
- Kenny, A. (2000). "Acoustic seabed survey techniques for monitoring marine SACs: a trial of three systems." *English Nature Research Report*, No. 411. English Nature, Peterborough, UK. 38p.
- Kenny, A.J., Cato, I., Desprez, M., Fader, G., Schüttenhelm, R.T.E. and Side, J. (2003). "An overview of seabed mapping technologies in the context of marine habitat classification." *ICES Journal of Marine Science* 60(2): 411-418.
- Kim, H.J., Chang, J.K., Jou, H.T., Park, G.T., Suk, B.C., and Kim, K.Y. (2002). "Seabed classification from acoustic profiling data using the similarity index." *Journal of the Acoustical Society of America* 111: 794-799
- Kitching, J.A. (1990). "Introduction to Lough Hyne." In: A.A. Myers, C. Little, M.J. Costello and J.C. Partridge (Editors), *The Ecology of Lough Hyne*. Royal Irish Academy, Dublin, pp. 13-18.
- Kitching, J.A., Ebling, F.J., Gamble, J.C., Hoare, R., McLeod, A.A.Q.R. and Norton, T.A. (1976). "The Ecology of Lough Ine." *Journal of Animal Ecology* 45(3): 731-758.
- Kloser, R.J., Sakov, P.V., Waring, J.R., Ryan, T.E. and Gordon, S.R. (1998). "Development of software for use in multi-frequency acoustic biomass assessments and ecological studies." *CSIRO Report to FRDC project T93/237*, 74pp.
- Kloser, R., Williams, A. and Butler, A. (2001a). "Acoustic, biological and physical data for seabed characterisation – Phase 1, Surveys April-June 2000". *Report to the National Oceans Office*, CSIRO Marine Research.
- Kloser, R.J., Bax, N.J., Ryan, T., Williams, A. and Baker, B.A. (2001b). "Remote sensing of seabed types in the Australian South East Fishery – development and application of normal incident acoustic techniques and associated "ground truthing"." *Journal of Marine and Freshwater Research* 552: 475-489.
- Knott, S.T., and Hersey, J.B. (1956). "Interpretation of high-resolution echo-sounding techniques and their use in bathymetry, marine geophysics, and geology." *Deep Sea Research* 14: 36-44
- Koniwinski, J., McKinney, A., Sagan, J. and Burns, J. (1999). "Hydroacoustic mapping of submerged aquatic vegetation in the lower St. Johns River, Florida." Poster presentation. *South Eastern Estuarine Research Society*, Spring 1999 Meeting, 8-9 April, Jacksonville, Florida. (The authors

affiliation: St. Johns River Water Management District, PO Box 1429, Palatka FL 32178)

- Kvitek, R., Iampietro, P., Sandoval, E., Castleton, M., Bretz, C., Manouki, T. and Green, A. (1999). "Early implementation of nearshore ecosystem database project." SIVA Resource Center, Monterey Bay, California, USA. 131pp.
- Lawrence, M.J. and Bates, C.R. (2001). "Acoustic ground discrimination techniques for submerged archaeological site investigations." *Marine Technology Society Journal* 35(4): 65-73.
- Lean, J., and Pratt, D.A. (1991). "Multi-sensor marine geophysical profiling and digital acquisition using SASI." *Exploration Geophysics* 22: 235-242.
- LeBlanc, L.R., Mayer, L., Rufino, M., Schock, S.G., and King J. (1992a). "Marine sediment classification using the chirp sonar." *Journal of the Acoustical Society of America* 91(1): 107-115.
- LeBlanc, L.R., Satchidanandan, P., and Schock, S.G. (1992b). "Sonar attenuation modelling for classification of marine sediments." *Journal of the Acoustical Society of America* 91(1): 116-126.
- Lee, H.Y., Park, K.P., Koo, N.H., Yoo, D.G., Kang, D.H., Kim, Y.G., Hwang, K.D. and Kim, J.C. (2004). "High-resolution shallow marine seismic surveys off Busan and Pohang, Korea, using a small-scale multichannel system." *Journal of Applied Geophysics* 56(1): 1-78.
- Linnett, L.M. (1991). "Multi-texture Image Segmentation." PhD Thesis, Heriot-Watt University, UK. 237pp.
- Linnett, L.M., Carmichael, D.R. and Clarke, S.J. (1995). "Texture classification using a spatial point process model." *Proceedings on Visual Image Signal Processing* 142(1): 1-6.
- Linnett, L.M., Clarke, S.J., Graham, C. and Langhorne, D.N. (1991). "Remote sensing of the seabed using fractal techniques." *Electronics and Communication Engineering Journal* 3(5): 195-203.
- Lubniewski, Z., Moszynski M, and Stepnowski A. (2000). "Modelling of surface and volume backscattering of echosounder signals on seabed using fractal analysis and impulse response", *Proceedings of ECUA 2000 Conference*, Gdansk, Poland, 2000, vol. 1: 307-312.
- Luskin, B., Heezen, B.C., Ewing, M., and Landisman, M. (1954). "Precision measurements of ocean depth." *Deep Sea Research* 1: 131-140.
- Magorrian, B.H., Service, M. and Clarke, W. (1995). "An acoustic bottom classification survey of Strangford Lough, Northern Ireland." *Journal of the Marine Biological Association of the United Kingdom* 75: 987-992.
- Myers, A.A., Little, C., Costello, M.J. and Partridge, J.C. (eds). (1990). *The Ecology of Lough Hyne: Proceedings of a conference 4-5 September, 1990*. Royal Irish Academy, Dublin.

- McGee, T.M. (1995). "High-resolution marine reflection profiling for engineering and environmental purposes. Part A: Acquiring analogue seismic signals." *Journal of Applied Geophysics* 33: 271-285.
- McKinney, C.M. and Anderson C.D. (1964). "Measurements of backscattering of sound from the ocean bottom." *Journal of the Acoustical Society of America* 36(1): 158-163.
- McRea, J.E., Greene, H.G., O'Connell, V.M. and Wakefield, W.W. (1999). "Mapping marine habitats with high resolution sidescan sonar". *Oceanologica Acta* 22: 679-686.
- McQuillin, R., Bacon, M., and Barclay, W. (1984). *An introduction to seismic interpretation: reflection seismics in petroleum exploration, 2nd Ed.* Graham & Trotman Ltd., London.
- Mignotte, M., Collet, C., Perez, P. and Bouthemey, P. (2000). "Markov Random Field Model And Fuzzy Formalism-Based Data Modeling For The Sea-Floor Classification." *Groupe de Traitement du Signal, Ecole Navale, Lanvéoc-Poulmic*, BP 600-29240, Brest-Naval, France.
- Milligan, S.D., LeBlanc, L.R., and Middleton, F.H. (1978). "Statistical grouping of acoustic reflection profiles." *Journal of the Acoustical Society of America* 64(3): 795-807.
- Ojeda, GY., Gayes, P.T., Van Dolah, R.F. and Schwab, W.C. (2004). "Spatially quantitative seafloor habitat mapping: example from the northern South Caorolina inner continental shelf." *Estuarine, Coastal and Shelf Science* 59(3): 399-416.
- Ol'shevskii, V.V. (1967). *Characteristics of Seafloor Reverberation*. New York: Plenum Press.
- Pace, N. and Gao, H. (1988). "Swathe seabed classification." *IEEE Journal of Oceanic Engineering* 13(2): 83-90.
- Pace, N.G, Zerr B., Pouliquen E. and Canepa, G. (1998). "Overview of progress towards area seabed classification." *UDT Europe 98*. 23-25 June 1998. Wembley Conference Centre, London, U.K. pp41-45.
- Parent, M.D., and O'Brien, T.F. (1993). "Linear-swept FM (chirp) sonar seafloor imaging system." *Sea Technology* 34(6): 49-55.
- Parnum, I.M. (2003). "Mapping sublittoral habitats using acoustic techniques and geographic information systems in Lough Hyne, Ireland." MSc Thesis, University of Wales, Bangor, UK. 108pp.
- Penrose, J.D. and Siwabessy, P.J.W. (2001). "Acoustic Techniques for Seabed Classification." Report prepared for the Marine Conservation Branch of the Western Australian Department of Conservation and Land Management. Perth, Curtin University of Technology.
- Preston, J. (2004). "Acoustic Classification by Sonar." *Hydro International* 8(3): 23-25.

- Preston, M., Christney, A.C., Bloomer, S.F., and Beaudet, I.L. (2001). "Seabed classification of multibeam sonar images", *Proceedings of MTS/IEEE Oceans '01* vol. 4: 2616-2623.
- Preston, J.M., Rosenberger, A. and Collins, W.T. (2000). "Bottom classification in very shallow water." *Proceedings of the 5th European Conference on Underwater Acoustics*, 10-13 July 2000 vol. I: 293-299.
- QTC. (2002). *QTC Sideview*. Quester Tangent Corporation. 2002.
- Reed IV, T.B. and Hussong, D. (1989). "Digital image processing techniques for enhancement and classification of SeaMARC II sidescan sonar imagery", *Journal of Geophysical Research* 94(B6): 7469-7490.
- Riegl, B.M., Moyer, R.P., Morris L.J., Virnstein R.W., Purkis, S.J. (in press). "Distribution and seasonal biomass of drift macroalgae in the Indian River Lagoon (Florida, USA) estimated with acoustic seafloor classification (QTC View, ECHOplus)." *Journal of Experimental Marine Biology and Ecology*.
- RESON. (2000). Seabat 8101 Multibeam Echo sounder System Operator's Manual v. 2.20. Goleta, California.
- Reut, Z. (2000). "On the Computer Characterization of Seabeds by Sonars." *Journal of Sound and Vibration* 232(2): 490-491.
- Rinehart, R.W., Wright, D.J., Lundblad, E.R., Larkin, E.M., Murphy, J. and Cary-Kothera, L. (2004) "ArcGIS 8.x Benthic Terrain Modeler: Analysis in American Samoa." *Proceedings of the 24th Annual ESRI User Conference*, San Diego, CA, Paper 1433.
- Rollet, N., Fellows, M.E., Struckmeyer, H.I.M., and Bradshaw, B.E. (2001). "Seabed character mapping in the Great Australian Bight." *Geoscience Australia Record*, 2001/42.
- Rukavina, N.A. (1997). "Substrate mapping in the Great Lakes nearshore zone with a RoxAnn acoustic sea-bed classification system." *Proceedings of the Canadian Coastal Conference 1997*, 12pp.
- Ryan, D.A., Brooke, B., Wilson, J., Creasey, J., Elliot, C., and Pearson, R. (2004). "Acoustic mapping of estuarine benthic habitats: results of a trial in Wallis Lake, N.S.W." *Geoscience Australia Record* 2004/12, 47 pp.
- Ryan, T., Kloser, R.J. and Sakov, P. (1997). "Data management, analysis and mapping of acoustic seafloor indices." CSIRO Unpublished Internal Report. 38pp.
- Sabol, B.M. and Burczynski, J. (1998). "Digital echo sounder system for characterising vegetation in shallow-water environments." *Proceedings of the Fourth European Conference On Underwater Acoustics*, Rome. Eds A. Alipii and G.B. Canelli. Pp165-171.
- Sainsbury, K.J. (1991). "Application of an experimental approach to management of a tropical multispecies fishery with highly uncertain dynamics." *ICES Marine Science Symposium* 193: 301-320.

- Schlagintweit, G.E.O. (1993). "Real-time acoustic bottom classification: a field evaluation of RoxAnn." *Proceedings of Oceans '93*: 214-219.
- Schock, S. G., LeBlanc, L.R., and Mayer, L.A. (1989). "Chirp subbottom profiler for quantitative sediment analysis." *Geophysics* 54(4): 445-450.
- Shang, C. (1995). "Principle features based texture classifications using artificial neural networks." PhD Thesis, Heriot-Watt University, UK.
- Shippey, G. (1991). "Investigation of Digital Processing in Underwater Acoustic Imaging and Image Interpretation (Acoustic Imaging)." PhD Thesis, Heriot-Watt University, UK.
- Sinclair, M., Stephenson, M., and Spurling, T. (1999). "High Resolution Surveys in Shallow Water - The Laser Airborne Depth Sounder (LADS)." *Shallow Survey 99 Proceedings - International Conference On High Resolution Surveys In Shallow Water*, Sydney, Australia. 18-20 October 1999.
- Simmen, J.A., Stanic, S.J. and Goodman, R.R. (2001). "Guest Editorial" in Special Issue on High Frequency Acoustics, *IEEE Journal of Ocean Engineering* 26: 1.
- Siwabessy, P.J.W. (2001). "An investigation of the relationship between seabed type and benthic and bentho-pelagic biota using acoustic techniques." PhD Thesis, Curtin University of Technology, Perth, Western Australia.
- Siwabessy, P.J.W., Penrose, J.D., Kloser, R.J. and Fox, D.R. (1999). "Seabed habitat classification." *Shallow Survey 99 Proceedings - International Conference On High Resolution Surveys In Shallow Water*, Sydney, Australia. 18-20 October 1999.
- Siwabessy, P.J.W., Penrose, J.D., Fox, D.R. and Kloser, R.J. (2000). "Bottom Classification in the Continental Shelf: A Case Study for the North-west and South-east Shelf of Australia." *Proceedings of Acoustic 2000*, Australian Acoustical Society, 15-17 November 2000, Joondalup, Perth, Western Australia, 265-270.
- Smith, G.F., Bruce, D.G. and Roach, E.B. (2001). "Remote acoustic assessment techniques used to characterise the quality and extent of oyster bottom in the Chesapeake Bay." *Marine Geodesy* 24, 171-189.
- Snelgrove, P.V.R. and Butman, C.A., (1994). "Animal-sediment relationships revisited: cause versus effect." *Oceanography and Marine Biology: an Annual Review* 32: 111-177.
- Sorensen, P.S., Madsen, K.N., Nielsen, A.A., Schultz, N., Conradsen, K. and Oskarsson, O. (1998). "Mapping of the benthic communities common mussel and neptune grass by use of hydroacoustic measurements." *Proceedings of the 3rd European Marine Science and Technology Conference*, 26 May 1998, Lisbon, Portugal.
- Sotheran, I.S., Foster-Smith, R.L. and Davies, J., 1997. "Mapping of marine benthic habitats using image processing techniques within a raster-based geographic

- information system.” *Estuarine Coastal and Shelf Science* 44 (Supplement A): 25-31.
- Sternlicht, D.D. (1999). “High frequency acoustic remote sensing of seafloor characteristics”, PhD Thesis, Marine Physical Laboratory, Scripps Institution of Oceanography, La Jolla, California, USA.
- Stewart, W.K., Jiang, M. and Marra, M. (1994). “A neural network approach to classification of sidescan sonar imagery from a midocean ridge area.” *IEEE Journal of Oceanic Engineering* 19(2): 214-224.
- Stoker, M.S., Pheasant, J.B., Josenhans, H. (1997). “Seismic methods and interpretation.” In T.A. Davies, T. Bell, A.K. Cooper, H. Josenhans, L. Polyak, A. Solheim, M.S. Stoker, J.A. Stravers (Eds.), *Glaciated Continental Margins: An Atlas of Acoustic Images*. Chapman and Hall, London, 1997. 315 pp.
- Thrush, S.F. and Townsend, C.R. (1986). “The sublittoral Macrobenthic Community composition of Lough Hyne, Ireland.” *Estuarine, Coastal and Shelf Science* 23: 551-574.
- Thorsnes, T., Longva, O., Christensen, O., Andresen, K. and Sandberg, J.H. (2004). “Coastal habitat mapping in Norway, with examples of Interferometric sonar applications.” *Geohab 04*, Galway Ireland.
- Trabant, P.K. (1984). *Applied High-Resolution Geophysical Methods*. International Human Resources Development Corporation, Boston. 103 pp.
- Tress, A. (1996). “Practical classification and segmentation of large textural images.” PhD Thesis, Heriot-Watt University, UK.
- Tsemahman, A.S., Collins, W.T. and Prager, B.T. (1997). “Acoustic seabed classification and correlation analysis of sediment properties by QTC View.” *Proceedings of MTS/IEEE Oceans '97*: 921-926.
- Tseng, Y.-T., Gavrilov, A.N., Duncan, A.J., Harwerth, M. and Silva, S. (2005). “Implementation of genetic programming toward the improvement of acoustic classification performance for different seafloor habitats.” *Proceedings of Oceans '05*.
- US Army Corps of Engineers. (2002). “Acoustic multibeam survey systems for deep-draft navigation projects.” In *Engineering and Design - Hydrographic Surveying*, US Army Corps of Engineers, Maryland, USA, p. 33. Accessed from: <http://www.usace.army.mil/inet/usace-docs/eng-manuals/em1110-2-1003/toc.htm>.
- von Szalay, P.G. and McConnaughey, R.A. (2001). “The effect of slope and vessel speed on the performance of a single beam acoustic seabed classification system.” *Fisheries Research*, 14pp.
- Voulgaris, G. and Collins, M.B. (1990). “USP RoxAnn ground discrimination system: a preliminary evaluation.” ARE Portland UTH Tech Memo 36/90. RE005314. University of Southampton, Dept. of Oceanography, Marine Consultancy Services. *Tech. Rep.* No. SUDO/TEC/90/5C, 75pp.

- Verbeek, N.H., and McGee, T.M. (1995). "Characteristics of high-resolution marine reflection profiling sources." *Journal of Applied Geophysics* 33: 251-269.
- Vrbanich, J., Hallet, M. and Hodges, G. (2001a). "Airborne electromagnetic bathymetry of Sydney Harbour", *Exploration Geophysics* 31: 179-186.
- Vrbanich, J., Fullagar, P.K. and Macnae, J. (2001b). "Bathymetry and seafloor mapping via one dimensional inversion and conductivity depth imaging of AEM", *Exploration Geophysics* 31: 603-610.
- Walter, D.J., Lambert, D.N., and Young, D.C. (2002). "Sediment facies determination using acoustic techniques in a shallow-water carbonate environment, Dry Tortugas, Florida." *Marine Geology* 182: 161-177.
- Waring, J.R., Kloster, R.J. and Pauly, T. (1994). "ECHO -Managing fisheries acoustic data." *Proceedings of International Conference on Underwater Acoustics*, University of New South Wales, Dec. 1994, 22-24.
- West, G.R. and Lillycrop, W.J. (1999). "Feature Detection and Classification with Airborne Lidar - Practical Experience." *Shallow Survey 99 Proceedings - International Conference On High Resolution Surveys In Shallow Water*, Sydney, Australia. 18-20 October 1999.
- Whitmore, G.P., and Belton, D.X. (1997). "Sedimentology of the south Tasman Rise, south of Tasmania, from 'groundtruthed' acoustic facies mapping." *Australian Journal of Earth Sciences* 44: 677-688.
- Wilding, T.A., Sayer, M.D.J. and Provost, P.G. (2003). "Factors affecting the performance of the acoustic ground discrimination system RoxAnn™." *ICES Journal of Marine Science* 60(6): 1373-1380.
- Wilkins, H.R.A. and Myers, A.A. (1990). "The distribution of gobies (Teleostei: Gobiidae)." In: A.A. Myers, C. Little, M.J. Costello and J.C. Partridge (Editors), *The Ecology of Lough Hyne*. Royal Irish Academy. Dublin, 107-116.